

Analysis of animal models of neurodegenerative diseases with protein deposits

Dissertation

zur Erlangung des akademischen Grades

doctor rerum naturalium

(Dr. rer. nat.)

genehmigt durch die Fakultät für Naturwissenschaften
der Otto-von-Guericke-Universität Magdeburg

von M. Sc. Johannes Steffen

geb. am 01.06.1986 in Wismar

Gutachter: Prof. Dr. Dr. Jens Pahnke
Prof. Dr. Oliver von Bohlen und Halbach

eingereicht am 25.08.2015

verteidigt am 19.01.2016

"Eine neue wissenschaftliche Wahrheit pfl egt sich nicht in der Weise durchzusetzen, dass ihre Gegner überzeugt werden und sich als belehrt erklären, sondern vielmehr dadurch, dass ihre Gegner allmählich aussterben und dass die heranwachsende Generation von vornherein mit der Wahrheit vertraut gemacht ist."

- Max Plank -

Table of contents

Abbreviations	IV
List of tables	V
List of figures	VI
Summary	VII
1 Introduction.....	1
1.1 Neurodegenerative diseases and protein aggregation	1
1.2 Alzheimer’s disease	2
1.2.1 Molecular fundamentals	3
1.2.2 Pathology.....	5
1.2.3 Molecular organisation and physiological functions of APP	6
1.2.4 Sporadic and inherited disease variants	7
1.3 Disease models.....	9
1.3.1 Transgenic animals expressing wild-type APP.....	9
1.3.2 Disease models expressing mutant transgenes	10
1.3.3 Advanced and natural models.....	11
2 Motivation and aims	15
3 Material and methods.....	17
3.1 Material	17
3.1.1 Chemicals.....	17
3.1.2 Kits	18
3.1.3 Antibodies.....	18
3.1.4 Primers	18
3.1.5 Animal feed	18
3.1.6 Equipment	19
3.1.7 Buffers and solutions.....	19
3.1.8 Software	21
3.2 Methods	22
3.2.1 Animal models.....	22
3.2.2 Animal husbandry.....	23
3.2.3 Genotyping	23
3.2.4 Tissue preparation.....	24

3.2.5	Immunohistochemistry	24
3.2.6	Histochemistry.....	25
3.2.7	Analysis of microscopic slides.....	26
3.2.8	Protein biochemistry	26
3.2.9	Statistics.....	28
4	Results	29
4.1	Murine APP-deficient mice.....	29
4.1.1	Plaque deposition is diminished by murine APP expression.....	29
4.1.2	Knockout of murine APP elevates intracerebral A β ₄₂ levels	33
4.1.3	Murine APP-deficiency does not affect APP processing	35
4.1.4	Co-expression of murine APP accelerates vascular deposition of A β	36
4.1.5	Microglial response is reduced in upon murine APP knockout.....	37
4.1.6	Pronounced gliosis in aged, murine APP-deficient mice	41
4.1.7	Neuronal density was not affected in murine APP-deficient mice	43
4.1.8	Caspase expression illustrates unchanged apoptosis	44
4.1.9	Correlating results	44
4.2	Octodon degus	45
4.2.1	Absence of unspecific signs of neuropathological changes	45
4.2.2	Lack of amyloid deposition in degus	48
4.2.3	Age-independent tau pathology in wild-type degus.....	50
5	Discussion.....	53
5.1	Murine APP-deficient mice.....	55
5.1.1	Impact of murine APP expression on plaque and amyloid load	55
5.1.2	Increased amyloid solubility exacerbates cortical amyloid angiopathy.....	57
5.1.3	Impact of cellular amyloid clearance	58
5.1.4	Neuronal density and apoptosis.....	60
5.1.5	Perspective and implications for research	60
5.2	Octodon degus	62
5.2.1	Natural aging without development of marked neurodegeneration	62
5.2.2	Phosphorylation of cytoskeletal tau.....	64
5.2.3	Cellular clearance, molecular markers and cognitive defects.....	65
5.2.4	Degus as model for natural aging.....	65
5.2.5	Conclusion	66

6	References.....	67
7	Supplement.....	81
8	Appendix.....	87
8.1	Declaration / Erklärung	87
8.2	Curriculum vitae	89
8.3	List of publications.....	91
8.4	Acknowledgements	93

Abbreviations

ABCB1	ATP-binding cassette sub-family B member 1	TAE	Tris acetate ethylenediaminetetraacetic acid
ABCC1	ATP-binding cassette sub-family C member 1	Taq	<i>Thermus aquaticus</i>
AD	Alzheimer's disease	TBS	Tris buffered saline
ADAM10	A disintegrin and metalloproteinase domain-containing protein 10	TBST	Tris buffered saline tween
AICD	Intracellular domain of APP	TEMED	Tetramethylethylenediamine
ANOVA	Analysis of variance	Thr	Threonine
APH1	Anterior pharynx-defective 1	ThS	Thioflavin S
APLP1/2	APP-like protein 1/2	ThT	Thioflavin T
APP	Amyloid precursor protein	Thy1	Thymocyte antigen 1
APS	Ammonium persulfate	Tris	Tris(hydroxymethyl)aminomethane
A β	β -amyloid	Vim	Vimentin
BACE1	β -site APP cleaving enzyme 1	ZnT3	Zinc transporter 3
BCA	Bicinchoninic acid	α CTF	α -secretase cleaved C-terminal fragment
BSA	Bovine serum albumin	β CTF	β -secretase cleaved C-terminal fragment
CA	<i>Cornu Ammonis</i>		
CAA	Cerebral amyloid angiopathy		
dATP	Deoxyadenosine triphosphate		
dCTP	Deoxycytidine triphosphate		
dGTP	Deoxyguanosine triphosphate		
DNA	Deoxyribonucleic acid		
dTTP	Deoxythymidine triphosphate		
EDTA	Ethylenediaminetetraacetic acid		
H&E	Haematoxylin and eosin		
His ¹³	Histidine at position 13		
IDE	Insulin-degrading enzyme		
ITCN	Image-based tool for counting nuclei		
LRP1	Low density lipoprotein receptor-related protein 1		
LTD	Long-term depression		
LTP	Long-term potentiation		
NCT	Nicastrin		
ND	Neurodegenerative disease		
NEP	Nepriylisin		
NFT	Neurofibrillary tangles		
NSE	Neuron-specific enolase		
p3	p3 peptide		
PAGE	polyacrylamide gel electrophoresis		
PBS	Phosphate buffered saline		
PCR	Polymerase chain reaction		
PD	Parkinson's disease		
PDGF	Platelet-derived growth factor		
PEN2	Presenilin enhancer 2		
PFA	Paraformaldehyde		
PHF	Paired helical filaments		
PrP	Prion protein		
PS1/2	Presenilin 1/2		
<i>PSEN1/2</i>	Presenilin 1/2 gene		
PVDF	Polyvinylidene difluoride		
sAPP α	Soluble APP α		
sAPP β	Soluble APP β		
SDS	Sodium dodecyl sulphate		
SEM	Standard error of the mean		
Ser	Serine		

List of tables

Table 3-1: PCR reaction mix for detection of APP/PS1-transgene.....	23
Table 3-2: PCR reaction mix for detection of murine APP knock-out.	24
Table 3-3: Thermocycler protocol for DNA amplification.	24
Table 3-4: Dehydration protocol for fixed hemispheres.....	25
Table 7-1: Accession numbers of compared proteins.....	81
Table 7-2: Linear regression analysis of plaque number.....	81
Table 7-3: Statistical analysis of plaque number, size and cortical coverage.	82
Table 7-4: Two-way analysis of variance (ANOVA) of the obtained parameters.....	82
Table 7-5: Separate analysis of 'small', medium and 'large' plaques in mAPP ^{0/0} and mAPP ^{+/+} mice....	83
Table 7-6: Comparison of cortical amyloid angiopathy in mAPP ^{0/0} and mAPP ^{+/+} mice.....	83
Table 7-7: Statistical analysis of microglia response in mAPP ^{0/0} and mAPP ^{+/+} mice.	84
Table 7-8: Neuronal density in mAPP ^{0/0} and mAPP ^{+/+} mice.	84
Table 7-9: Cortical astrocyte coverage in mAPP ^{0/0} and mAPP ^{+/+} mice.	84
Table 7-10: Statistical analysis of age-dependent astrogliosis in mAPP ^{0/0} and mAPP ^{+/+} mice.	84
Table 7-11: Cortical levels of soluble and insoluble A β ₄₂ in mAPP ^{0/0} and mAPP ^{+/+} mice.	85
Table 7-12: Nonparametric Spearman correlation coefficients in mAPP ^{0/0} mice.	85
Table 7-13: Nonparametric Spearman correlation coefficients in mAPP ^{+/+} mice.	86
Table 7-14: Semi-automatic evaluation of cortical microglia, astrocytes and neurons in degus.	86

List of figures

Figure 1-1: Proteolytic processing of the amyloid precursor protein.	4
Figure 1-2: Mutation-based changes of the human amyloid precursor protein.	8
Figure 1-3: Species-dependent differences in the β -amyloid sequence.	13
Figure 4-1: Progression of cortical amyloidosis in mAPP ^{0/0} and mAPP ^{+/+} mice.	31
Figure 4-2: Cortical amyloidosis is exacerbated in murine APP-deficient mice.	32
Figure 4-3: Influence of endogenous APP on cerebral A β ₄₂ levels in transgenic mice.	34
Figure 4-4: Expression of APP- and A β -cleaving enzymes.	35
Figure 4-5: Frequency and severity of cerebral amyloid angiopathy.	36
Figure 4-6: Similar sized microglial populations in 150 d old mice.	37
Figure 4-7: Microglial response is decreased in murine APP-deficient mice.	39
Figure 4-8: Plaque size and corresponding microglial coverage follow a distinct pattern.	40
Figure 4-9: Pronounced astrogliosis in aged mAPP ^{0/0} but not mAPP ^{+/+} mice.	42
Figure 4-10: Neuronal density is unchanged in murine APP-deficient mice.	43
Figure 4-11: Expression levels of major caspases remain unchanged in mAPP ^{0/0} mice.	44
Figure 4-12: Basic histological stains provide no evidence for any neurodegeneration in degus.	46
Figure 4-13: Absence of age-dependent astrocytic, microglial and neuronal changes in degus.	47
Figure 4-14: Degus display no signs of extracellular β -amyloid deposition.	49
Figure 4-15: Degus lack age-dependent tau pathology.	51

Summary

Alzheimer's disease is the most common cause of dementia and accompanied by vast socio-economic problems. To meet these challenges, basic research makes great efforts to provide a better understanding and develop treatment strategies. However, the final success depends also on the quality and precision of the utilised disease models. To reproduce the disease state in animals, mutant human transgenes are overexpressed. Although most animals still express the endogenous variants, the potential interactions with transgenic proteins have rarely been addressed so far.

This study was conducted to provide new insights on the impact of endogenous proteins on deposition of the corresponding transgenic proteins in animal models of neurodegenerative diseases. To do so, an established model of cortical amyloidosis expressing mutant human variants of amyloid precursor protein (APP) and presenilin 1 was crossed with an APP knockout strain to create a model that exclusively expresses human APP. The absence of murine APP led to an increased number of cortical plaques and higher levels of cerebral A β . In contrast, accumulation of amyloid in leptomeningeal blood vessels was diminished. Deficiency of murine APP further altered cellular response to amyloid deposition, as animals developed a pronounced, age-dependent astrogliosis and presented with significantly reduced microglial coverage of plaques. Neuronal density, caspase levels and expression of APP- and A β -processing enzymes were unchanged within the analysed period.

Nevertheless, these mice are genetically modified and rather mimic the rare inherited form of the disease. The most promising model for the common sporadic variant is the South American rodent *Octodon degus* (degu). Degus are supposed to combine the general advantages of rodents with the natural development of plaques and tangles. The second part of the study investigates the age-dependent histopathological changes in degus, to evaluate their suitability for serving as model of Alzheimer's disease. Firstly, basic histological stains were performed, but revealed neither major deviations between young and aged degus and nor any signs for lesions, spatial displacement, neurodegeneration or neuronal loss. Silver impregnations, fluorescent and immunohistological stains unveiled no evidence for extracellular deposits. Astrocytes showed no indication for either activation or any age-dependent changes. Accordingly, resting microglia were evenly distributed in the cortex without any clustering. Finally, the staining of phosphorylated tau revealed reactivity in most cells throughout cortex and hippocampus, but neither spatially nor morphologically resembled tangles.

The first part of the study showed that remaining expression of endogenous APP crucially altered the deposition of amyloid in transgenic mice. It therefore provides an opportunity for further improving current models and thereby enhance the transferability of results to the human system. Secondly, utilisation of degus as model of Alzheimer's disease seems inadequate, as current analyses discovered exclusively normal aging. The presumed progressive aggregation of tau and amyloid was consistently absent and not even unspecific signs for degeneration or inflammation were present.

1 Introduction

1.1 Neurodegenerative diseases and protein aggregation

The term 'neurodegeneration' is collectively used for a large number of neurological disorders^[1]. Neurodegenerative diseases (NDs) are characterised by progressive dysfunction and neuronal loss in specific regions of the central nervous system, which thereby determine course and clinical manifestation^[2]. The vast majority of NDs occur sporadically^[1] and are presumably provoked by a complex interaction of genetic, endogenous and environmental factors^[3]. Age is the most consistent risk factor, especially for the most frequent, Alzheimer's disease (AD) and Parkinson's disease (PD)^[1]. The increasing life expectancy is therefore accompanied by a growing incidence of NDs^[4]. A small subset of those is hereditary and caused by known genetic mutations, related to only a few pathways^[1, 2]. Although exceptional, heritable forms proved particularly valuable for understanding the basic pathogenetic mechanism of NDs^[5]. Neurodegenerative diseases are therefore no longer divided by their predominant clinical features and primarily affected brain regions^[1, 3], but are classified on the basis of the underlying genetic mechanisms and the major compounds of the generated deposits^[2, 3].

Despite the heterogeneity of NDs, common pathogenic mechanisms have been identified^[2, 3, 5], including (i) disturbed dynamics and aggregation of proteins (reviewed in^[6]), (ii) mitochondrial dysfunction and oxidative stress (reviewed in^[7]) and (iii) neuroinflammatory processes (reviewed in^[4]). The pathologic extent of protein aggregation is a common feature of NDs (reviewed in^[1, 3]) and includes for instance β -amyloid (A β) and tau in AD, α -synuclein in PD and huntingtin in Huntington's disease^[3, 5]. Interestingly, the disease-causing mutations typically increase either aggregation propensity or cellular abundance of these proteins^[5]. The characteristic localisation of protein aggregates in the most affected brain regions made them hallmarks of their corresponding disorder^[5]. Although the deposits are prominent features of particular diseases, most protein aggregates are not disease-specific and occur in different disorders^[5, 8]. Aggregated tau, for instance, appears in AD, frontotemporal dementia, Pick's disease, progressive supranuclear palsy and many others (reviewed in^[9]). The intracellular inclusion of α -synuclein is not only a renowned feature of PD, but was also detected in Lewy body dementia, multiple systems atrophy, amyotrophic lateral sclerosis and others (reviewed in^[10]). There are further similarities at the molecular level, where the formation of β -sheet and β -strand structures is a common structural element of aggregating proteins^[11].

1.2 Alzheimer's disease

Since its first description in 1907^[12], Alzheimer's disease became the most frequently cited cause of dementing cerebral cortex pathology^[13]. AD commonly progresses slowly and the first related changes already occur decades before the emergence of initial symptoms^[14]. Clinically, the disease can be roughly divided into three stages. In the (i) early stage (mild AD), patients and their social environments recognise disturbances of short-time memory for the first time. The early stage symptoms further include difficulties in concentration, organisation and performance of complex tasks. The (ii) middle stage (moderate AD) is typically the longest phase and characterised by the increasing loss of autonomy. Difficulties to perform routine tasks (nutrition, hygiene and clothing) and deteriorated memory performance (spatial and temporal confusion) lead to an increasing dependency. Moreover, patients become emotional unstable and undergo personality and behavioural changes. Sleep patterns change and patients can become depressed and withdrawn or restless and irritable. Memory performance impairs progressively and patients have trouble in remembrance of personal history and recognising even near relatives. In the (iii) late stage (severe AD), patients require continuous assistance for daily activities. They lose physical abilities (walk, sit and eat) as well as the awareness of recent events and their environment. Patients finally depend on full-time care, become bedridden and vulnerable to infections^[13], e.g. pneumonia, the leading cause of death in AD patients (reviewed in^[15]).

By 2001, 24.3 million people worldwide suffered from dementia^[16], of which about 70% was attributed to AD^[17]. Until 2040, the number of cases is predicted to double every 20 years^[16]. But prevalence and incidence of AD are age-dependent and show regional differences^[18]. They are highest in Western Europe, North and Latin America^[16, 18], lower in Eastern Europe, China, Western Pacific, North Africa and the Middle East^[16] and lowest in India, South Asia and Africa^[16, 18]. In return, the proportional increase of demented between 2001 and 2040 is presumed strongest in Latin America (393%), North Africa and Middle East (385%) and in China and the developing western Pacific region (336%)^[16].

1.2.1 Molecular fundamentals

In 1907, Alois Alzheimer reported two characteristic changes in the brain of his former patient Auguste Deter, which became *the* histopathological hallmarks of the disease. The intracellular formation of dense neurofibrillary bundles and the deposition of a peculiar substance in the cerebral cortex^[12].

The extracellularly located plaques consist of aggregated β -amyloid^[19]. It is generated by sequential enzymatic proteolysis of the amyloid precursor protein (APP)^[20], a type I transmembrane protein^[21, 22] with various physiological functions in neuronal development and homeostasis (described more detailed in section 1.2.3). The A β sequence is located at the transition of the extracellular juxtamembrane region to the transmembrane helix^[21]. The proteolytic processing of APP is principally realised by two divergent pathways (reviewed in^[23]).

The common, non-amyloidogenic pathway prevents the generation of A β by α -secretase cleavage within the A β -region^[20] and produces a N-terminal, soluble APP fragment (sAPP α) and a membrane-bound C-terminal fragment (α CTF)^[23] (Figure 1-1). In the less frequent amyloidogenic pathway, β -secretase (β -site APP cleaving enzyme, BACE1) initially also generates a soluble, N-terminal APP fragment (sAPP β) and a membrane-bound C-terminal fragment (β CTF)^[23]. Both C-terminal fragments are further processed by γ -secretase, a complex of 4 essential subunits: presenilin (PS), nicastrin (NCT), anterior pharynx-defective 1 (APH1) and presenilin enhancer 2 (PEN2)(reviewed in^[24]). The cleavage of α CTF thereby releases a 24 to 26 amino acid long peptide (p3) and the intracellular domain of APP (AICD)^[25], while β CTF cleavage produces AICD and A β ^[23]. But the γ -secretase cleavage is inaccurate to a certain extent and generates a variety of A β species with different lengths, spanning from 34 to 50 amino acids (reviewed in^[25]). The 40 amino acid long fragment (A β ₄₀) is the most abundant isoform and accounts for 90% of the generated A β ^[26]. Although being produced in a much lesser extent^[26], A β ₄₂ is the crucial pathogenic isoform^[26]. The increased hydrophobicity and aggregation propensity of A β ₄₂ trigger its toxicity^[27] and make A β ₄₂ the major component of plaques^[20]. The aggregation process of A β starts with the spontaneous formation of small oligomers, namely dimers and trimers, proceeds with the generation of larger oligomers and linear protofibrils and results in the generation of larger, insoluble fibrils and ultimately their deposition as plaques^[28, 29].

Neurofibrillary tangles (NFTs) on the contrary, are intracellular bundles of paired helical filaments (PHFs), consisting of hyperphosphorylated species of the microtubule-binding, cytoskeletal protein tau^[19]. Homologous to A β , tau filaments exhibited the same characteristic cross- β structure in the aggregated state^[30]. Due to their exceptional stability, NFTs can remain in the extracellular space upon neuronal death^[12, 31]. The microtubule binding of tau is controlled by phosphorylation and disrupted by hyperphosphorylation, which thereby initiates the aggregation of tau^[32]. In the

disease state, the phosphate/tau ratio increases from physiologic 1.9 to 2.6 and even to 6 - 8 in PHFs^[33].

The exact sequence of molecular events that lead to AD is still debated. Although β -amyloid and tau mediate toxicity through different pathways, they closely interact^[34]. Several lines of evidence thereby assign tau a subsequent but not less crucial role in disease progression^[35]. Accordingly and in contrast to APP, mutations of *tau* have only been implicated in the development of hereditary frontotemporal dementia^[36] but not AD^[37]. Furthermore, $A\beta$ is sufficient to induce tau phosphorylation^[38] and accelerates the formation of NFTs^[39] in animal models. Finally, the combination of APP and tau transgenes in mice solely exacerbate tau pathology, while $A\beta$ deposition is unchanged^[40, 41]. But as β -amyloid basically drives tau pathology, its toxic effects are mediated, at least to a certain extent, by tau^[35].

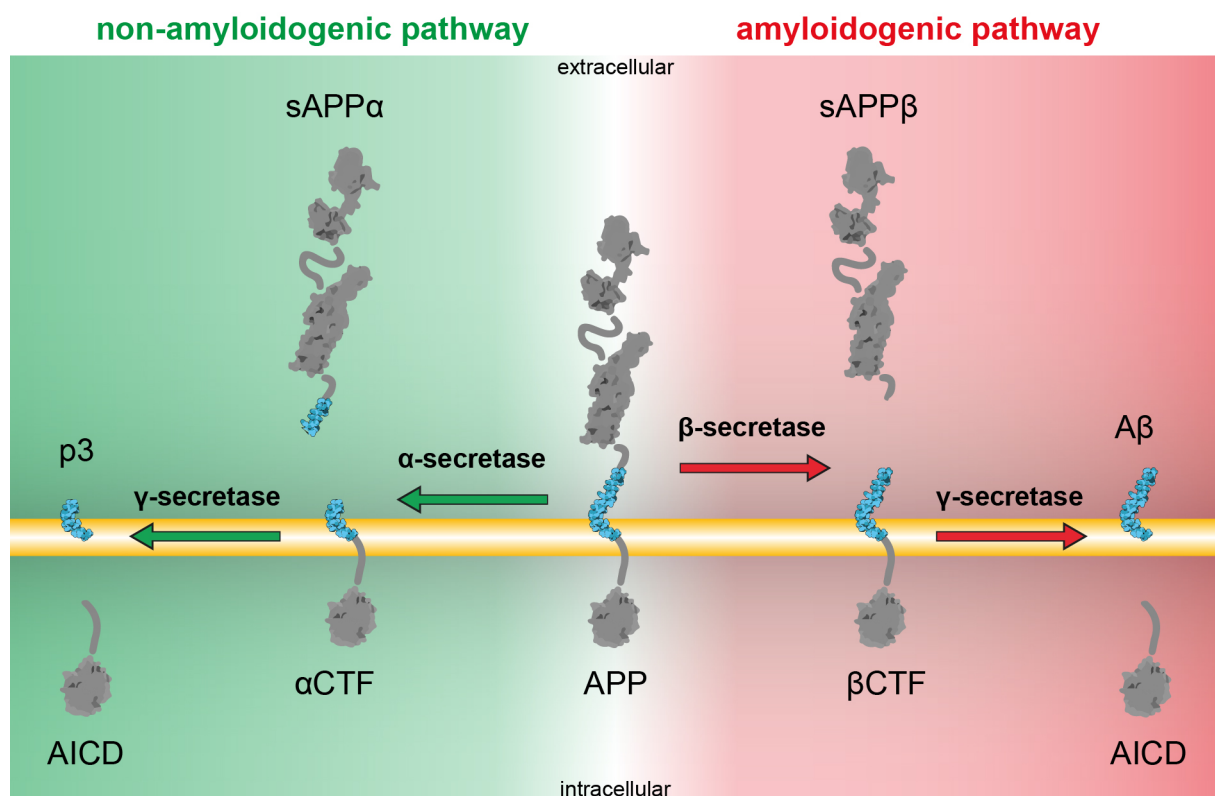


Figure 1-1: Proteolytic processing of the amyloid precursor protein.

There are two general pathways of amyloid precursor protein (APP) cleavage. The non-amyloidogenic pathway (green) prevents $A\beta$ generation by sequential α - and γ -secretase cleavage, producing sAPP α , p3 and AICD. In the amyloidogenic pathway (red), the initial β -secretase cleavage also generates two fragments, sAPP β and β CTF. The subsequent γ -secretase cleavage then releases AICD and the aggregation-prone $A\beta$ (blue). (Adapted from^[42, 43])

1.2.2 Pathology

Alzheimer's disease pathology enfold a series of biochemical and morphological changes that clinically manifest as cognitive decline and dementia^[27, 44]. The persistent neuronal death leads to brain atrophy, which progressively accelerates^[44]. The volume loss particularly affects anterior frontal lobe, inferior and lateral temporal lobe, posterior and medial parietal lobe, precuneus^[45] hippocampus^[46] and cingulate gyrus and is accompanied by ventricular enlargement^[45]. Histologically, the previously described extracellular plaques and intracellular neurofibrillary tangles are most characteristic, but their spatial and temporal development differs. The common histopathological staging of Alzheimer's disease is based on the appearance of neurofibrillary tangles, which precede plaques. NFTs occur initially in the entorhinal cortex, subsequently in the limbic system and finally also in isocortical regions^[47]. By contrast, plaques first appear in the basal proportions of frontal, temporal and occipital lobe. As the disease progresses, amyloid pathology continuously aggravates and affects isocortical association fields, while hippocampus is only mildly affected. Finally, amyloid deposits occur in all isocortical and even subcortical areas^[48]. But A β is also deposited in media and adventitia of cerebral arteries and arterioles^[49]. The cerebral amyloid angiopathy (CAA) first affects leptomeningeal vessels and continues in vessels of the neocortical grey matter and the olfactory cortex. Deposition starts thereafter in hippocampus and cerebellum and finally includes even vessels in the deep grey and white matter (reviewed in^[49]). The sustained deposition of A β in vessel walls causes thickening and loss of smooth muscle cells. The affected vessels thereby become increasingly vulnerable, as they lose their ability to adapt to blood flow changes. The final stage of CAA is characterised by vessel fragmentation, fibrinoid necrosis and aneurysm formation and thereby sets the basis for haemorrhages (reviewed in^[49]). Moreover, the accumulation of A β in vessel walls progressively impairs functionality and thereby impedes vascular elimination of A β ^[50].

The deposition of A β further leads to a sustained activation of microglia and astrocytes, which were long perceived to surround and closely associate with plaques in AD. Both cell types are complexly involved in pathogenesis and possess beneficial as well as detrimental effects (reviewed in^[51]).

The early recruitment of microglia promotes the neuroprotective clearance of A β ^[52] through extracellular and intracellular degradation^[53]. Insulin-degrading enzyme (IDE) and neprilysin (NEP) are thereby the most important proteolytic enzymes and implicated in both pathways^[53]. While extracellular degradation is accomplished by secreted and membrane-bound enzymes^[53], the intracellular pathway depends on receptor-mediated endocytosis and subsequent targeting to the lysosomal pathway^[53]. Microglial cells are able to clear soluble^[54] and fibrillary^[55] forms of A β . But as AD progresses, phagocytic and enzymatic capacity of microglial cells decreases and further accelerates deposition^[52].

On the other hand, microglial activation induces production and release of various proinflammatory and cytotoxic factors like reactive oxygen species^[56], nitric oxide^[57], tumor necrosis factor- α (TNF- α)^[58], and different interleukins^[51], which directly contribute to the pathogenesis and increase during disease progression. The importance of microglial cells is underlined by the identification of microglia-associated risk factors for AD, like *CD33* polymorphism^[51], mutations in *TREM2* or *TLR4*^[51], upregulation of *TYROBP*^[59] and downregulation or deficiency of *PGRN*^[60].

Together with microglia, activated hypertrophic astrocytes gather in the vicinity of amyloid plaques^[61]. Upon A β exposure, astrocytes similarly release various cytokines and chemokines and thereby contribute to the neuroinflammatory response^[51]. Thus, interference with inflammatory pathways ameliorated cognition and reduced plaque load^[62]. But astrocytes also degrade A β ^[63] and upregulate IDE, NEP and different matrix metalloproteinases upon A β exposure^[51]. Attenuation of the reactive gliosis therefore increased plaque load^[64], while further activation of astrocytes promoted phagocytosis and decreased plaque load^[65, 66]. In summary, astrocytes and microglial cells complexly respond to A β deposition. Their overall effect changes during disease progression from neuroprotective to destructive^[52].

1.2.3 Molecular organisation and physiological functions of APP

Although the amyloid precursor protein has a wide range of important physiological functions, it is almost exclusively perceived in the context of Alzheimer's disease. Accordingly, the *APP* gene was discovered in 1987 as precursor of the β -amyloid protein from AD^[67, 68] and not as trophic factor^[69, 70]. *APP* is located at chromosome 21^[67, 68], organised in 20 exons (Entrez Gene database^[71, 72], Gene ID: 350) and transcribed/spliced to 17 variants (Ensembl^[73], ID: ENSG00000142192). There are three major isoforms (*APP*₆₉₅, *APP*₇₅₁, *APP*₇₇₀) of which *APP*₆₉₅ is the most abundant in human cortex^[74]. These major APP variants are type I transmembrane glycoproteins^[22], with a large ectodomain and a small intracellular domain^[21] (Figure 1-2). *APP* is part of a small gene family, which further includes the two APP-like proteins *APLP1* and *APLP2*^[26, 75]. Evolutionary, APP-like proteins emerged simultaneous with early nervous systems and functional synapses and were preserved ever since^[76]. The A β sequence, however, is not well conserved and exclusive to APP^[26]. The amyloid precursor protein and its proteolytic products play important roles in various stages of neuronal development. They stimulate neural differentiation of embryonic stem cells^[77] and proliferation of neural stem^[70] and progenitor cells^[78]. *APP* and sAPP α further regulate migration of neuronal progenitor cell and promote neurite outgrowth^[78, 79]. Finally, an essential role for development and maintenance of peripheral and central synapses^[80, 81] and dendritic spines^[82] is assigned to APP. The sum of functions provided by *APP* gene family is literally vital. In *Caenorhabditis elegans* with a single APP-related

gene, a knock-out is lethal^[78]. In higher organisms, the APP paralogues seem functionally redundant to a certain extent^[76] and a single knockout of either *APP*, *APLP1* or *ALPL2* is not fatal^[78].

1.2.4 Sporadic and inherited disease variants

According to the amyloid hypothesis, Alzheimer's disease is caused by the imbalance of A β production and clearance^[83]. In sporadic AD, decreased clearance^[83] was found to be the major contributor, while production was unchanged^[84]. A β clearance thereby refers to the sum of several elimination pathways, which can be attributed to two fundamental mechanisms, (i) proteolytic degradation or (ii) elimination by transport. As previously described, A β is extracellularly degraded by several secreted and membrane-bound proteases. Intracellularly, endocytosed A β is mainly degraded in endo- and lysosomes, while generated membrane-associated A β can additionally be degraded in endoplasmic reticulum, mitochondria and cytosol (reviewed in^[85]). Degradation of A β physiologically operates at its functional capacity and decreases age-dependently^[85]. Secondly, A β is eliminated by active and passive transport through the brain barriers for instance by the low density lipoprotein receptor-related protein 1 (LRP1)^[86] and different ATP-binding cassette transporters like ABCB1^[87] and ABCC1^[88]. As A β removal decreases age-dependently, the activation of transport processes was suggested to reduce the cortical amyloid load^[89]. This strategy has conceptionally already been proved for LRP1^[90], ABCB1^[90, 91] and ABCC1^[88, 92].

Another and far less frequent cause for developing AD are inheritable mutations. Although their effects are heterogeneous, they generally affect either production or aggregation propensity of A β ^[93]. A sum of 231 disease-causing mutations has been identified so far^[37]. These mutations affect only three genes, namely *APP* (33 mutations), *PSEN1* (185 mutations) and *PSEN2* (13 mutations)^[37, 94]. As PS1 and PS2 are part of the γ -secretase complex (section 1.2.1), mutations either enhance A β production or increase the A β_{42} /A β_{40} ratio (reviewed in^[93, 94]).

Mutations in the *APP* gene have different effects, depending on their specific localisation^[93] (Figure 1-2). The Swedish *APP* mutation [KN670/671ML] is a double substitution flanking the C-terminus of A β , which affects the β -secretase cleavage^[95]. It increases A β production two to threefold^[93] while leaving A β sequence and A β_{42} /A β_{40} ratio unchanged^[96, 97]. An extra copy of APP likewise increases A β levels and initiates the inevitable cascade of neuropathological changes in certain forms of familial AD^[98, 99] and trisomy 21^[100] (Down's syndrome). *APP* mutations at the C-terminus of the A β sequence affect γ -secretase cleavage^[93] and thus increase A β_{42} level and A β_{42} /A β_{40} ratio^[93]. Mutations within the A β sequence and a certain distance to cleavage sites elevate the A β accumulation rather by raising aggregation propensity than increasing amount or A β_{42} /A β_{40} ratio^[101]. Expedited aggregation is apparent in English [H677R]^[102, 103], Tottori [D678N]^[102, 103], Taiwanese [D678H]^[104, 105], Dutch [E692Q]^[106], Arctic [E693G]^[101], Osaka [E693 Δ]^[107], and Iowa [D694N]^[106] *APP* mutations.

1.3 Disease models

The discovery of *APP* and the various mutations of *APP*, *PSEN1* and *PSEN2* not only inspired the development of the amyloid hypothesis but also created the prerequisites for the generation of animal disease models. Alzheimer's disease is a complex disorder, virtually involving and influencing every aspect of the brain's physiology. However, the methodological and temporal limitations of exploring aetiology and pathogenesis in humans made it necessary to develop appropriate animal disease models. These models largely drove understanding of the disease as well as the development of therapeutic strategies. Thus far, animal models are unable to reproduce the full spectrum of pathological changes observed in AD. The generated models are therefore commonly judged on reproducing the characteristic histopathological features (plaques, tangles, gliosis, neuronal loss) and the main symptom of memory loss^[111]. Due to their many advantages, rodents are the most commonly used species in basic research^[112]. Unfortunately, they naturally develop none of the characteristic changes of AD^[113], a constraint that has been resolved by inducing pathology through genetic manipulation or injection of toxins^[111].

1.3.1 Transgenic animals expressing wild-type APP

After identifying the origin of A β in 1987^[67, 68], first attempts to reproduce the cortical amyloidosis and related histopathological and cognitive characteristics in mice were published in 1991^[114-117]. To resemble the differences in mRNA expression which have been reported for AD^[118-120], human wild-type APP₇₅₁ was expressed by rat neuron-specific enolase (NSE) promoter in mice, creating an imbalance of the most abundant isoforms, APP₆₉₅ and APP₇₅₁^[114]. Although extracellular deposits were apparent^[114, 121], modified Bielschowsky silver impregnation and thioflavin S (ThS) stains were rarely positive and Congo red positive aggregates were not present^[121]. The deposits have been suspected unspecific^[122], and animals have lately been described to develop diffuse^[123, 124], preamyloid^[124] deposits but no plaques^[123].

Virtually simultaneously, a second murine model was presented, using the human APP promoter to express a sequence encoding the A β peptide^[115]. The initially described amyloid-like deposits were later revealed unspecific, as they were also present in non-transgenic animals^[122].

Based on the discovery, that the 100 C-terminal amino acids contain the A β sequence^[125], C-terminal APP fragments were expressed in mice using either JC viral early region^[116] or brain dystrophin^[126] promoters. But despite higher expression of A β , mice did not show extracellular aggregates of A β ^[116, 126-128].

The first murine model that manifested with thioflavin S positive, dense-core amyloid plaques, neurofibrillary tangles and neuronal loss used a C-terminal APP fragment and the human Thy1-promoter for expression^[129]. These mice seemed a major breakthrough for the next four months,

until the study was retracted^[130] as histopathological findings were not reproducible^[131]. The expression of APP₆₉₅ using the metallothionine IIA promoter also failed to induce plaque deposition^[117, 128].

To better recreate the human situation in terms of spatial and temporal expression patterns and splice variants, the entire and unarranged human APP gene was introduced into mice^[127, 132, 133]. Although mice expressed all of the most abundant human APP isoforms (APP₆₉₅, APP₇₅₁, APP₇₇₀) at a level similar to endogenous murine transcripts^[127, 132], plaque deposition was not evident^[128].

In sum, none of these early models mimicked the characteristic features of AD^[69, 122, 127, 128, 134] and the missing deposition of A β even indicated a certain physiologic protection against its aggregation. These drawbacks were mainly attributed to insufficient transgene expression and the genetic background of mice^[128], but raised the question if mice are generally capable of reproducing an AD-like pathology^[121].

1.3.2 Disease models expressing mutant transgenes

The discovery of point mutations strongly associated with early onset AD^[135] entailed the generation of animal models with mutant transgenes. In 1994, the first models were described^[69] which expressed the London mutant [V717I]^[136, 137] variant of APP₆₉₅ or APP₇₅₁ under control of the rat NSE promoter^[69]. Nevertheless, the neuronal overexpression of mutant APP did not provoke amyloid deposition or neurodegeneration^[69].

In 1995, Games et al. presented the transgenic PDAPP mice^[134]. Here, the platelet-derived growth factor- β (PDGF) promoter drives the expression of Indiana mutant [V717F]^[138] cDNA^[134] of APP. The PDAPP mice exhibit thioflavin S positive plaques, astro- and microgliosis and synaptic loss^[134]. Moreover, impairments in spatial memory (water maze^[139]) working memory (radial arm maze^[140]) and cognition (novel object recognition task^[140]) preceded the appearance of plaques^[139, 140].

A still very common strain was introduced in 1996 by Hsiao et. al.^[141]. The Tg2576 mice fivefold overexpress Swedish mutant [KM670/671NL]^[142] APP₆₉₅ under the control of the prion protein (PrP) promoter^[141]. These mice display dense, thioflavin S and Congo red positive deposits^[141], spine loss, hippocampal LTP impairment and a distinct astro- and microgliosis^[143]. Tg2576 mice have deficits in learning and memory (water maze^[141], Y-maze^[141, 144] and passive avoidance task^[144]) and cognition (novel object recognition task^[145]). Disease progression is relatively slow in Tg2576 mice, as first memory deficits occur about six months of age^[146] and amyloid plaques emerge between nine and twelve months^[141, 146, 147]. To accelerate pathology and increase A β ₄₂ production^[148], Tg2576 animals were crossed with mice expressing mutant PS1 (M146L)^[147]. In these double transgenic mice, plaques and behavioural changes already appeared at an age of three to four months^[147].

In contrast to *APP* mutations, the expression of AD-causing, mutant presenilin failed to induce plaque deposition in mice (reviewed in^[149]). But $A\beta_{42}$ levels and $A\beta_{42}/A\beta_{40}$ ratios were consistently elevated in different mutant PS1 and PS2 transgenic mice^[148, 149].

Interestingly, the second prominent histopathological hallmark of AD, intracellular neurofibrillary tangles, was not evident in any of the APP transgenic mice. Despite their joint appearance in AD, mutations of tau are only linked to frontotemporal dementia^[36] but not to AD^[37]. Consequently, expression of mutant tau, either alone^[150-152] or in combination with PS1^[153], was not sufficient to induce plaque deposition.

To reproduce both pathological features in mice, 3xTg-AD mice were generated^[153]. These mice express the Swedish APP₆₉₅ variant [KM670/671NL] and mutant tau [P301L], both controlled by the Thy1.2-promoter^[153] and mutant PS1 [M146V] by its endogenous promoter^[154]. 3xTg-AD mice present with extracellular $A\beta$ deposits at six and hippocampal tau pathology at twelve months of age^[153]. Impairments in synaptic plasticity (LTP^[153, 155]), spatial memory (Barnes maze^[156], Morris water maze^[155]) and working memory (8-arm radial maze^[157]) are also apparent in 3xTg-AD mice. However, intracellular $A\beta$ aggregation in 3xTg-AD mice has been questioned^[158] by a controversial and already retracted^[159] study. Moreover, one author of the initial study recently reported the phenotype was not complying with the initially described observations in males^[160].

All these results demonstrate that high levels of the aggregation-prone human $A\beta$ are necessary to induce deposition and associated symptoms in mice. Most of the current murine models therefore combine strong expression by specific promoters, mutant transgenes and vulnerable background strains. However, the heterogeneity of the utilised promoters, transgenes and background strains in these models make the originating phenotypes extremely variable. Overall, the PDGF-, Thy1- and PrP-promoters, the APP₆₉₅ isoform with the Swedish double mutation, and the C57BL/6, 129, FVB/N and DBA strains are most commonly used for the generation of murine disease models^[161]. Almost all of these 'common' AD mouse models simultaneously express the corresponding murine proteins. But, as overexpression of mutant human APP, PS1 and tau reliably provoke the desired phenotype, interactions between transgenic and endogenous proteins have rarely been addressed.

1.3.3 Advanced and natural models

To eliminate potential interactions with endogenous proteins, animals expressing human transgenes can be combined with appropriate knockout models. This approach has been previously described for tau^[162], whereby human tau transgenic^[163] and murine tau-deficient^[164] mice were crossed to create a model exclusively expressing human tau^[162]. These mice showed intracellular aggregates of tau^[162, 165, 166] consisting of paired helical filaments^[162], which are similar to the early 'pre-tangle stage' in humans^[162]. The tau pathology was accompanied by impairments in learning and memory

(Morris water maze^[165, 167], Y-maze^[167]), cognition (novel object recognition task^[165, 167]), synaptic plasticity (hippocampal LTP^[165]) and even neuronal loss^[167]. By contrast, these pathological signs were not apparent in mice that additionally expressed murine tau^[162]. The cause of this aggregation-preventing effect is still unclear^[168]. Although murine tau is known to have a lower aggregation propensity^[168], it was shown to co-aggregate with human tau^[169].

Mice expressing human APP in the absence of endogenous murine APP have also been previously described and were generated by crossing transgenic and knockout mice^[170, 171]. APP23 mice^[170, 171] (expressing mutant [KM670/671NL] APP₇₅₁ controlled by the Thy1-promoter^[172]) and APP/PS1 mice^[171] (expressing mutant [KM670/671NL] APP₇₅₁ and mutant PS1 [L166P] both controlled by the Thy1-promoter^[173]) were used for providing the human APP transgenes. The elimination of murine APP in transgenic mice was initially described to affect neither A β deposition nor cerebral amyloid angiopathy (CAA)^[170]. But that conclusion was very recently questioned by Mahler et al., who reported an increase in cortical plaque load and CAA by eliminating endogenous APP in certain transgenic models^[171].

Animals that physiologically reproduce certain characteristics of AD are potential alternatives for transgenic models. Several mammalian species naturally develop histopathological changes, similar to those of AD patients. Amyloid β deposits have been described in primates (gray mouse lemur (*Microcebus murinus*)^[174], rhesus monkey (*Macaca mulatta*)^[175], hamadryas baboon (*Papio hamadryas*)^[175]), carnivorans (dog (*Canis lupus familiaris*)^[176, 177], polar bear (*Ursus maritimus*)^[177], california sea lion (*Zalophus californianus*)^[176], american black bear (*Ursus americanus*)^[176], tsushima leopard cat (*Prionailurus bengalensis euptilurus*)^[176], cheetah (*Acinonyx jubatus*)^[176]), bovids (sheep (*Ovis aries*)^[178]) and even-toed ungulates (Bactrian camel (*Camelus bactrianus*)^[179]). Interestingly, what these animals have in common (so far sequenced), is the human identical A β segment in their APP gene^[180] (see Table 7-1). But beyond the identical A β sequence, progression and characteristics significantly differ from the human disease. However, due to numerous impediments, these animals are not well suited for research. The main hindrances are their body size and the slow disease progression.

Rodents, however, are an ideal research model as they combine the benefits of mammalian models in terms of anatomy, physiology and genetics with a short generation time and an accelerated lifespan. Since mice, as rodent archetype, do not naturally develop AD pathology^[113], the same has been concluded for all rodents, regardless of the apparent differences.

The small, South American rodent *Octodon degus* (degu) has recently been described to 'naturally develop a full range of AD-like pathologies including A β plaques and neurofibrillary tangles'^[181]. Thus, degus were the first rodents described developing amyloid plaques and NFTs without genetic modification. Two specific properties likely make degus particularly susceptible for developing

AD-like symptoms, (i) their high average lifespan of up to ten years in captivity, which is considered equivalent to 120 human years^[182] and (ii) the high sequence homology to human APP, with only one amino acid variation in A β ^[182] (Figure 1-3). Degus manifest with a profound number of age-dependent changes, including prominent intra- and extracellular, thioflavin S positive deposits of A β in entorhinal cortex, hippocampus and even frontal and parietal cortex^[183]. Thioflavin S positive plaques rapidly develop and are already apparent at twelve months of age^[183]. A β deposition was accompanied by intracellular aggregation of phosphorylated tau^[182, 183] and pronounced astrogliosis^[182]. Degus showed further age-dependent deficits in memory, cognition and synaptic plasticity (determined by LTP measurement, T-maze and novel object recognition task)^[183]. The degu is a quite new model and first results were very promising, but studies employing degus are still rare and the obtained results are sparse and not consistent. Additional research is therefore urgently needed to elucidate the physiological processes during natural aging of degus.

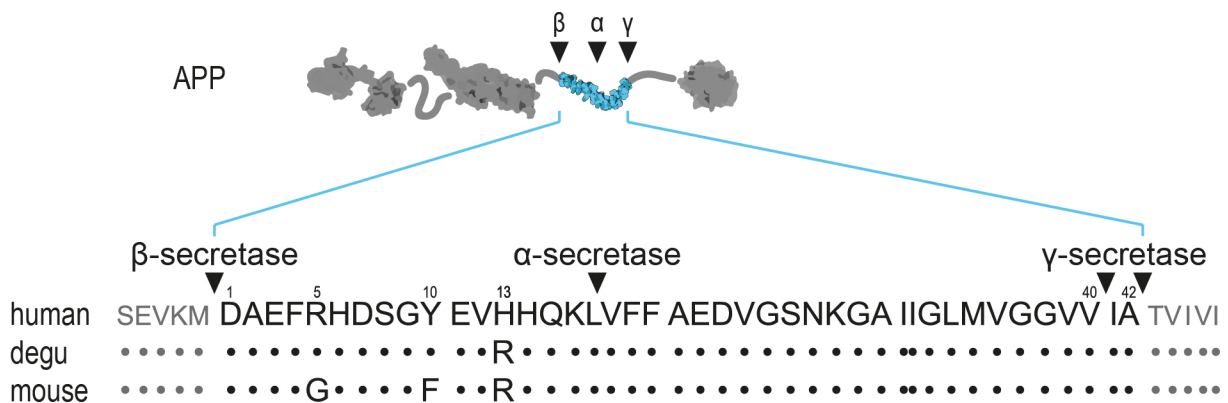


Figure 1-3: Species-dependent differences in the β -amyloid sequence.

The alignment of human, degu and murine A β sequence reveals the species-dependent differences at the molecular level. While mice have three amino acid variations (positions 5, 10 and 13), degus possess only the histidine to arginine substitution at position 13. (Adapted from^[43, 182]).

2 Motivation and aims

Alzheimer's disease is one of the greatest future socio-economic challenges with the demographic development as its major driving force. Various animal models have been generated to gain a better understanding and develop treatment strategies against this complex disease. The major breakthrough in resembling AD pathology in animals was achieved by expressing mutant APP and presenilin variants. Although they separately mimic only individual aspects, animal models have substantially contributed to the current understanding of Alzheimer's disease.

Virtually all of the utilised transgenic models still co-express the corresponding endogenous proteins. Potential interactions between endogenous and transgenic proteins have rarely been considered, as strong overexpression ensured the desired phenotype. Nevertheless, there are still many differences between AD and its reproduction in animal models, for instance the necessity of strong overexpression of A β to induce plaque deposition or the missing causal link between plaques and neurofibrillary tangles. Strategies for refinement of current models, to reproduce more comprehensive and physiologic phenotypes, would therefore be highly appreciated.

This study was performed to elucidate the effects of murine APP co-expression in an established transgenic model of cortical amyloidosis. With special regard to A β deposition in brain parenchyma and blood vessels and cellular response, the following questions arose:

- I. Can endogenous murine APP relevantly affect the deposition of A β in transgenic models of AD and, if so, is additional co-expression deteriorating or ameliorating A β accumulation?
- II. Does murine APP influence general A β aggregation propensity and affect the balance between soluble and insoluble amyloid or parenchymal plaque deposition and cerebral amyloid angiopathy?
- III. Can murine APP expression alter the microglial and astrocytic response to A β deposition?

The second part of this study dealt with the small rodent *Octodon degus*, 'the new face of sporadic Alzheimer's research?'^[184]. A large variety of histological analyses was conducted to assess quality and quantity of neurodegenerative changes that naturally occur in aging degus. The central question was:

- IV. Are degus a convenient model of Alzheimer's disease and which histopathological features of AD do they reproduce?

3 Material and methods

3.1 Material

3.1.1 Chemicals

Substance	Supplier	Catalog number
1 kb DNA ladder	Bioron GmbH, Germany	305105
100 bp plus DNA ladder	Bioron GmbH, Germany	304105
2-Mercaptoethanol	Carl Roth GmbH & Co. KG, Germany	4227.3
Acetic acid	Carl Roth GmbH & Co. KG, Germany	T179.1
Acrylamid/Bisacrylamid-solution	Carl Roth GmbH & Co. KG, Germany	A124.2
Ammonium nitrate (NH ₄ NO ₃)	Carl Roth GmbH & Co. KG, Germany	X988.1
Ammonium persulfate (APS)	Carl Roth GmbH & Co. KG, Germany	9592.2
Bond™ dewax solution	Leica Biosystems Nussloch GmbH, Germany	AR9222
Bond™ primary antibody diluent	Leica Biosystems Nussloch GmbH, Germany	AR9352
Bond™ wash solution 10X concentrate	Leica Biosystems Nussloch GmbH, Germany	AR9590
Cresol red	Sigma-Aldrich Co. LLC., USA	114472
D(+)-Sucrose	Carl Roth GmbH & Co. KG, Germany	4621.1
Disodium hydrogen phosphate (Na ₂ HPO ₄)	Carl Roth GmbH & Co. KG, Germany	P030.2
EDTA	Zentralapotheke, Universität Rostock, Germany	34070720
Eosin Y	Medite GmbH, Germany	41-5141-00
Ethanol	Zentralapotheke, Universität Rostock, Germany	23210271
Ethidium bromide	Carl Roth GmbH & Co. KG, Germany	2218.1
Formaldehyde solution 37%	Carl Roth GmbH & Co. KG, Germany	7398.1
Glycine	Zentralapotheke, Universität Rostock, Germany	34040290
Guanidine hydrochloride	Sigma-Aldrich Co. LLC., USA	G4505
Hematoxylin (Harris/Gill II)	Medite GmbH, Germany	41-5136-00
Hydrochloric acid (HCl)	Merck KGaA, Germany	1003171000
Igepal® CA-630	Sigma-Aldrich Co. LLC., USA	I8896
Kaiser's glycerol gelatine	Merck KGaA, Germany	109242
Magnesium chloride (MgCl ₂)	Carl Roth GmbH & Co. KG, Germany	3532.1
Methanol	VWR International, USA	20903.368
PageRuler Plus Prestained Protein Ladder	Thermo Fisher Scientific Inc., USA	26620
Paraformaldehyde	Carl Roth GmbH & Co. KG, Germany	0335.4
Pertex® mounting medium	Leica Biosystems Nussloch GmbH, Germany	3808706E
Potassium carbonate (K ₂ CO ₃)	Carl Roth GmbH & Co. KG, Germany	P743.2
Potassium chloride (KCl)	Carl Roth GmbH & Co. KG, Germany	P017.2
Potassium dihydrogen phosphate (KH ₂ PO ₄)	Merck KGaA, Germany	3904.2
Protease inhibitors (Complete-mini)	Roche Diagnostics GmbH, Germany	11836153001
Proteinase K solution	AppliChem GmbH, Germany	A4392
Pyridine	Carl Roth GmbH & Co. KG, Germany	CP07.1
RNAlater®	Sigma-Aldrich Co. LLC., USA	R0901
Rockland blocking buffer	Biomol GmbH, Germany	MB-070-003
Silver nitrate (AgNO ₃)	Carl Roth GmbH & Co. KG, Germany	6207.1
Sodium acetate (C ₂ H ₃ NaO ₂)	Carl Roth GmbH & Co. KG, Germany	6773.2
Sodium carbonate (Na ₂ CO ₃)	Carl Roth GmbH & Co. KG, Germany	A135.2
Sodium chloride (NaCl)	Carl Roth GmbH & Co. KG, Germany	3957.1
Sodium dodecyl sulfate (SDS)	Carl Roth GmbH & Co. KG, Germany	CN30.3
Tetramethylethylenediamine (TEMED)	Carl Roth GmbH & Co. KG, Germany	2367.3
Thioflavin T	Sigma-Aldrich Co. LLC., USA	T3516-25G
Tris	Carl Roth GmbH & Co. KG, Germany	4855.1
Tungstosilicic acid (H ₄ [W ₁₂ SiO ₄₀])	Merck KGaA, Germany	1006590025
Tween 20 (polysorbate 20)	Carl Roth GmbH & Co. KG, Germany	9127.2

3.1.2 Kits

Name	Supplier	Catalog number
Bond Enzyme Pretreatment Kit	Leica Biosystems Nussloch GmbH, Germany	AR9551
Bond Polymer Refine Detection	Leica Biosystems Nussloch GmbH, Germany	DS9800
Bond Polymer Refine Red Detection	Leica Biosystems Nussloch GmbH, Germany	DS9390
Bond™ Epitope Retrieval 1	Leica Biosystems Nussloch GmbH, Germany	AR9961
dNTP-Set	Steinbrenner Laborsysteme GmbH, Germany	SL-Set-M-dNTPs
Pierce™ BCA protein assay	Thermo Fisher Scientific Inc., USA	23225
V-PLEX Aβ42 Peptide (4G8)	Meso Scale Diagnostics, LLC., USA	K150SLE-1

3.1.3 Antibodies

Name	Supplier	Catalog number
Anti-ADAM10	Abcam plc., UK	ab1997
Anti-BACE1	Abcam plc., UK	ab2077
Anti-caspase-3	Cell Signaling Technology Inc., USA	9662
Anti-caspase-9	Cell Signaling Technology Inc., USA	9504
Anti-GFAP	Dako Deutschland GmbH, Germany	Z033401
Anti-IBA1	Wako Chemicals, Germany	019-19741
Anti-Insulin-degrading enzyme	Abcam plc., UK	ab32216
Anti-NeuN	Millipore, Germany	MAB377
Anti-tau AT100	Thermo Scientific, Germany	MN1060
Anti-tau AT180	Thermo Scientific, Germany	MN1040
Anti-tau AT8	Thermo Scientific, Germany	MN1020
Anti-β-actin, clone AC-15	Sigma-Aldrich Co. LLC., USA	A1978
Anti-β-Amyloid, clone 4G8	HISS-DX, Germany	SIG-39220
Anti-β-Amyloid, clone 6E10	Covance Inc., Germany	SIG-39320
Anti-β-Amyloid, clone 6F3D	Dako Deutschland GmbH, Germany	M0872
IRDye® 680LT Goat anti-Mouse IgG (H + L)	LI-COR Biosciences – GmbH, Germany	925-68020
IRDye® 800CW Goat anti-Rabbit IgG (H + L)	LI-COR Biosciences – GmbH, Germany	925-32211

3.1.4 Primers

Target	Name	Direction	Sequence
β-actin ^[185]	N 278	forward	5'-CCT CAT GAA GAT CCT GAC CG-3'
	N 279	reverse	5'-GCA CTG TGT TGG CAT AGA GG-3'
APP/PS1 transgene ^[173]	N 205	forward	5'-GAA TTC CGA CAT GAC TCA GG-3'
	N 206	reverse	5'-GTT CTG CTG CAT CTT GGA CA-3'
Murine APP ^[186]	N 135	forward	5'-AGA GCA CCG GGA GCA GAG-3'
	N 136	reverse	5'-AGC AGG AGC AGT GCC AAG-3'
Neomycin resistance gene ^[187]	N 227	forward	5'-TGT CAA GAC CGA CCT GTC CG-3'
	N 228	reverse	5'-TAT TCG GCA AGC AGG CAT CG-3'

3.1.5 Animal feed

Name	Supplier	Catalog number
M-Z Ereich	ssniff Spezialdiäten GmbH, Germany	V1185-0
R/M-H	ssniff Spezialdiäten GmbH, Germany	V1535-0

3.1.6 Equipment

Device	Company
Analytik scale	Sartorius AG, Germany
BOND-III autostainer	Leica Microsystems GmbH, Germany
Dewar vessel	Karlsruher Glastechnisches Werk - Schieder GmbH, Germany
Eppendorf Research® pipettes	Eppendorf AG, Germany
Eppendorf Research® plus pipettes	Eppendorf AG, Germany
EV231 power supply	PEQLAB Biotechnologie GmbH, Germany
Freezer -20 °C	Gorenje Vertriebs GmbH, Germany
Freezer -80 °C	Kryotec-Kryosafe GmbH, Germany
Histokinette STP 120	Microm International GmbH, Germany
Leica EG 1160 embedding center	Leica Microsystems GmbH, Germany
Li-Cor Odyssey infrared imaging system	LI-COR Biosciences – GmbH, Germany
LSM 700	Carl Zeiss Imaging Solutions GmbH, Germany
MESO QuickPlex SQ 120	Meso Scale Diagnostics, LLC., USA
Pannoramic MIDI	3DHISTECH Ltd., Hungary
Paradigm™ detection platform	Molecular Devices, LLC., USA
Refrigerator	Liebherr-Hausgeräte GmbH, Germany
RM 2155 microtome	Leica Microsystems GmbH, Germany
Scandrop spectrophotometer	Analytik Jena AG, Germany
SpeedMill PLUS homogenisator	Analytik Jena AG, Germany
Thermoshaker	EuroClone S.p.A., Italy
TPersonal thermocycler	Analytik Jena AG, Germany
TProfessional thermocycler	Analytik Jena AG, Germany
Universal 320R centrifuge	Andreas Hettich GmbH & Co.KG, Germany
UVsolo TS	Analytik Jena AG, Germany
VTX-3000L Vortex	LMS Consult GmbH & Co. KG, Germany

3.1.7 Buffers and solutions

12% polyacrylamid separation gel

0.375 M Tris, 40% (v/v) acrylamid/bisacrylamid-solution (30 %; 29:1), 0.1% (w/v) SDS, 0.1% (w/v) APS, 0.1% (v/v) TEMED

4% buffered paraformaldehyde solution

4% (w/v) paraformaldehyde, 137 mM NaCl, 10 mM Na₂HPO₄, 2.7 mM KCl, 1.8 mM KH₂PO₄, pH 6.9

5 M guanidine buffer

5 M guanidine hydrochloride, 50 mM Tris, pH 8.0

5% polyacrylamid stacking gel

0.125 M Tris, 16,7% (v/v) acrylamid/bisacrylamid-solution (30 %; 29:1), 0.1% (w/v) SDS, 0.1% (w/v) APS, 0.1% (v/v) TEMED

8.2 M guanidine buffer

8.2 M guanidine hydrochloride, 82 mM Tris, pH 8.0

Acetate buffer

33.6 mM sodium acetate, 14.4 mM acetic acid, pH 4.99

Carbonate buffer

100 mM Na₂CO₃, 50 mM NaCl, protease inhibitors (1 tablet/10 mL), pH 11.5

Citric acid buffer pH 6.0

10 mM citric acid, 0.05% (v/v) polysorbate 20, pH 6.0

Developer solution

236 mM Na₂CO₃, 12.5 mM NH₄NO₃, 5.9 mM AgNO₃, 1.7 mM H₄[W₁₂SiO₄₀], 0.87 mM formaldehyde

DNA extraction buffer

1 M KCl, 10 mM Tris, > 3.6 mAnsonU/mL proteinase K, 0.4% (v/v) Igepal® CA-630, 0.4% (v/v) polysorbate 20, pH 9.0

EDTA buffer pH 9.0

1 mM EDTA, 0.05% (v/v) polysorbate 20, pH 9.0

Electrophoresis buffer

192 mM glycine, 25 mM Tris, 0.1% (w/v) SDS

PAGE transfer buffer

192 mM glycine, 25 mM Tris, 20% (v/v) methanol

Phosphate buffered saline (PBS)

137 mM NaCl, 10 mM Na₂HPO₄, 2.7 mM KCl, 1.8 mM KH₂PO₄, pH 7.4

Protein sample buffer

200 mM Tris, 40% (v/v) glycerine, 16% (w/v) SDS, 4% (v/v) 2-mercaptoethanol

RIPA buffer

150 mM NaCl, 50 mM Tris, 1% (v/v) Igepal® CA-630, 1% (v/v) SDS, 0.5% (w/v) sodium deoxycholate, protease inhibitors (1 tablet/10 mL), pH 8.0

Silver-pyridine-carbonate solution

14% (v/v) pyridine, 0.49% (w/v) silver nitrate, 0.37% (w/v) potassium carbonate

Taq PCR master mix

100 mM KCl, 20 mM Tris, 1.5 mM MgCl₂, 0.4 mM dATP, 0.4 mM dCTP, 0.4 mM dGTP, 0.4 mM dTTP, 0.2 mM cresol red, 50 U/mL Taq DNA polymerase, 10% (w/v) sucrose, 0.08% (v/v) Igepal® CA-630, 0.08% (v/v) polysorbate 20, pH 8.6

Tris acetate EDTA buffer (TAE)

40 mM Tris, 20 mM acetic acid, 1 mM EDTA, pH 8.4

Tris buffered saline Tween20 (TBST)

50 mM Tris, 150 mM NaCl, 1% (v/v) polysorbate 20, pH 7.5

Tris buffered saline (TBS)

50 mM Tris, 150 mM NaCl, pH 7.5

3.1.8 Software

Name	Developer
AxioVision 4.8.1.0	Carl Zeiss Imaging Solutions GmbH, Germany
Endnote X6	Thomson Reuters Corp., USA
GraphPad Prism 6.01	GraphPad Software Inc., USA
ImageJ 1.48v	Wayne Rasband, National Institutes of Health, USA
Microsoft Office 14.0	Microsoft Corporation, USA
Pannoramic Viewer 1.15.4	3DHISTECH Ltd., Hungary
Adobe Creative Suite	Adobe Systems Inc., USA
ITCN Plug-in	Thomas Kuo and Jiyun Byun, University of California, USA

3.2 Methods

3.2.1 Animal models

Inbred C57BL/6J mice provided the genetic background of all analysed mice and were purchased from the Jackson Laboratory (C57BL/6J, #000664).

3.2.1.1 APP-deficient mice

APP knockout mice were purchased as congenic strain in the C57BL/6J genetic background from the Jackson Laboratory (B6.129S7-Apptm1Dbo/J, #004133). APP-deficiency was introduced by replacing the promoter and first exon of murine APP with a neomycin resistance cassette in AB2.1 ES cells^[188].

3.2.1.2 APP/PS1 transgenic mice

Transgenic C57BL/6J mice harbouring two mutant human transgenes, amyloid precursor protein [KM670/671NL] and presenilin 1 [L166P] both driven by the murine Thy1.2-promoter^[173] (B6-Tg(Thy1-APP^{swe}; Thy1-PS1 L166P)) were used as model for cortical amyloidosis. Expression by Thy1.2-promoter starts postnatal^[189] in various neuronal cells (reviewed in^[190]) including cortical and hippocampal neurons^[189, 191]. Mice are referred to as APP/PS1 and were kindly provided by M. Herzig, R. Radde and M. Jucker (University of Tübingen, Germany). As homozygous mice have a reduced viability due to excessive transgene expression, only heterozygous APP/PS1 mice were used for experiments. For breeding, heterozygous males (APP/PS1^{+/-}) were throughout mated with female C57BL/6J mice. APP/PS1 transgenic mice (APP/PS1^{+/-}) naturally expressing the murine APP gene were used as controls for experiments and are referred to as mAPP^{+/+}.

3.2.1.3 Combined murine APP-deficient and APP/PS1 transgenic mice

To induce cortical amyloidosis in APP-deficient mice (B6.129S7-Apptm1Dbo/J), homozygous females were mated with heterozygous male APP/PS1 mice. First generation male offspring with desired genotype (B6-Apptm1Dbo^{+/-}-Tg(Thy1-APP^{swe}; Thy1-PS1 L166P)^{+/-}) were again mated with female homozygous APP-deficient mice. Second generation offspring males harbouring the required genotype (B6-Apptm1Dbo^{+/-}-Tg(Thy1-APP^{swe}; Thy1-PS1 L166P)^{+/-}) were used for further breeding. Murine APP-deficient mice with human APP/PS1 transgene (B6-Apptm1Dbo^{+/-}-Tg(Thy1-APP^{swe}; Thy1-PS1 L166P)^{+/-}) were used for experiments and are referred to as mAPP^{0/0}.

3.2.1.4 Degus

Wild-type degus (*Octodon degus*) for the respective experiments were provided by A. K. Braun (Institute of biology, Otto von Guericke-University, Magdeburg).

3.2.2 Animal husbandry

All mice were bred in the animal care facility of the Neurodegeneration Research Lab (Otto von Guericke-University, Magdeburg). Degus were bred at the animal care facility of the Institute of Biology (Otto von Guericke-University, Magdeburg). Animals were housed in a 12 h/12 h light/dark cycle at 22 °C with free access to food and water. All experiments were conducted according to the European Union and state law of the government of Saxony-Anhalt and were approved by the local animal ethics committee.

3.2.3 Genotyping

Animals were genotyped, as far as necessary, to determine actual genetic status of transgenes and targeted mutations and to monitor breeding procedures.

3.2.3.1 DNA extraction

Samples for genotyping were obtained from mice upon 20 d of age. The tail tip was cut off and digested overnight in DNA extraction buffer at 55 °C under vigorous agitation. Proteinase K was then inactivated by incubation at 95 °C for 30 min. Samples were subsequently centrifuged (20,000 g, 15 min, 4 °C) to remove debris and finally stored at 4 °C until further use.

3.2.3.2 Polymerase chain reaction

To determine genetic status, presence of indicative DNA sequences was qualitatively evaluated by amplification using polymerase chain reaction (PCR). Reaction was performed using DNA samples, Taq PCR master mix and the specific primers (see Table 3-1, Table 3-2). Amplification was achieved using a thermocycler (Table 3-3).

Table 3-1: PCR reaction mix for detection of APP/PS1-transgene.

	Stock concentration in pmol/μl	Final concentration in pmol/μl	Volume in μl
H ₂ O			3.520
Taq PCR master mix			5.500
Primer N 205	10	0.450	0.495
Primer N 206	10	0.450	0.495
Primer N 278	10	0.450	0.495
Primer N 279	10	0.450	0.495
PCR master mix			11.00
DNA			1.000
Reaction mix			12.00

Table 3-2: PCR reaction mix for detection of murine APP knock-out.

	Stock concentration in pmol/ μ l	Final concentration in pmol/ μ l	Volume in μ l
H ₂ O			3.740
Taq PCR master mix			5.500
Primer N 135	10	0.40	0.440
Primer N 136	10	0.40	0.440
Primer N 227	10	0.40	0.440
Primer N 228	10	0.40	0.440
PCR master mix			11.00
DNA			1.000
Reaction mix			12.00

Table 3-3: Thermocycler protocol for DNA amplification.

Step	Temperature	Duration	Number of cycles
Initial denaturation	95 °C	5 min	
Denaturation	95 °C	45 s	35
Annealing	62 °C	60 s	
Elongation	72 °C	90 s	
Final elongation	72 °C	5 min	
Storage	4 °C	∞	

3.2.3.3 Agarose gel electrophoresis

10 μ l amplificate were used for electrophoresis on an agarose gel (2% (w/v) agarose and 76.09 nM ethidium bromide in TAE buffer). After electrophoretic separation of DNA fragments, gels were evaluated and documented using ultra violet imaging system (UVsolo TS).

3.2.4 Tissue preparation

3.2.4.1 Mice

Mice were sacrificed by cervical dislocation and transcardially perfused with PBS. The brain was removed and hemispheres were separated. One Hemisphere was immediately snap-frozen in liquid nitrogen and stored at -80 °C for biochemical analysis, the second hemisphere was stored in buffered 4% paraformaldehyde solution for paraffin-embedding and immunohistochemistry.

3.2.4.2 Degus

Degus were likewise sacrificed by cervical dislocation and transcardially perfused with PBS and subsequently with PFA. The brain was removed and stored in buffered 4% paraformaldehyde for paraffin-embedding and immunohistochemistry.

3.2.5 Immunohistochemistry

After removal, tissue was post-fixed in 4% buffered paraformaldehyde solution for 72 hours, dehydrated and embedded in paraffin (Table 3-4).

Table 3-4: Dehydration protocol for fixed hemispheres.

Step	Reagent	Duration in min
1	Buffered PFA 4% (w/v)	5
2	Ethanol 70% (v/v)	180
3	Ethanol 80% (v/v)	60
4	Ethanol 80% (v/v)	120
5	Ethanol 90% (v/v)	60
6	Ethanol 90% (v/v)	60
7	Ethanol absolute	120
8	Ethanol absolute	120
9	Xylene	120
10	Xylene	120
11	Paraffin wax 60 °C	240
12	Paraffin wax 60 °C	240

For immunostaining, tissue was cut into 4 μm thick coronal sections (~ 1.5 mm caudal of bregma) using a microtome and mounted on glass slides. Sections were then deparaffinised, rehydrated, peroxidase blocked and immunostained using BOND-III autostainer. Epitope retrieval was carried out as follows: 5 min in 95% (v/v) formic acid for 6F3D, 4G8 and 6E10; 20 min in EDTA buffer pH 9.0 for IBA1 and AT180; 10 min enzymatic digestion (Bond Enzyme Pretreatment Kit) for GFAP or 20 min in citric acid buffer pH 6.0 for NeuN, AT8 and AT100. A β was generally detected using anti- β -amyloid clone 6F3D (1:100, 15 min). Additional β -amyloid stains were conducted, where indicated, using clones 4G8 (1:2000, 15 min) and 6E10 (1:100, 15 min). Furthermore antibodies against ionised calcium-binding adapter molecule 1 (IBA1, 1:1000, 15 min), glial fibrillary acid protein (GFAP, 1:500, 15 min), neuronal nuclear antigen (NeuN, 1:500, 15 min) and different epitopes of phosphorylated tau, clones AT8 (1:50, 30 min), AT100 (1:500, 30 min) and AT180 (1:50, 30 min) were used and detected with Bond Polymer Refine Detection kit (Leica). For double-stained slides, A β was stained on the same slide using anti- β -amyloid clone 6F3D (1:100, 15 min) and the Bond Polymer Refine Red Detection kit (Leica, Germany). All sections were finally counterstained with haematoxylin (5 min) subsequently dried and embedded using Pertex[®] mounting medium.

3.2.6 Histochemistry

For haematoxylin and eosin (H&E) slides, deparaffinised 4 μm thick sections were stained using haematoxylin (30 s, Harris/Gill 2), blued in water (30 s) and washed with distilled water. Sections were then stained using eosin Y (60 s), washed with distilled water, dehydrated and embedded using Pertex[®] mounting medium.

For Campbell-Switzer staining deparaffinised 4 μm thick sections were stirred in ammonium hydroxide (5 min) and washed twice in distilled water (60 s). Sections were then incubated in silver-pyridine-carbonate solution (40 min) followed by citric acid (3 min) and afterwards washed in acetate buffer. Slides were processed in developer solution under a light source for about 6 min and

subsequently washed three times in acetate buffer (30 s) and then once in distilled water (30 s). Slides were finally placed in 0.5% (w/v) sodium thiosulfate solution (45 s), washed twice in distilled water, dehydrated and finally embedded using Pertex® mounting medium.

For thioflavin T staining, deparaffinised 8 µm thick sections were stained in 1% (w/v) thioflavin T solution for 30 min and subsequently washed with 96% (v/v) ethanol for 5 min. Slides were then washed with distilled water and mounted using Kaiser's glycerol gelatine.

3.2.7 Analysis of microscopic slides

Slides were digitised using Pannoramic MIDI digital slide scanner at a resolution of < 0.23 µm/pixel for further analysis.

3.2.7.1 Semi-automatic analysis

Scanned slides were processed using Pannoramic Viewer and neocortical areas were analysed under blinded conditions, computer-assisted using either AxioVision (Aβ, GFAP, IBA1 and IBA1/Aβ double stains) or ImageJ (NeuN stains) and the ITCN plugin^[192].

3.2.7.2 Manual Analysis

Cerebral amyloid angiopathy (CAA) was analysed manually using digitised slides. To evaluate severity of CAA, leptomeningeal vessels were divided in five categories. Unaffected vessels were assigned to group 0. Affected vessels were categorised depending on percentage of labelled circumference as follows: group I: ≤ 25%, group II: 26 – 50%, group III: 51 – 75%, group IV: > 75%.

3.2.8 Protein biochemistry

3.2.8.1 Preparation of protein samples

Frozen hemispheres (-80 °C) were slowly thawed in 500 µl RNeasy Lysis Buffer for one hour on ice at 300 rpm. Access liquid was removed and hemisphere was homogenised using metal beads for 30 s in SpeedMill PLUS homogeniser. Samples were centrifuged (20,000 g, 2 min, 4 °C) and stored at -80 °C until further use.

For western blot analysis, 20 mg of brain homogenate were mixed with 500 µL RIPA buffer for 30 s using a metal bead and the SpeedMill PLUS homogeniser. Samples were centrifuged (20,000 g, 5 min, 4 °C) and supernatant was transferred to new tube and stored at -20 °C until further use.

For immunoassays, 20 mg brain homogenate were mixed with 400 µL carbonate buffer for 30 s using a metal bead and the SpeedMill PLUS homogeniser. Homogenate was centrifuged (20,000 g, 20 min, 4 °C). Supernatant (carbonate soluble fraction) and pellet (for guanidine extraction) were further processed separately. Carbonate soluble fraction was mixed with 8.2 M guanidine buffer (610 µL/mL), rigorously vortexed and centrifuged (20,000 g, 20 min, 4 °C). Supernatant was stored at -20 °C until further use. Pellet for guanidine extraction was mixed with 5 M guanidine buffer

(8 $\mu\text{L}/\mu\text{g}$ protein) for 3 h (1,500 rpm at room temperature). Samples were then centrifuged (20,000 g, 20 min, 4 °C) and supernatants (guanidine-soluble fraction) were stored at -20 °C until use.

3.2.8.2 Spectrophotometric protein quantification

Protein concentration of samples for immunoassays was measured using ScanDrop® spectrophotometer according to the manufacturer's instructions using appropriate dilutions. Absorption at 280 nm (protein content) and 320 nm (background correction) was measured in parallel at 0.1 and 1 mm path length for each sample against appropriate reference. Dark signal and background corrected protein concentrations were automatically calculated.

3.2.8.3 Biochemical protein quantification

Protein concentration of samples for western blot was determined using Pierce™ BCA protein assay, according to the manufacturer's instructions using appropriate dilutions. Absorption at 562 nm was measured using Paradigm™ detection platform. Concentrations were calculated using the corresponding BSA calibration curve (linear regression).

3.2.8.4 Polyacrylamide gel electrophoresis and western blot

Samples for western blot analyses were mixed with protein sample buffer (0.25 $\mu\text{L}/\mu\text{L}$) and denatured for 5 min at 95 °C. 25 μg protein of each sample was loaded on a polyacrylamide gel (5% stacking gel, 12% separation gel). Electric field was applied to the gel (80 V for 30 min and subsequently 120 V for 2 h) to separate proteins which were afterwards blotted (50 V, 2 h) onto a PVDF membrane in PAGE transfer buffer. The blot was then blocked using Rockland blocking buffer for 1 h at room temperature and subsequently probed using either anti-ADAM10 (1:500), BACE1 (1:1,000), anti-caspase-3 (1:1,000), anti-caspase-9 (1:1,000) or anti-Insulin-degrading enzyme (1:50) and anti- β -actin (1:30,000). Primary antibodies were diluted in Rockland blocking buffer and incubated overnight with gentle agitation at 4 °C. IRDye®-labeled anti-mouse and anti-rabbit antibodies (diluted 1:15,000 in Rockland blocking buffer) were used for detection and incubated for 1 h at room temperature with gentle agitation. Blots were visualised using the Odyssey infrared imaging system.

3.2.8.5 *Electrochemiluminescence immunoassays*

Immunoassays were used to determine A β ₄₂ concentration in buffer- and guanidine-soluble fractions. V-PLEX A β ₄₂ Kits were used according the manufacturer's instructions using appropriate dilutions. Assays were read with a MESO QuickPlex SQ 120 and concentrations were calculated using the corresponding calibration curve. Calibration curve was generated using 5-parameter logistic regression (equation 3.1) and fitted using sum of weighted squared errors (equation 3.2)^[193].

$$y = f(x; a, b, c, d, g) = d + \frac{(a - d)}{\left(1 + \left(\frac{x}{c}\right)^g\right)^e} \quad 3.1$$

$$\sum_{i=1}^n \frac{1}{(y_i)^2} (y_i - \hat{y}_i)^2 \quad 3.2$$

3.2.9 **Statistics**

Results of immunohistochemistry and immunoassays were, in general, statistically analysed using unpaired t test with Welch's correction in GraphPad Prism and considered significant for $p \leq 0.05$. Furthermore, the two-way analysis of variance (two-way ANOVA, GraphPad Prism) was additionally performed, where appropriate. Data are presented as arithmetic mean with corresponding standard error of the mean (SEM).

4 Results

4.1 Murine APP-deficient mice

To explore the effect of endogenous APP expression on A β aggregation in transgenic mice, murine APP-deficient mice expressing mutant human *APP* and *PEN1* transgenes were utilised (mAPP^{0/0}; hAPP_{swE}⁺⁰; PS1_{L166P}⁺⁰, referred to as mAPP^{0/0}). APP/PS1 transgenic mice with natural expression of murine APP served as control (mAPP^{+/+}; hAPP_{swE}⁺⁰; PS1_{L166P}⁺⁰, referred to as mAPP^{+/+}). Animals were first analysed at an age of 50 d, when first plaques occur, until an age of 200 d. Neocortical plaque deposition was thereby studied in short intervals of 25 d to accurately portray the aggregation process. Additionally, intracerebral amyloid load was biochemically quantified to verify results and to screen for differences in soluble and deposited fractions of A β . To detect changes in generation or degradation of A β , expression levels of the most important enzymes were determined. Microglia and astrocytes were examined to characterise the cellular response to A β deposition in the altered environment. At last, neuronal density and expression of caspases were determined to detect developmental changes and signs for enhanced apoptosis.

4.1.1 Plaque deposition is diminished by murine APP expression

To analyse cortical deposition of transgenic human A β , brain sections were immunostained using the human-specific anti- β -amyloid antibody clone 6F3D. First plaques occurred similarly about the age of 50 d in both, mAPP^{0/0} and mAPP^{+/+} mice (Figure 4-1, Figure 4-2A and Table 7-2). The number of plaques rapidly rose upon an age of 100 d and continued afterwards in a slower fashion. The knockout of murine APP thereby led to a considerably faster formation of plaques (Table 7-2) and mAPP^{0/0} mice possessed significantly more cortical deposits at all analysed ages (Table 7-3). At 200 d, mice lacking murine APP displayed about 50% more plaques (Figure 4-1, Figure 4-2). The two-way analysis of variance (two-way ANOVA) confirmed the significance of age and murine APP expression as mainsprings of amyloid deposition (Table 7-4). The average size of plaques, however, strongly increased only until about 100 to 125 d of age and remained rather constant thereafter in both strains (Figure 4-2). Although the mean size of plaques was generally higher in mAPP^{0/0} (two-way ANOVA, Table 7-4), the actual differences at specific ages were low and only reach significance at 100 d and 200 d (unpaired t-test with Welch's correction, Table 7-3). As a result of plaque number and size, the cortical plaque coverage (percentage of cortex covered by plaques) was also significantly higher in mAPP^{0/0} mice compared to the mAPP^{+/+} mice at all ages (Figure 4-2, Table 7-3). To further analyse aggregation, all plaques were classified according to their size. Plaques smaller than 400 μm^2 were defined 'small', between 400 and 700 μm^2 'medium' and above 700 μm^2 'large'. In absolute terms, mAPP^{0/0} mice displayed throughout more plaques of all magnitudes (Figure 4-2, Table 7-4 and Table 7-5). The amount of 'small' plaques increased more rapidly in mAPP^{0/0} mice,

which had significantly more 'small' deposits at young ages (50 d, 75 d and 100 d). Beyond 100 d of age, the number of 'small' plaques rose in a similar fashion in both groups.

In contrast, 'medium' and 'large' plaques emerged later. At the earliest time point (50 d), only few animals already displayed deposits larger than $400 \mu\text{m}^2$, but they occurred more frequently in mAPP^{0/0} mice. Upon 75 d, all analysed mice had 'medium' sized plaques. Their number was again consistently higher in mAPP^{0/0} animals and reached significance upon 100 d of age (Figure 4-2, Table 7-5). 'Large' plaques were found in all animals older than 125 d. The amount of 'large' plaques was constantly rising in both groups and the amount was again significantly larger in mAPP^{0/0} mice upon 100 d of age (Figure 4-2, Table 7-5).

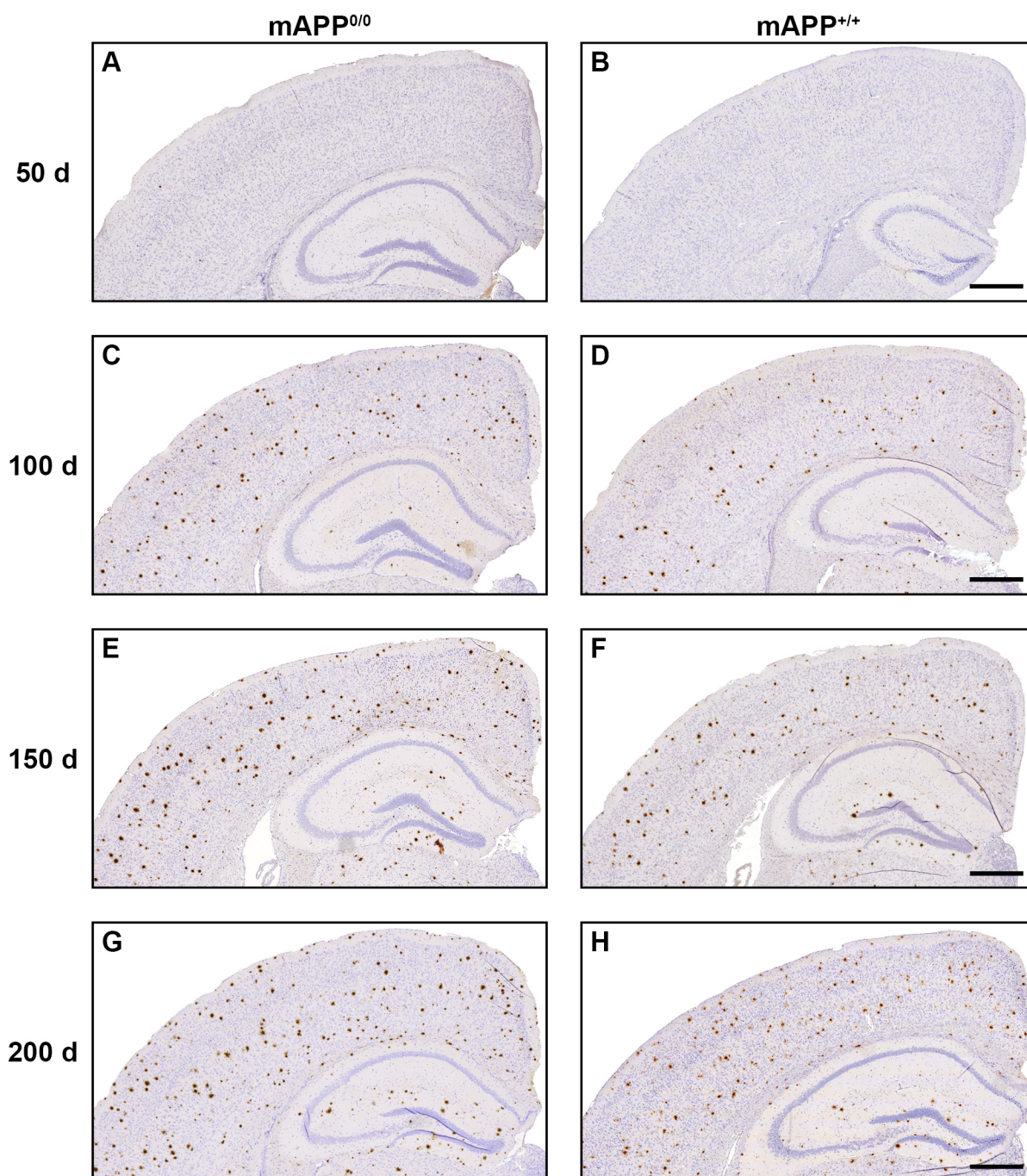


Figure 4-1: Progression of cortical amyloidosis in mAPP^{0/0} and mAPP^{+/+} mice.

Representative brain sections of 50 - 200 d old mice illustrate the differences in plaque deposition between mAPP^{0/0} and mAPP^{+/+} mice. Sections were immunostained for human A β and contrasted using haematoxylin. Deposition of A β (brown) started at an age of about 50 d with few small plaques in both strains (A, B). At the age of 100 d, a distinct number of plaques was visible and mAPP^{0/0} mice already presented with considerably more deposits than mAPP^{+/+} mice (C, D). The amyloidosis progressed continuously with age in both strains, and APP-deficient mice (E, G) manifested constantly with higher numbers of cortical plaques compared to mAPP^{+/+} controls (F, H). (Scale bars: 500 μ m).

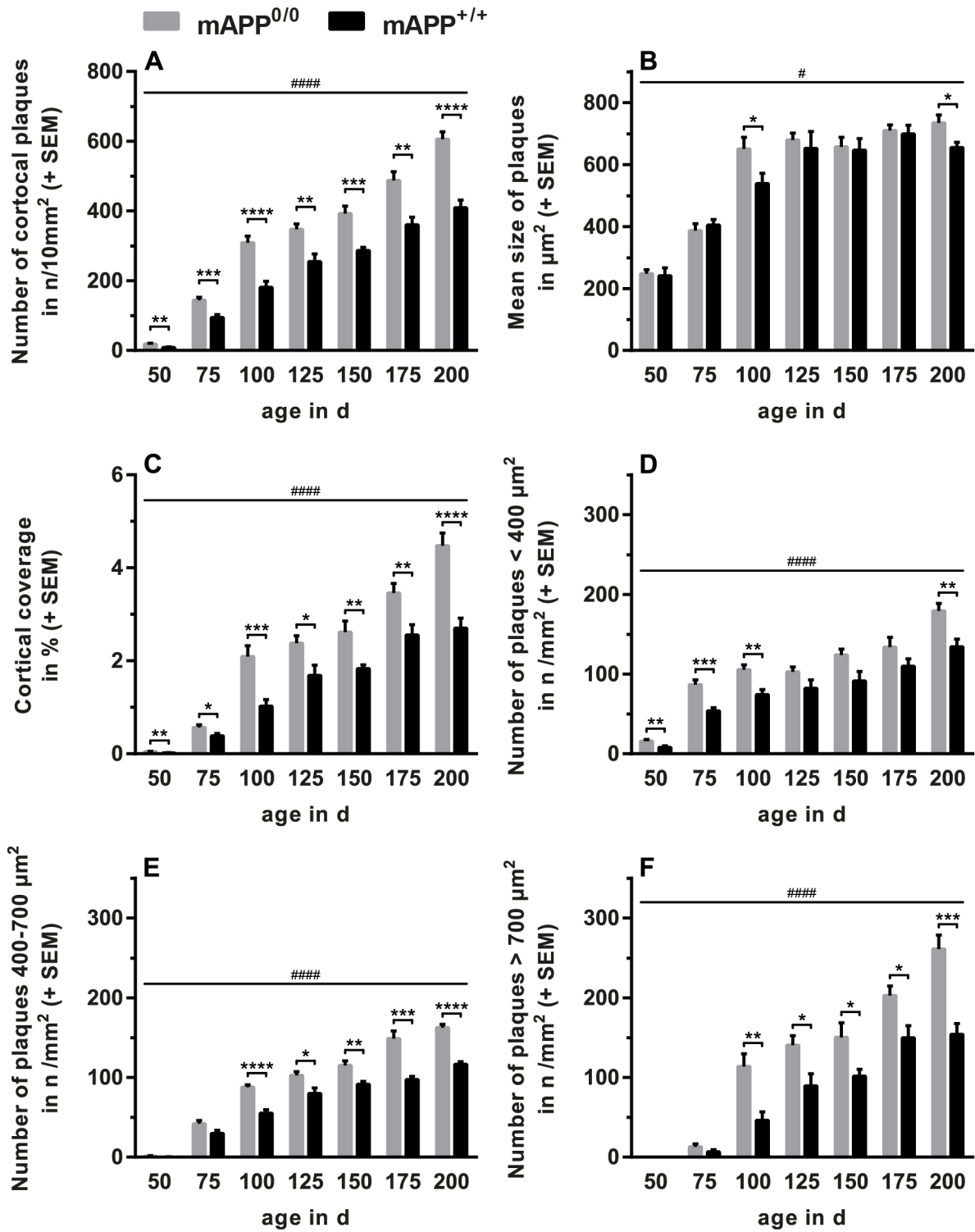


Figure 4-2: Cortical amyloidosis is exacerbated in murine APP-deficient mice.

(A) The amount of plaques continuously rose in *mAPP^{0/0}* and *mAPP^{+/+}* mice. The increase was stronger in *mAPP^{0/0}* mice, which possessed significantly more plaques at all ages. (B) The mean size of plaques rose sharply until 100 d of age and remains rather stable thereafter. Nevertheless, mean size was generally slightly higher in *mAPP^{0/0}* mice. (C) The cortical coverage with plaques was also significantly higher in *mAPP^{0/0}* mice at all ages. Individual analysis of (D) 'small' (< 400 µm²), (E) 'medium' (400-700 µm²) and (F) 'large' (> 700 µm²) deposits confirmed the previous results, as increase and absolute number of plaques were higher in *mAPP^{0/0}* mice for all magnitudes. (Statistical analysis: unpaired t-test with Welch's correction for individual time points, * p < 0.05, ** p < 0.01, *** p < 0.001, **** p < 0.0001; two-way ANOVA for comparison of strains, # p < 0.05, ##### p < 0.0001).

4.1.2 Knockout of murine APP elevates intracerebral A β ₄₂ levels

Quantitative measurements of A β ₄₂ levels were performed using sandwich immunoassays. The assays employed the well-established anti-A β antibody clone 4G8 for detection, which recognises both, human and murine A β . Two different fractions were generated (buffer- and guanidine-soluble) and individually analysed, to discriminate between soluble and deposited β -amyloid.

The amount of insoluble A β ₄₂ (guanidine-soluble fraction) steadily rose with age in both, mAPP^{0/0} and mAPP^{+/+} mice (Figure 4-3). The increase was thereby more rapid in mAPP^{0/0} mice, which also presented with higher amounts of cerebral A β ₄₂ at all ages. The difference between the groups was finally about 40% (200 d of age, Table 7-11). In mAPP^{+/+} mice, the rise in A β ₄₂ levels slowed down upon 150 d, while it continued unabatedly in mAPP^{0/0} mice. Overall, levels of insoluble A β ₄₂ were highly variable and differences at individual time points reached significance only at 75 and 100 d. However, analysis of all ages using two-way ANOVA showed that missing murine APP expression significantly increased the cerebral deposition of A β ₄₂ (Table 7-4). In comparison to deposited amyloid, soluble A β ₄₂ had an essentially lower concentration. The amount of soluble amyloid increased rapidly until 100 d to 125 d of age, whereby the accumulation was more pronounced in mAPP^{0/0}. Upon 125 d of age, the amount of soluble A β ₄₂ decreased in both groups and mAPP^{0/0} mice finally demonstrated even lower levels of soluble A β ₄₂ than mAPP^{+/+} animals (Figure 4-3, Table 7-11). The levels of total A β ₄₂ (calculated sum of buffer- and guanidine-soluble fraction) showed a continuous increase with a tendency to slow age-dependently down. The total A β ₄₂ levels were again constantly higher in mAPP^{0/0} mice. Statistical analysis showed that co-expression of murine APP significantly decreased total levels of cerebral A β (two-way ANOVA, Table 7-4).

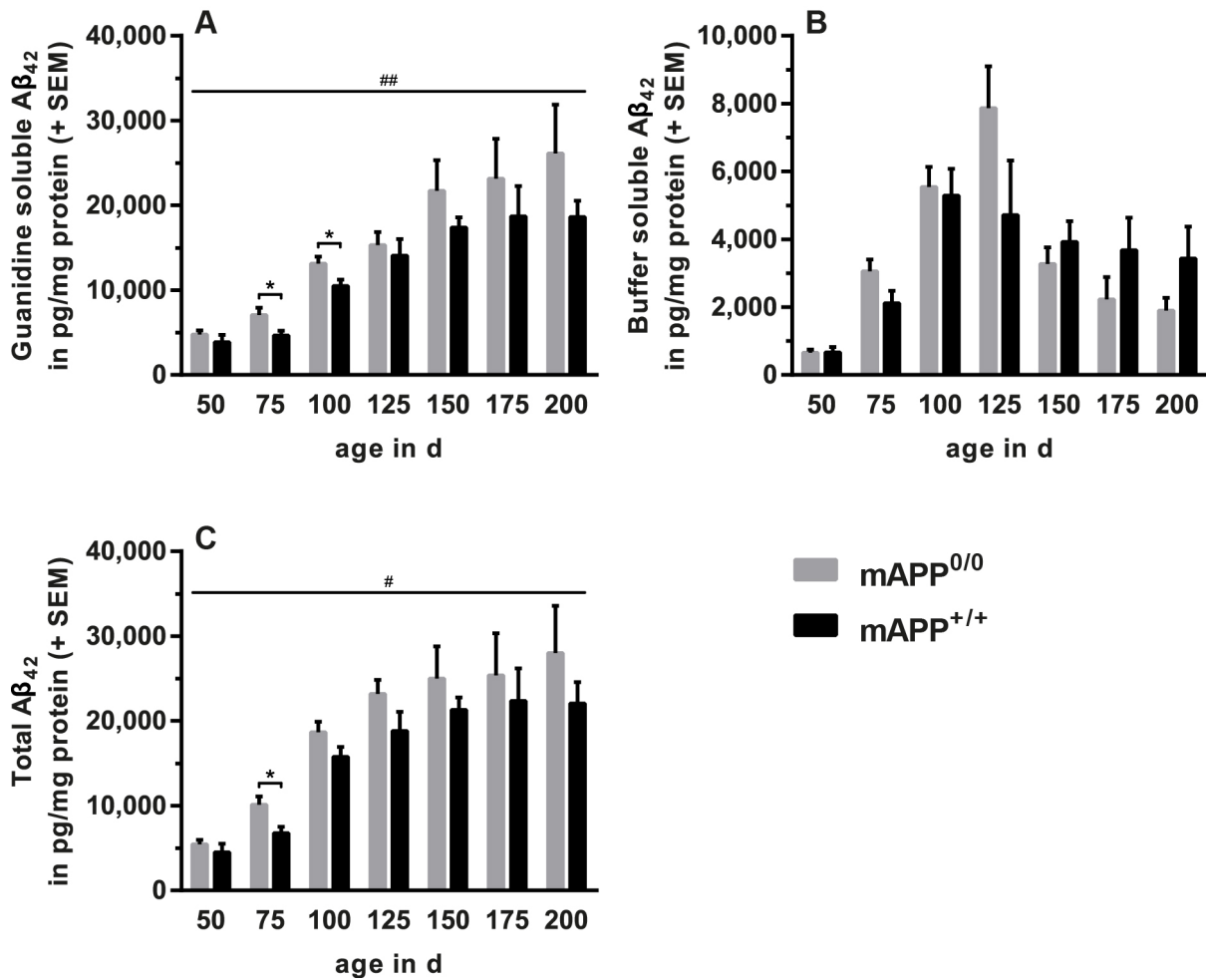


Figure 4-3: Influence of endogenous APP on cerebral Aβ₄₂ levels in transgenic mice.

Concentrations of (A) guanidine- and (B) buffer-soluble Aβ₄₂ in brain homogenates were measured using immunoassays. (A) The levels of deposited (guanidine-soluble) Aβ₄₂ constantly increased with age in both strains. However, mAPP^{0/0} mice presented consistently with higher concentrations of insoluble Aβ₄₂. (B) The amount of soluble Aβ₄₂ (buffer-soluble) initially rose until 100 – 125 d of age and subsequently decreased in both strains. The murine APP-deficient mice displayed higher levels of soluble Aβ₄₂ only until 125 d, thereafter mAPP^{+/+} mice had higher levels of soluble Aβ₄₂. Nevertheless, (C) total Aβ₄₂ levels (calculated sum of guanidine- and buffer-soluble fraction) were again consistently higher in mAPP^{0/0} mice at all ages. (Statistical analysis: unpaired t-test with Welch's correction for individual time points, * p < 0.05; two-way ANOVA for comparison of strains, # p < 0.05, ## p < 0.01).

4.1.3 Murine APP-deficiency does not affect APP processing

Generation and degradation of A β are controlled by different proteases. To assess whether the different progression of A β deposition was caused by an altered cleavage, the expression levels of the most important proteases were determined by western blot. ADAM10 (A disintegrin and metalloproteinase domain-containing protein 10) is the primary neuronal α -secretase and prevents the generation of β -amyloid by cleavage within the A β -sequence. Expression levels of ADAM10 revealed neither age- nor strain-specific differences until 200 d of age (Figure 4-4). The cerebral levels of BACE1, which initiates the production of A β , were likewise unchanged.

Once generated, A β can also be eliminated by enzymatic degradation. The insulin-degrading enzyme (IDE) is one of the most important enzymes for proteolytic degradation of A β . However, expression levels were independent of age and endogenous APP expression in the analysed and age range.

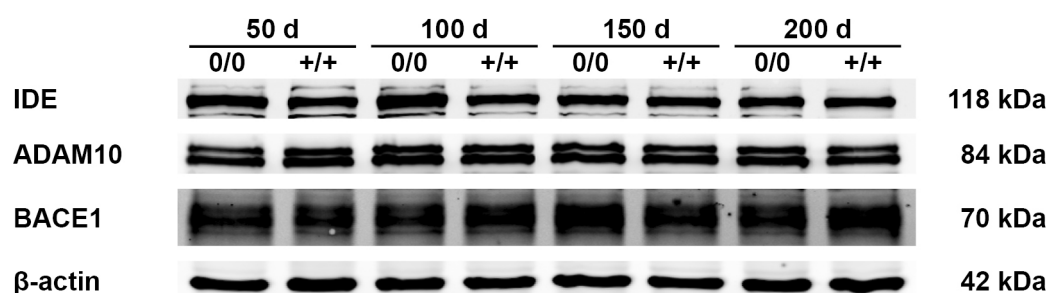


Figure 4-4: Expression of APP- and A β -cleaving enzymes.

Western blots of ADAM10 (α -secretase) and BACE1 (β -secretase) showed that their expression was independent of age and murine APP expression between 50 and 200 d of age in the utilised model. Blots of the insulin-degrading enzyme (IDE) revealed no evidence for enhanced expression as well. (β -actin was used as loading control).

4.1.4 Co-expression of murine APP accelerates vascular deposition of A β

Deposition of A β in leptomeningeal and cortical vessel is a common pathological feature of Alzheimer's disease. To analyse the effect of murine APP on cerebral amyloid angiopathy (CAA) in transgenic mice, leptomeningeal vessels were categorised depending on A β deposition (Figure 4-5A). At 50 d of age, only a small proportion of vessels was already affected (Table 7-6). With increasing age, vascular deposition of A β became more frequent and severe. CAA progressed thereby faster in mice that still expressed murine APP. Accordingly, the proportion of affected blood vessels was overall significantly higher in mAPP^{0/0} mice (two-way ANOVA, Table 7-4). Upon 100 – 125 d of age, the proportion of affected vessels reached a rather stable level in both groups and the severity equalised with age as well. In general, CAA was primarily observed in meningeal vessels and only rarely in cortical vessels.

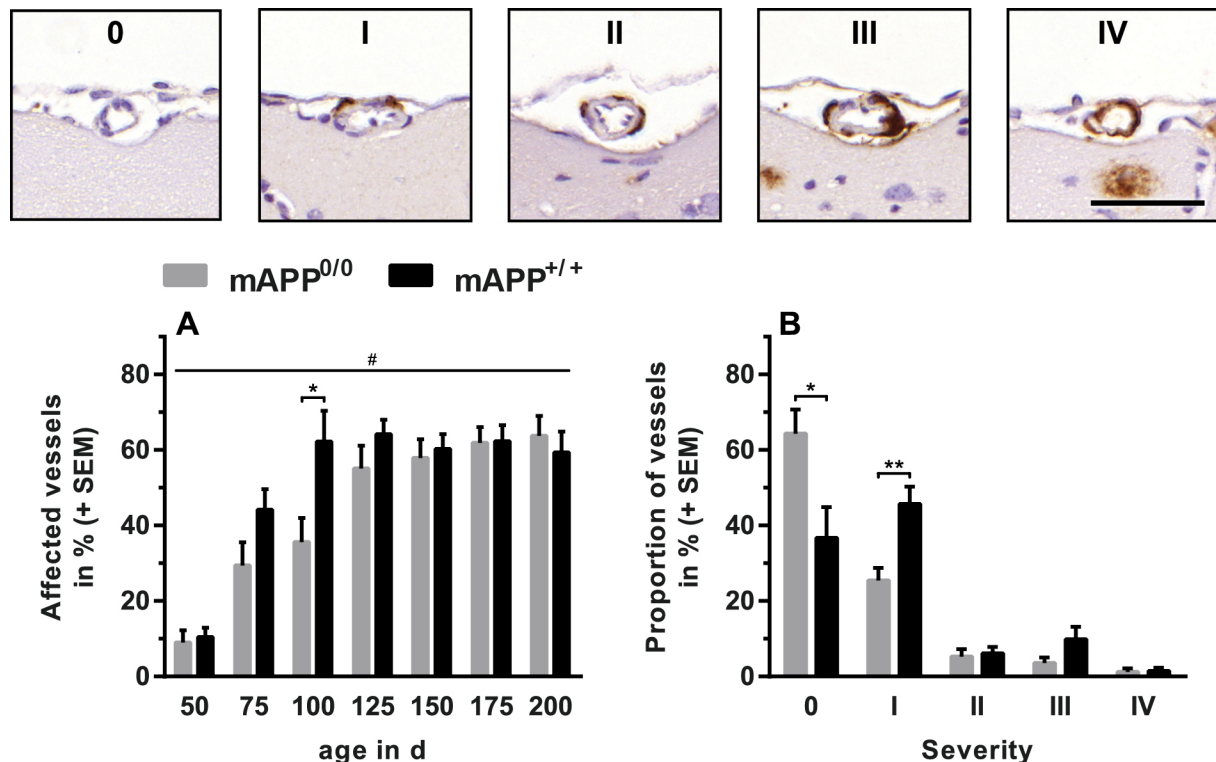


Figure 4-5: Frequency and severity of cerebral amyloid angiopathy.

Brain sections, immunostained for A β and contrasted by haematoxylin show deposition of A β in leptomeningeal blood vessels. Severity of cerebral amyloid angiopathy was defined based on deposited A β as follows: **0**: no A β deposition; **I**: \leq 25% of circumference labelled; **II**: 26 – 50% of circumference labelled; **III**: 51 – 75% of circumference labelled; **IV**: $>$ 75% of circumference labelled. The proportion of affected vessels (I – IV) increased age-dependently (A), whereby the knockout of murine APP decelerated the deposition of A β in vessel walls. Severity of CAA is exemplarily shown for 100 d old mice (B), where mAPP^{0/0} mice exhibited significantly more unaffected vessels. The majority of labelled vessels was only mildly affected ($<$ 25%) at this time point. (Scale bar: 50 μ m; statistical analysis: unpaired t-test with Welch's correction for individual time points and severity, * $p < 0.05$, ** $p < 0.01$; two-way ANOVA for comparison of strains, # $p < 0.05$).

4.1.5 Microglial response is reduced in upon murine APP knockout

Microglial cells are activated by high A β concentrations in the vicinity of amyloid plaques and interfere with further deposition thereafter. To assess their impact in transgenic, murine APP-deficient mice, microglial presence was determined using IBA1 (ionised calcium-binding adapter molecule 1) as marker. Initially, microglial reaction and corresponding cortical coverage were analysed at 150 d. This specific age was chosen, because cortical amyloidosis was pronounced and plaque load already significantly different between the two groups, while microglial response was still in its acute phase. The cortical density of IBA1⁺ cells was not notably changed between mAPP^{0/0} and mAPP^{+/+} mice (Figure 4-6). Microglial cells frequently appeared in clusters of several cells and presented characteristically with enlarged cell bodies and short, sparsely ramified processes. Semi-automatic evaluation of digitised slides revealed that the total area covered by IBA1⁺ cells was identical in both groups (Figure 4-6C, Table 7-7).

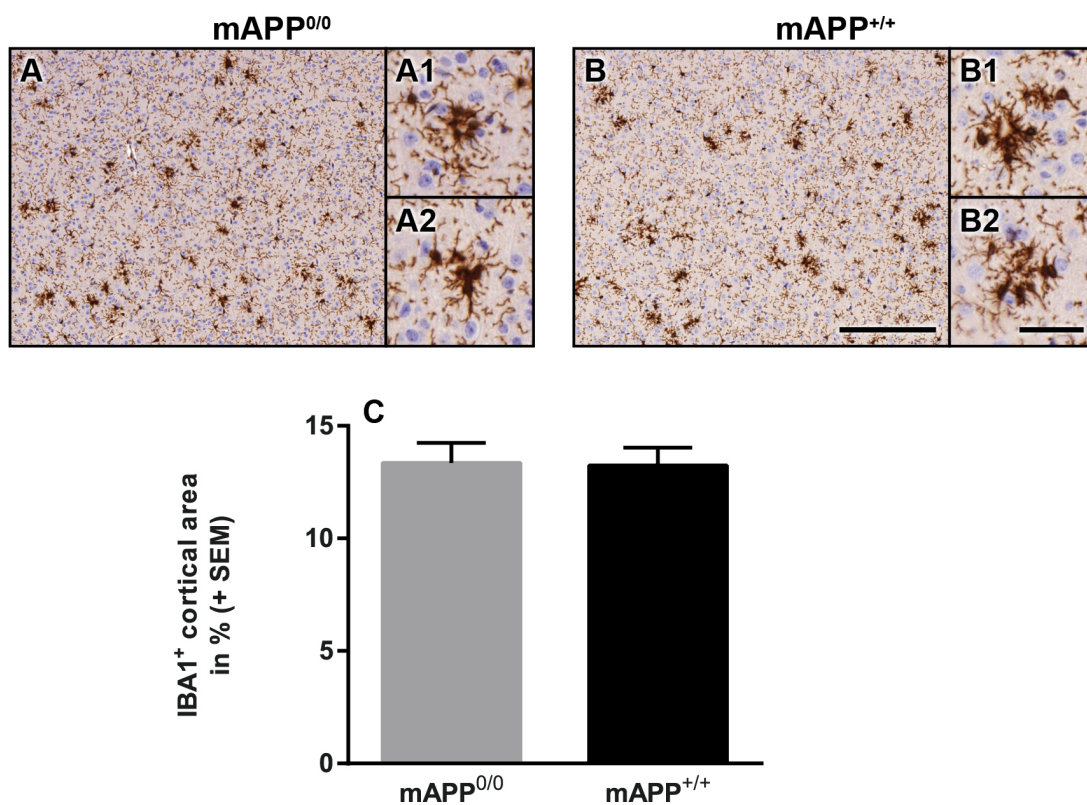


Figure 4-6: Similar sized microglial populations in 150 d old mice.

Representative brain sections, immunostained for microglial marker IBA1 and contrasted using haematoxylin, showed clustering of IBA1⁺ cells in cortices of (A) mAPP^{0/0} and (B) mAPP^{+/+} mice. Microglia thereby presented with short, barely branched processes and enlarged cell bodies (A1, A2, B1, B2). Semi-automatic evaluation of slides demonstrated similar cortical coverage by microglial cells (C) in both groups. (Scale bars: 250 μ m in overviews; 50 μ m in enlarged insets, unpaired t-test with Welch's correction revealed no significant difference for cortical microglia coverage).

To explore potential differences in microglia-plaque interaction between mAPP^{0/0} and mAPP^{+/+} mice, plaques and microglia were stained consecutively on the same sections (double staining). In both groups, microglial cells appeared frequently in close proximity of amyloid plaques (Figure 4-7). At 100 d of age, amyloid deposits were notably covered by microglial cells, which presented with an activated phenotype. The mean microglial coverage of plaques was thereby remarkably lower in mAPP^{0/0} mice (Figure 4-7, Table 7-7). With advancing age and thus higher plaque load, microglial coverages increased as well. At 150 d of age, the microglial coverage of plaques was again significantly lower in mAPP^{0/0} mice. At the last analysed time point (200 d), microglial coverage of plaques sharply dropped in both groups. The same course was apparent when 'small', 'medium' and 'large' plaques were analysed separately (Table 7-7). Statistical analysis confirmed the significant influence of murine APP expression on microglial coverage of plaques (two-way ANOVA, Table 7-4). Plotting individual size of plaques and their corresponding microglial coverage revealed a general distribution pattern (Figure 4-8). On average, microglial coverage of plaques was highest in 'small' plaques and declined with increasing size of deposits. To further analyse the relation of plaque size and microglial coverage, plaques were separated using the established categories 'small' (< 400 μm^2), 'medium' (400 – 700 μm^2) and 'large' (> 700 μm^2). The size-separated analysis of microglial coverage was in line with the previous observation, that microglia coverage was lower in mAPP^{0/0} and decreased size-dependently (Figure 4-8, Table 7-7).

To evaluate whether these changes in microglial coverage of plaques were exclusively caused by different density of amyloid deposits, the total area of plaque-associated microglia was determined. This area was consistently lower in mAPP^{0/0} mice (Figure 4-8). Although differences did not reach significance at individual time points (unpaired t-test with Welch's correction, Table 7-7), in general, murine APP-deficiency significantly lowered the total area of plaque-associated microglia (two-way ANOVA, Table 7-4).

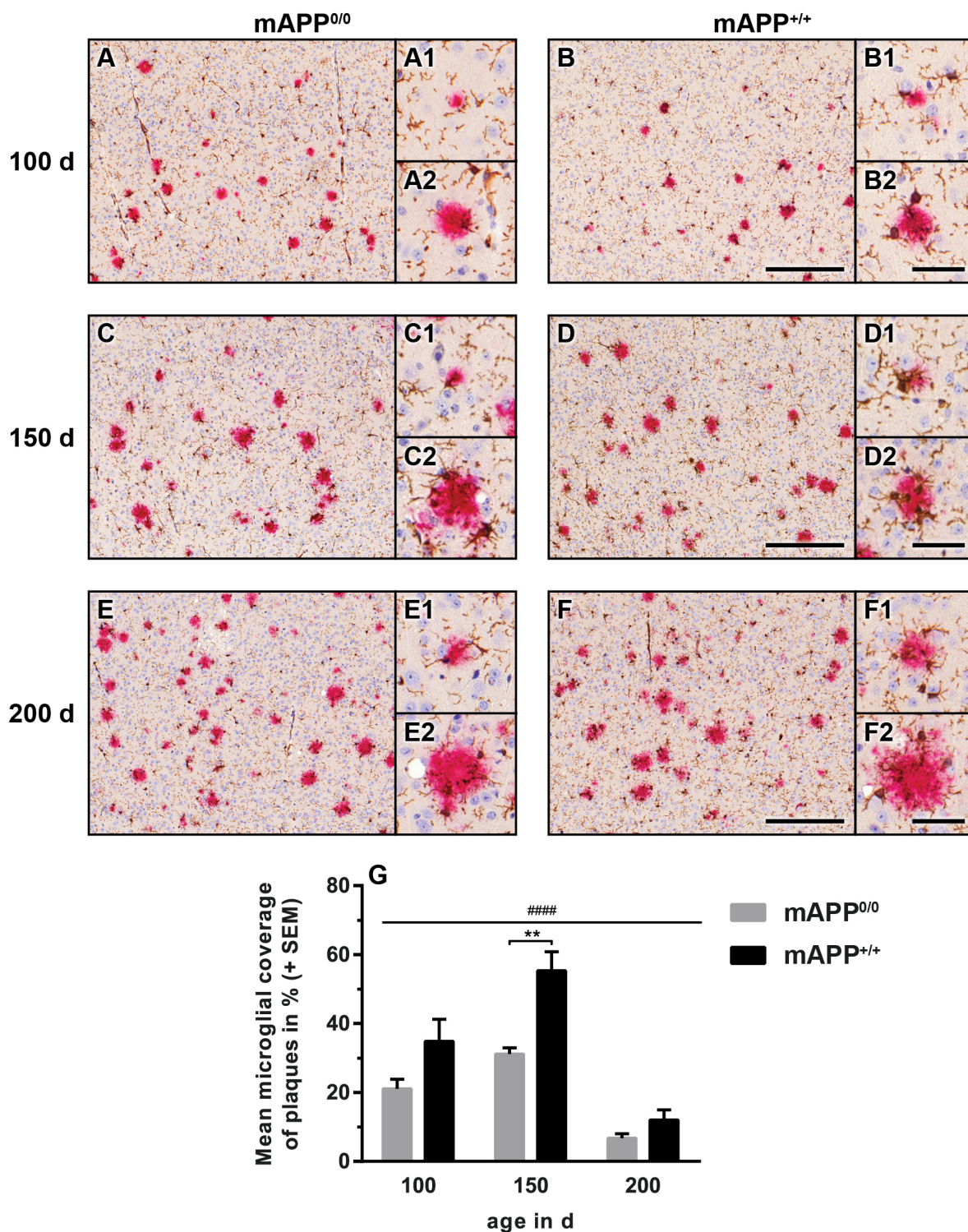


Figure 4-7: Microglial response is decreased in murine APP-deficient mice.

Representative cortical micrographs of immunostained brain sections and corresponding enlargements of ‘small’ and ‘large’ plaques (red) and microglia (brown) indicate a decreased microglial response in *mAPP^{0/0}* mice. Microglial reaction is visible at 100 d (A, B) and strongly increased at 150 d (C, D). As individual plaques grow further (E, F) proportional microglial coverage declines. In general, coverage of plaques by microglial cells was consistently lower in *mAPP^{0/0}* mice (G). (Scale bars: 250 μ m in overviews; 50 μ m in enlarged insets; statistical analysis: unpaired t-test with Welch’s correction for individual time points, ** p < 0.01; two-way ANOVA for comparison of strains, #### p < 0.0001).

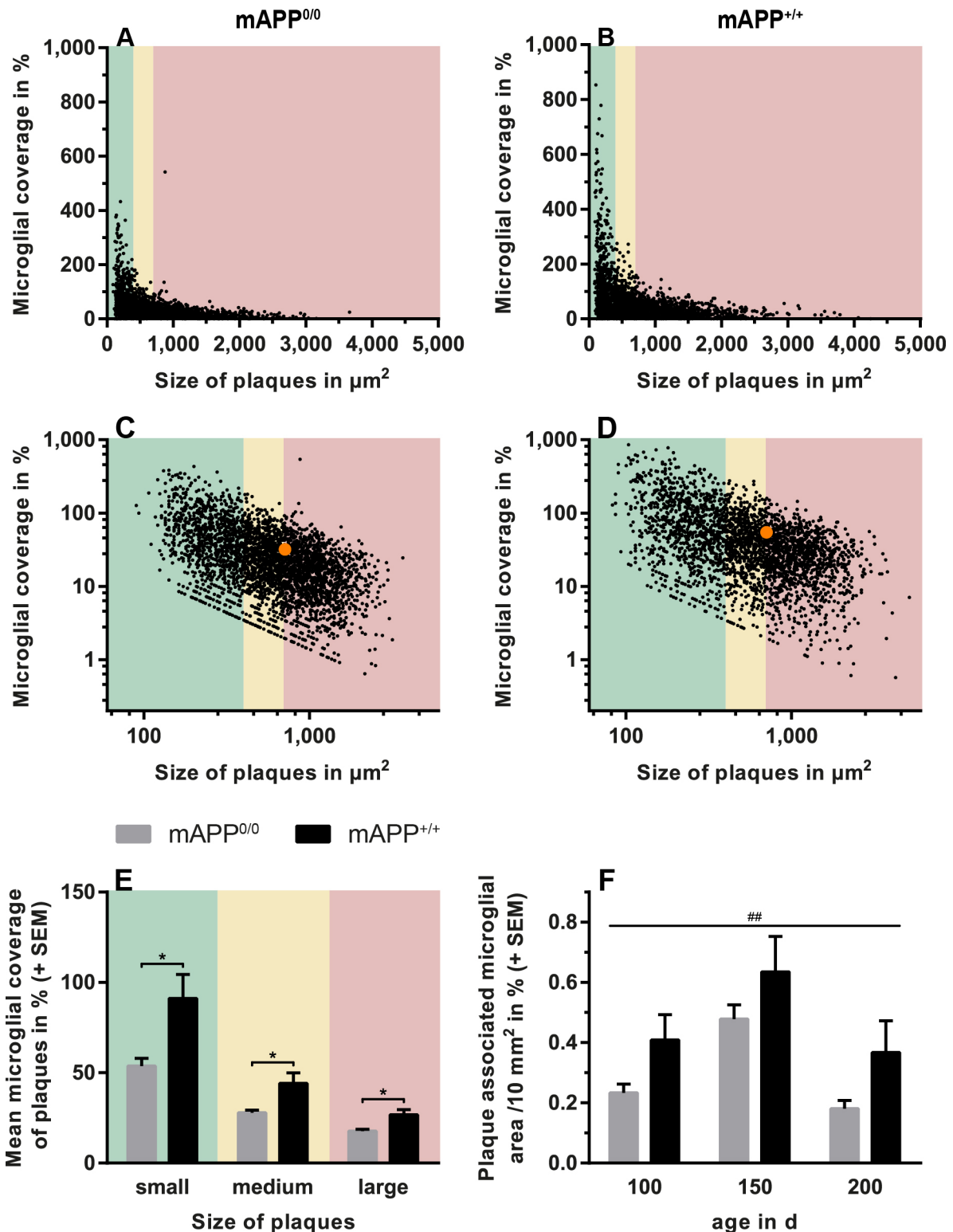


Figure 4-8: Plaque size and corresponding microglial coverage follow a distinct pattern.

Exemplary diagrams show the general distribution pattern of plaque size and corresponding microglial coverage in $mAPP^{0/0}$ (A, C) and $mAPP^{+/+}$ (B, D) mice at 150 d. The size categories of plaques are highlighted in green ('small', $< 400 \mu m^2$), yellow ('medium', $400 - 700 \mu m^2$) and red ('large', $> 700 \mu m^2$). The logarithmic representation (C, D) displays a lowered mean coverage of plaques by microglia in $mAPP^{0/0}$ mice as vertical shift of the point cloud (the centroid as additional indicator is plotted in orange). (E) Microglial coverage was significantly lower for all sizes of plaques in $mAPP^{0/0}$ mice, exemplarily shown at 150 d of age. (F) The total area of plaque-associated microglial cells was as well consistently reduced in $mAPP^{0/0}$ mice. (Statistical analysis: unpaired t-test with Welch's correction for microglial coverage of different plaque sizes, * $p < 0.05$; two-way ANOVA for comparison of strains, ## $p < 0.01$).

4.1.6 Pronounced gliosis in aged, murine APP-deficient mice

Beside microglial cells, activated astrocytes encircle amyloid plaques. They initially interfere with further A β deposition, but as activation prolongs, detrimental effects prevail. To characterise astrocyte reaction in mAPP^{0/0} and mAPP^{+/+} mice, brain sections were stained using specific antibodies against the glial fibrillary acidic protein (GFAP) as astrocytic marker. To detect potential differences in astrocyte populations, total astrocyte area was determined using semi-automatic analysis of digitised slides. Mice were analysed at an early (100 d) and an advanced stage (200 d) to further reveal age-dependent changes. At 100 d of age, GFAP⁺ astrocytes were present in all cortical layers with a tendency to form clusters. Neither spatial distribution nor amount of GFAP⁺ cells differed between mAPP^{0/0} and mAPP^{+/+} controls at 100 d of age (Figure 4-9). While astrocyte coverage and spatial distribution remained similar in older mAPP^{+/+} mice (200 d), a pronounced astrogliosis developed in mAPP^{0/0} mice. Semi-automatic analysis of digitised slides revealed no age-dependent changes for GFAP⁺ area in mAPP^{+/+} mice, while it was increased about 60% in 200 d old mAPP^{0/0} mice (Figure 4-9, Table 7-9, Table 7-10). Statistical analysis confirmed the strong impact of murine APP expression on severity of astrogliosis, while age had a comparably low influence (two-way ANOVA, Table 7-4).

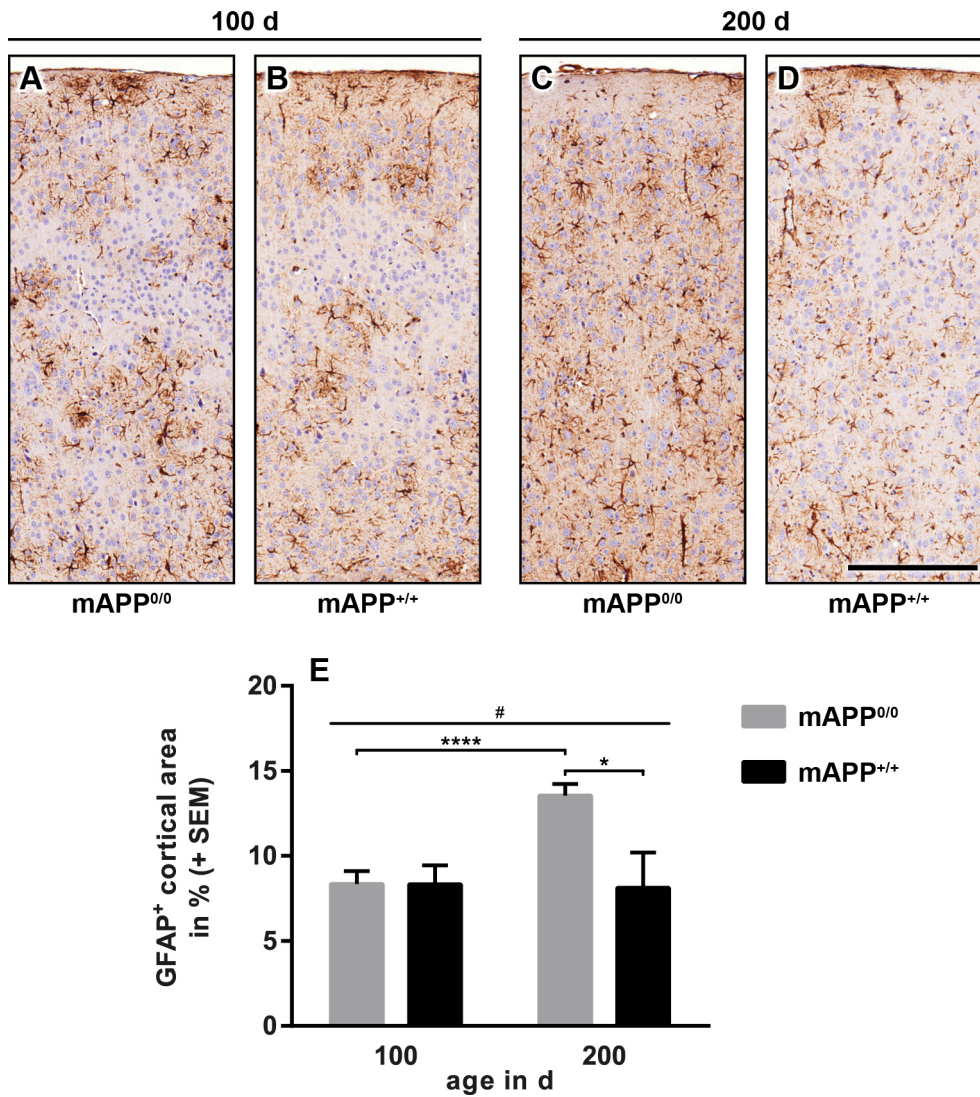


Figure 4-9: Pronounced astrogliosis in aged mAPP^{0/0} but not mAPP^{+/+} mice.

Brain sections immunostained for GFAP revealed no differences between mAPP^{0/0} and mAPP^{+/+} mice at 100 d (A, B). With advancing age, a notably stronger gliosis evolved in mAPP^{0/0} mice (C), whereas abundance of astrocytes remained unchanged in mAPP^{+/+} mice (D). Semi-automatic evaluation of slides confirmed the significant increase of GFAP⁺ area in mAPP^{0/0} mice (E). (Scale bar: 250 μ m; statistical analysis: unpaired t-test with Welch's correction for individual time points, * $p < 0.05$, **** $p < 0.0001$; two-way ANOVA for comparison of strains, # $p < 0.05$).

4.1.7 Neuronal density was not affected in murine APP-deficient mice

Progressive neuronal loss and consequential brain atrophy are characteristics of Alzheimer's disease that occur comparatively late in the pathogenesis of the disease. The synaptic and neuronal loss is thereby strongly driven by accumulation of amyloid in their vicinity. To estimate the effect murine APP-deficiency on neuronal density in APP/PS1 transgenic mice, brain sections of 150 d old mice were stained using a specific antibody against neuronal nuclei (NeuN). The number of cortical neurons in layers II to VI was determined by semi-automatic evaluation of digitised slides. However, the neuronal density was not significantly changed between $mAPP^{0/0}$ and $mAPP^{+/+}$ mice at 150 d of age (Figure 4-10, Table 7-8).

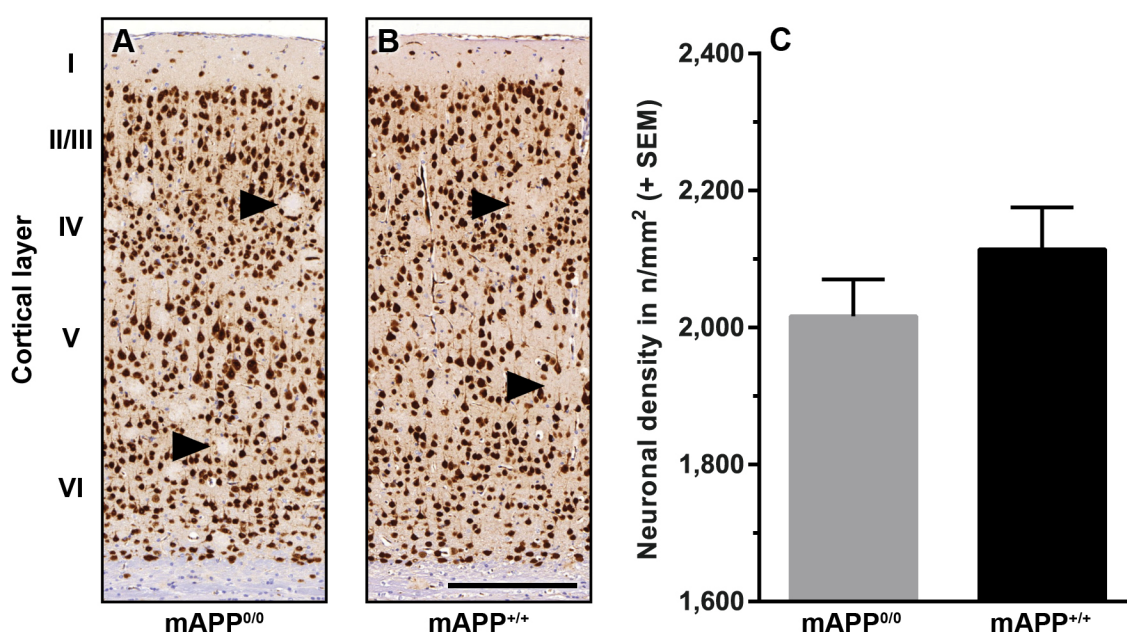


Figure 4-10: Neuronal density is unchanged in murine APP-deficient mice.

Brain sections of 150 d old $mAPP^{0/0}$ (A) and $mAPP^{+/+}$ mice (B) were immunostained for neuronal nuclei, but revealed no obvious changes in neuronal density. However, the spatial displacement by amyloid deposits (arrowheads) was clearly visible in both groups. Semi-automatic evaluation of digitised slides confirmed the similar density of neurons in both groups (C). (Scale bar: 250 μm , unpaired t-test with Welch's correction revealed no significant difference between $mAPP^{0/0}$ and $mAPP^{+/+}$ mice).

4.1.8 Caspase expression illustrates unchanged apoptosis

Apoptosis is a relatively late event in the pathogenesis of Alzheimer's disease, which has been recurrently described. The centre of interest includes inter alia caspase-3 and -9. The latter is an initiator caspase, triggering the apoptotic cascade by proteolytic activation of effector procaspase-3 and -7, which then cleave different target proteins within the cell. Expression levels of caspases were determined by western blot, to screen for signs of enhanced apoptosis. However, the blots demonstrated no age or strain-specific differences until 200 d of age (Figure 4-11).

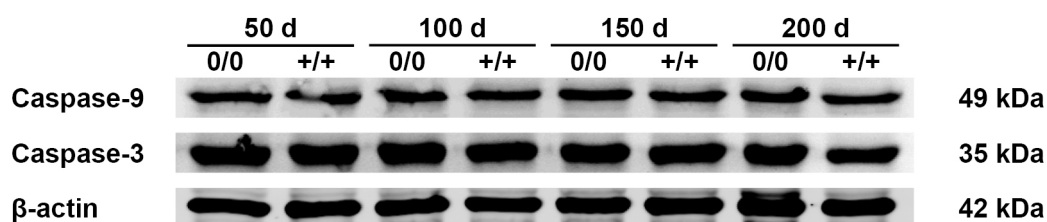


Figure 4-11: Expression levels of major caspases remain unchanged in mAPP^{0/0} mice.

Western blots of caspase-3 and -9 revealed neither strain- nor age-dependent changes of expression levels in mAPP^{0/0} or mAPP^{+/+} mice. (β-actin served as loading control).

4.1.9 Correlating results

To collectively analyse the obtained parameters, nonparametric Spearman correlation coefficients were calculated (Table 7-12, Table 7-13). The first obvious and logical observation was that insoluble Aβ₄₂ correlates generally more with plaque size and number than did soluble Aβ₄₂.

As previously observed, the microglial coverage of plaque strongly depends on the amount of cortical plaques. Accordingly, the higher the amount of amyloid deposits was, the smaller the average microglial coverage of plaques became.

The most prominent differences between correlation coefficients involved astrocytes. It was particularly striking, that insoluble Aβ₄₂ showed a moderate positive correlation with astrocytic coverage in mAPP^{0/0} mice ($r_s = 0.64$), whereas it correlated negatively in mAPP^{+/+} mice ($r_s = -0.54$). Furthermore, microglial and astrocyte coverage correlated positively in mAPP^{+/+} mice ($r_s = 0.60$) and negatively in mAPP^{0/0} mice ($r_s = -0.78$).

4.2 Octodon degus

To determine the adequacy of using the South American rodent *Octodon degus* (degu) as model of sporadic AD, cortices and hippocampi of young (1-year-old) and aged (5-year-old) animals were histologically analysed. Basic stains were used for the general comparison of young and aged brains. To detect histopathological hallmarks of AD, unspecific stains were performed to provide first evidence for neurodegeneration in aging animals. Immunohistochemical stains were further utilised to specifically identify aggregates of A β and phosphorylated tau. The cellular responses to potential protein aggregation and neurodegeneration were finally estimated by analysing the age-dependent changes in spatial distribution and abundance of astrocytes and microglial cells.

4.2.1 Absence of unspecific signs of neuropathological changes

Principal histologic staining with haematoxylin and eosin (H&E) provided a general overview of age-dependent changes in the degu brain. However, H&E stains showed no prominent deviations between young and aged animals. Unspecific signs for lesions, neurodegeneration, pronounced neuronal loss or spatial displacement were not apparent (Figure 4-12). To screen more specifically for extracellular plaques and intracellular tangles, Campbell-Switzer silver impregnation was performed. But even intense staining unravelled neither plaques nor tangles in cortices and hippocampi of young or aged animals (Figure 4-12). The fluorescent amyloid-binding dye thioflavin T (ThT) was also utilised to expose amyloid deposits, but no specific fluorescence was apparent in cortices or hippocampi (Figure 4-12).

GFAP was used as astrocytic marker, to evaluate their abundance and spatial distribution. In young degus, GFAP⁺ cells were comparatively rare in cortices and mainly located in the superficial region of lamina I and the vicinity of blood vessels (Figure 4-13). In the hippocampus, GFAP⁺ cells were mainly located in alveus, stratum lacunosum-moleculare and the vicinity of blood vessels of the hippocampal fissure. GFAP⁺ astrocytes without a visible link to a blood vessel were rarely found in cortical laminae II - VI or hippocampal stratum oriens and stratum radiatum. In aged animals, neither abundance nor spatial distribution was notably changed compared to young degus (Figure 4-13). IBA1 was used as marker, to screen for age-dependent changes in microglial phenotype, abundance and spatial distribution. Stained sections demonstrated an even distribution of microglial cells in cortex and hippocampus of young and aged animals, without any local clustering (Figure 4-13). Phenotypically, small cell bodies and long branched processes were characteristic. To compare the neuronal density, brain sections were immunostained for neuronal marker NeuN, but no obvious differences were evident between young and aged animals.

The digitised slides stained for GFAP, IBA1 and NeuN were finally semi-automatically evaluated. However, no significant differences were apparent between young and aged animals (Table 7-14).

The astrocytic and microglial area even tended to be lower in aged animals and the neuronal density was likewise unchanged between young and aged degus (Figure 4-13).

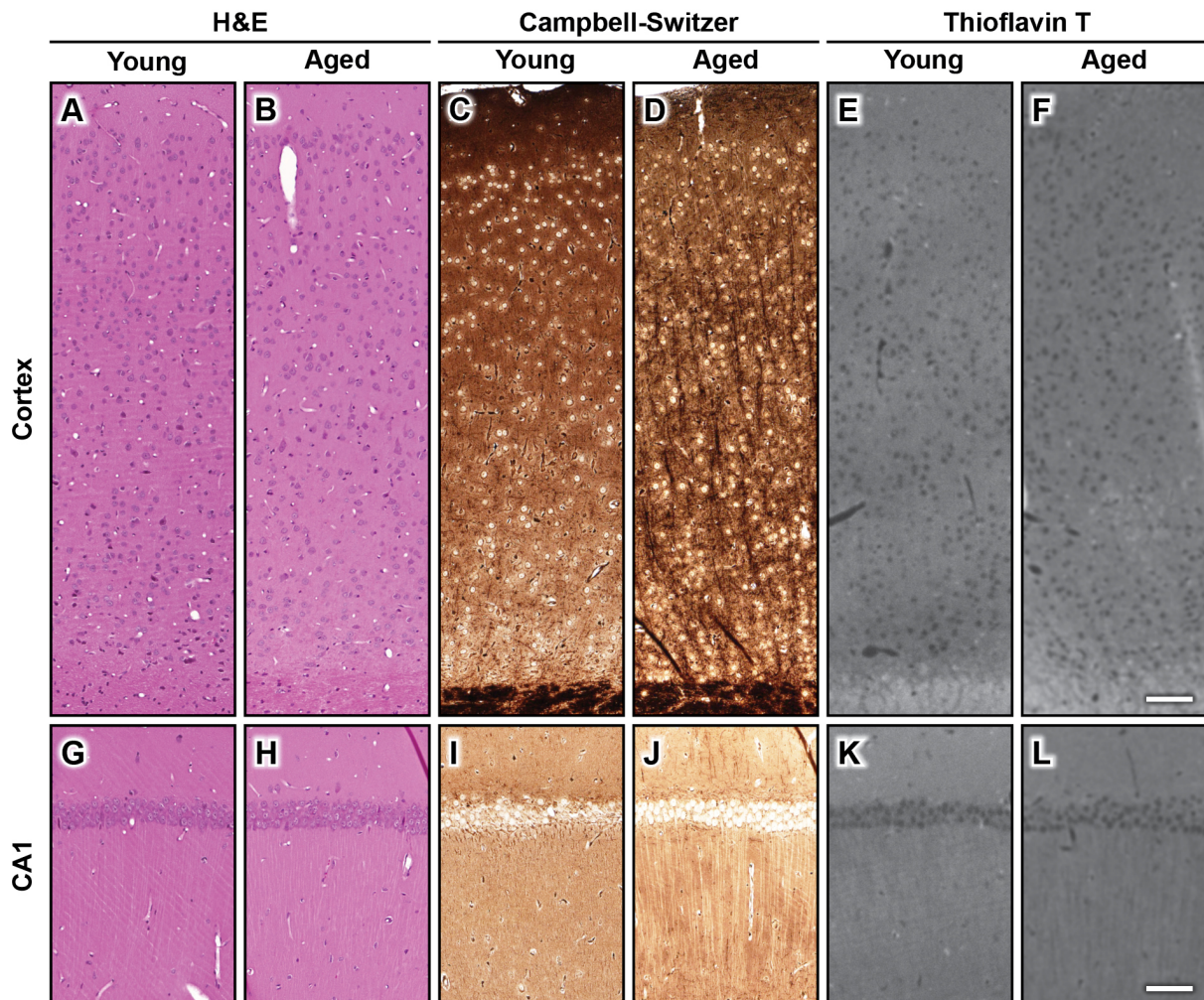


Figure 4-12: Basic histological stains provide no evidence for any neurodegeneration in degus.

Representative haematoxylin and eosin (H&E) stained sections revealed no signs for specific lesion, generalised neuronal loss or degeneration in cortex (A, B) or hippocampal CA1-region (G, H) of degus. Campbell Switzer silver impregnation displayed neither extracellular deposits nor intracellular tangles in young (C, I) or aged (D, J) animals. Accordingly, no specific cortical (E, F) or hippocampal (K, L) fluorescence could be detected in thioflavin T stained sections. (Scale bars = 100 μ m).

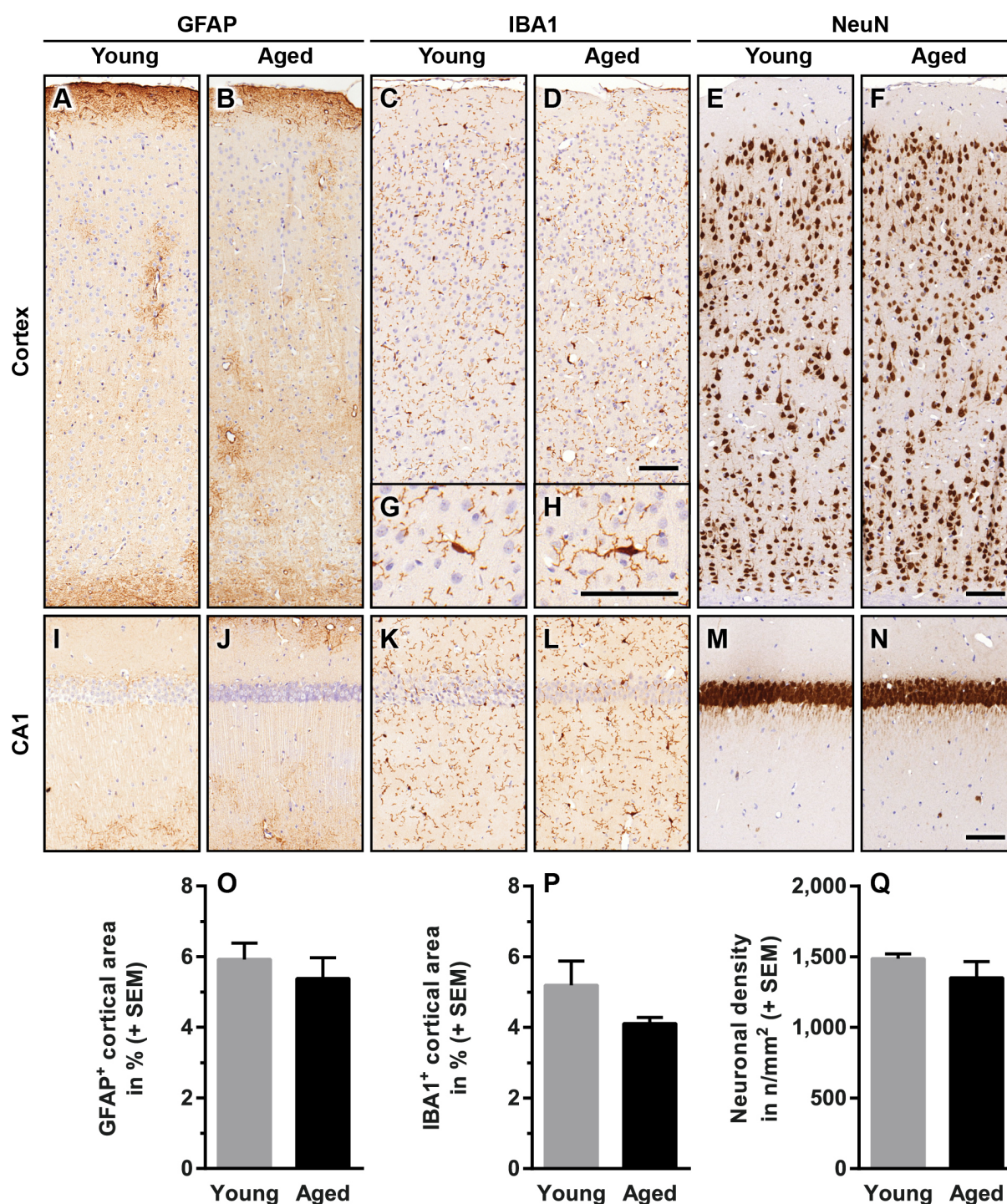


Figure 4-13: Absence of age-dependent astrocytic, microglial and neuronal changes in degus.

Representative cortical (A – H) and hippocampal (I – N) sections of young and aged degus demonstrate the lack of specific, age-dependent alterations. Astrocytes (GFAP⁺) were mainly located in cortical lamina I (A, B) and the proximity of blood vessels (A, B, I, J). Their spatial distribution and abundance (O) did not change with age. Microglia (IBA1⁺) were evenly distributed in cortices (C, D) and hippocampi (K, L) without any clustering and presented with long, branched processes and small cell bodies (G, H). The cortical area covered by microglial cells did not significantly change with age, but rather tended to decrease (P). Neuronal density (NeuN⁺) was likewise not notably changed in cortices (E, F) and hippocampi (M, N) of young and aged animals. Computer-assisted evaluation of slides confirmed this observation and indicated a similar neuronal density in young and aged degus (Q). (Scale bars = 100 μ m, unpaired t-test with Welch's correction was used for statistical analysis).

4.2.2 Lack of amyloid deposition in degus

Immunohistochemical methods are more sensitive and preferably used for detection of A β . Commonly employed and well-established antibodies against three different epitopes of A β were used for detection of potential deposits. The epitope of anti- β -amyloid clone 6E10 (amino acids 3 - 8) is located N-terminally of the H13R substitution in degu A β . Usage of clone 6E10 resulted in similar levels of unspecific background staining and further showed limited intracellular reactivity in cortices and hippocampi of all young and aged animals (Figure 4-14). However, extracellular reactivity (e.g. plaques) was not apparent.

The epitope of clone 6F3D includes the region of the H13R substitution (amino acids 8 - 17), but the corresponding slides indicated neither intra nor extracellular deposition of amyloid (Figure 4-14). The epitope of the third antibody (clone 4G8) is located C-terminally of position 13 (amino acids 18 - 22). Likewise, no aggregates could be detected in cortices and hippocampi of young or aged animals (Figure 4-14).

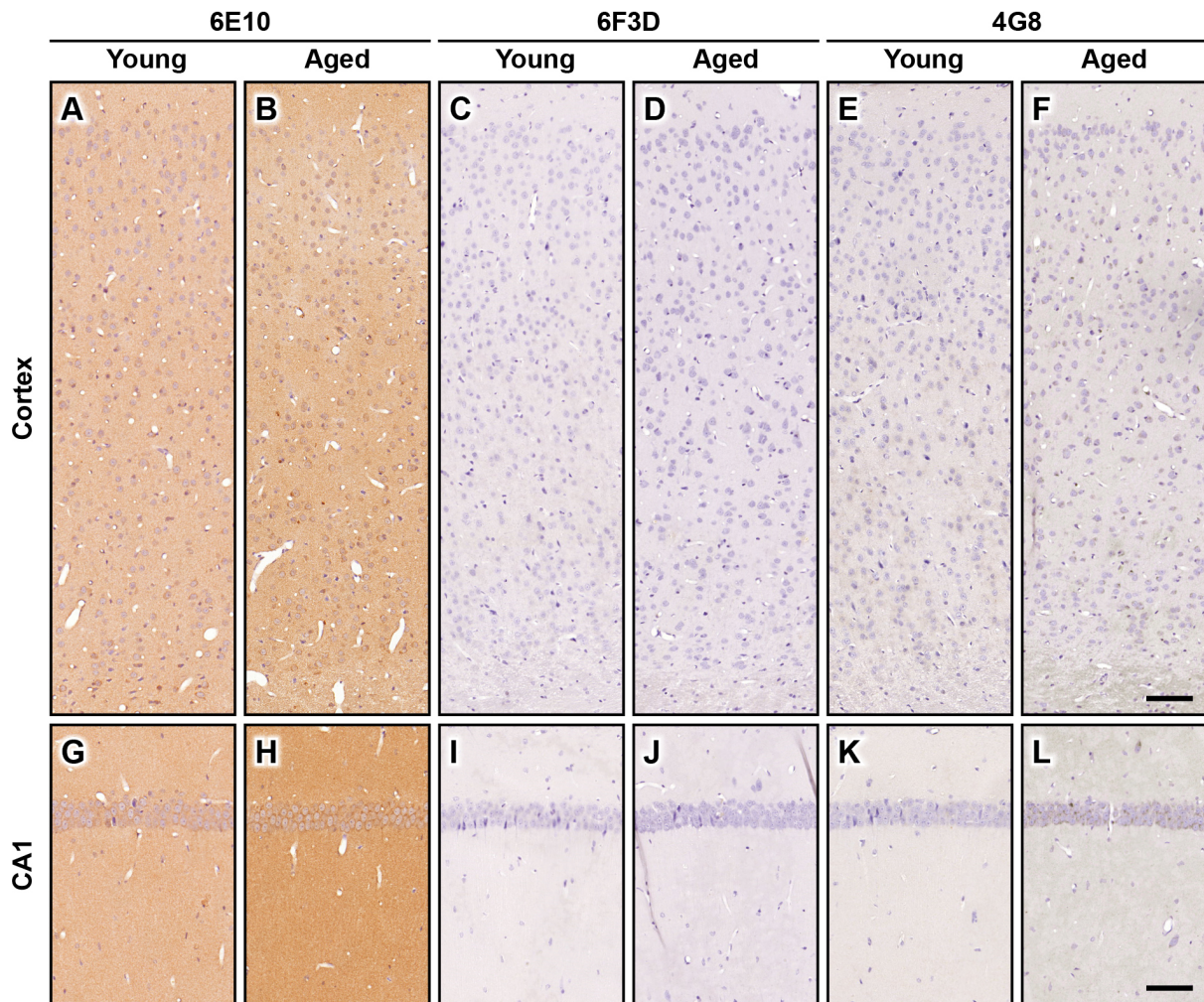


Figure 4-14: Degus display no signs of extracellular β -amyloid deposition.

Representative micrographs of A β -stained cortical (A - F) and hippocampal (CA1-region, G - L) sections of young and aged degus. Anti- β -amyloid antibody clone 6E10 revealed sparse intracellular reactivity, but no extracellular deposits in young (A, G) and aged (B, H) animals. By contrast, neither 6F3D nor 4G8 demonstrated any intra- or extracellular reactivity in young (C, I, E, K) or aged (D, J, F, L) degus. (Scale bars = 100 μ m).

4.2.3 Age-independent tau pathology in wild-type degus

Three antibodies directed against particular phosphoepitopes of tau were used to screen for neurofibrillary tangles in degus. Despite the overall differences between human and degu tau, the phosphorylation sites and adjacent amino acids are identical (Table 7-1). The anti-tau antibody clone AT8 recognises the phosphorylation of residues Ser²⁰²/Thr²⁰⁵ and labelled cortical and hippocampal neurons with a similar intensity in young and aged animals (Figure 4-15). Hippocampal reactivity was thereby more pronounced in CA3-region and mossy fibres. Although AT100 (Thr²¹²/Ser²¹⁴) showed mainly nuclear localised reactivity in cortex and hippocampus, the particular reactivity against the mossy fibres in CA3-region was preserved. AT180 (Thr²³¹) showed again intracellular reactivity in cortical and hippocampal neurons and a slight accentuation of hippocampal mossy fibres (Figure 4-15).

In sum, phospho-tau reactivity was not restricted to specific regions, but appeared in cerebral cortex, hippocampus, thalamus, hypothalamus, brainstem and cerebellum. Intensity was consistently higher in hippocampal CA3-region compared to CA1- and cortical regions. Furthermore, neither intensity nor spatial distribution of labelled epitopes was notably changed between young and aged animals. Finally, the intracellular reactivity of cortical and hippocampal neurons seen in AT8 and AT180 stained sections did neither spatially nor morphologically resemble the characteristics of neurofibrillary tangles.

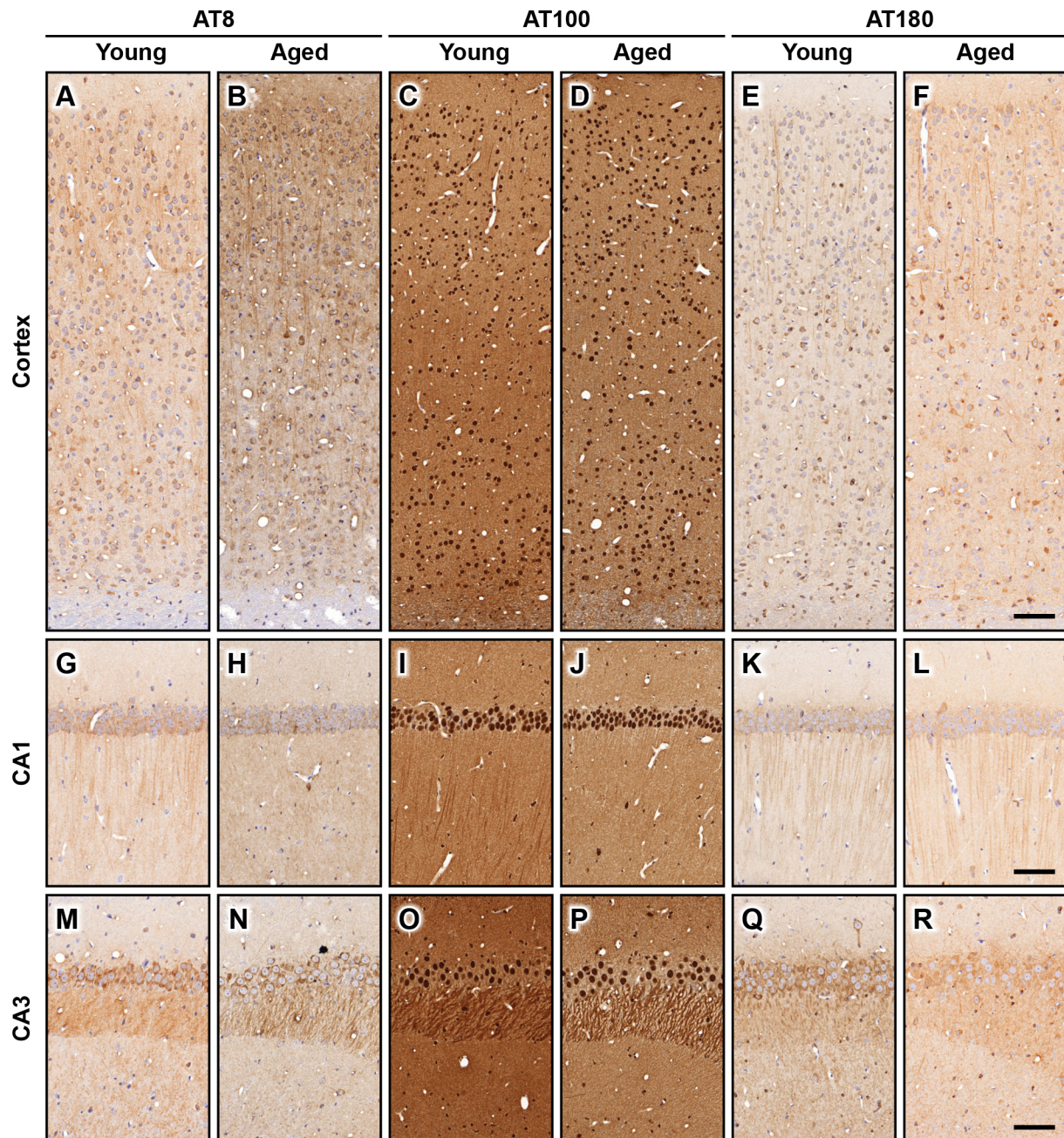


Figure 4-15: Degus lack age-dependent tau pathology.

Sections were stained using phosphoepitope specific antibodies against tau. Representative micrographs of cortices (A - F) and hippocampi (CA1-region: G - L, CA3-region: M - R), revealed no obvious differences between young and aged animals. AT8 labelled cortical (A, B) and hippocampal (G, H, M, N) neurons with similar spatial distribution and intensity in young and aged animals. AT8-reactivity was thereby more pronounced in CA3-region and mossy fibres (M, N). AT100 stain resulted in strong background and nuclear localised reactivity in cortex (C, D) and hippocampus (I, J, O, P), mossy fibres of hippocampal CA3-region were again specifically labeled (O, P). Stains using AT180 showed an analogical intracellular reactivity in young (E, K, Q) and aged (F, L, R) degus with visible but yet diminished accentuation of mossy fibres (Q, R). (Scale bars = 100 μ m).

5 Discussion

Extracellular plaques and intracellular neurofibrillary tangles are the major histopathological hallmarks of Alzheimer's disease. The importance of β -amyloid deposits was already very early hypothesised^[194], and later on supported by inherited mutations^[136, 137] which increased production or enhanced aggregation propensity of $A\beta$ ^[93]. These disease-causing mutations are constrained to the amyloid precursor protein and its proteases^[37]. Even the only protective mutation known so far affects *APP*^[109, 110]. But the causal role of plaques was questioned when evidence emerged showing that disease progression correlates better with soluble than with aggregated $A\beta$ ^[195]. Today, small soluble oligomers are mainly considered the primary toxic species^[27].

To elucidate causes, influential factors and to develop therapeutic strategies, a broad range of different and most commonly murine disease models is utilised for research. The obstacle that mice not physiologically develop amyloid deposits was quickly overcome by overexpression of mutant human transgenes. The characteristic manifestation and especially the extent of $A\beta$ deposition in these disease models depends strongly on the introduced promoter and APP variant. The herein used model is quite representative, as the promoter, transgenes, mutations and genetic background are very frequently utilised for the creation of AD models. The mice express *APP_{swe}* and *PS1_{L166P}* transgenes postnatally in neurons of the neocortex, hippocampus and brain stem and less pronounced the striatum and thalamus by Thy1-promoter^[173]. As in nearly all other models, the transgenes are expressed in addition to endogenous murine variants. The ratio of endogenous murine and transgenic human APP is about 1:3 in the analysed model^[173]. Despite their potential importance, interactions between murine and human APP have rarely been addressed so far. Considering transgenic models as a decisive indicator for further research and therapeutic strategies, the precise reproduction of the aggregation process in the utilised models is of paramount importance. The present study therefore aimed for deciphering and estimating the effects of endogenous murine APP in transgenic models of Alzheimer's disease.

Although the utilised animal models of Alzheimer's disease are constantly refined and replaced, most of them are still based on overexpression of mutant human proteins. Despite all accompanied successes, the overexpressed proteins introduce only a limited number of AD associated symptoms. Furthermore, they pathogenetically rather mimic the rare inherited variants than the generally occurring sporadic form. Suitable models of the sporadic disease are therefore urgently required.

The South American rodent *Octodon degus* has been the most promising rodent candidate model of sporadic AD. Degus have a long lifespan and their $A\beta$ is very similar to the human variant, differing in only one amino acid. Initial analyses of degus supposed, that aged animals 'naturally develop a full range of AD-like pathologies including $A\beta$ plaques and neurofibrillary tangles'^[181]. These results were

enthusiastically noticed^[184] and degus attracted increasing attention. However, analyses of the neurodegenerative changes in degus are still rare and not consistent. To determine the adequacy of employing degus as 'natural model' of Alzheimer's disease, the second part of this study intensively analysed histopathological changes in aging degus.

5.1 Murine APP-deficient mice

Although APP-deficient mice are viable and fertile, they display a number of abnormalities that should be kept in mind for the evaluation of the results. Animals present with a reduced body weight^[188, 196-198], weakened forelimb grip strength^[188, 196, 198], diminished locomotor activity^[188, 196, 198] and reduced brain weight^[199]. Interestingly, the impact of an APP knockout strongly depends on the genetic background^[199]. The developmental consequences (size reduction of ventral hippocampal commissure and corpus callosum) were substantially reduced by the C57BL/6 genetic background compared to 129/Sv and 129/Ola strains^[199]. APP-deficient mice further develop a marked and age-dependent cortical^[188, 196] and hippocampal gliosis^[200] with variable onset and progression. At the cellular level, dendrites were shown to be shorter, less branched and possess a reduced density of dendritic spines^[82, 201]. Hence, long-term potentiation was age-dependently^[201] impaired^[196]. Branching and number of dendritic spines was partially rescued by sAPP α but not sAPP β treatment^[201]. In striatal GABAergic neurons, an absence of APP lead to dysregulation of calcium channels (namely upregulation of Ca_v1.2)^[202]. The cellular abnormalities entailed behavioural changes, as spatial learning (water maze^[196, 197]) and memory (passive avoidance^[198]) were impaired. No differences were seen in thermal nociception^[196], motoric functions (visible platform water maze and rotarod test^[196]) and exploratory behaviour^[198]. At the neuromuscular junction, APP is necessary in both, motor neurons and muscle cells, for proper formation and function of the neuromuscular junction^[81]. Together with its role in regulating voltage-dependent calcium channels^[203], this explains the lower grip strength in APP knockout mice. Beside the focused role in the central nervous system, APP and its metabolites have additional functions various organs (reviewed in^[204]). It is interesting to note that despite the functional overlap of APP paralogues, there is no evidence for a compensatory upregulation of either APLP1 or APLP2 in APP-deficient mice^[188]. Although these phenotypic alterations are comparatively mild, especially in the C57BL/6 strain, they considerably restrict the spectrum of reasonable experiments.

As the APP-deficient mice in this study expressed high levels of human APP, a partial compensation of the missing endogenous APP can be speculated. But the mitigation of the described symptoms would likely be restricted by the Thy1-promoter, expressing transgenes only postnatally in neuronal cells^[173]. However, from the aforementioned abnormalities, the reported astrogliosis was the most critical factor for the conducted experiments in this particular study.

5.1.1 Impact of murine APP expression on plaque and amyloid load

Overall, murine APP-deficiency significantly altered the cortical deposition of β -amyloid. The onset of the amyloidosis was not substantially changed in mAPP^{0/0} mice because A β deposition starts rapidly upon activation of the utilised Thy1^[173]. Due to the missing expression of endogenous APP, the total

amount of APP is generally lowered about one-fourth in mAPP^{0/0} mice^[171, 173]. But despite decreased total APP, deposition of A β was accelerated in murine APP-deficient mice, especially upon its onset in young animals. This is surprising because murine A β was so far assumed to contribute to plaque deposition^[171], as plaques of transgenic mice consist of both, human and about 5% endogenous murine A β ^[171, 205]. An alteration of the general aggregation propensity would be a possible explanation for the evidently increased deposition of β -amyloid in mAPP^{0/0} mice. As murine A β does not aggregate under physiological conditions^[113, 206], it could impede the aggregation of overexpressed human A β to a certain extent. A similar effect was observed in heterozygous carriers of a rare human APP mutation. The A2V-mutated form of A β slowed the aggregation process of wild-type A β and generated aggregates were far more unstable^[108]. The human A2T variant of A β likewise increases solubility, when mixed with wild-type A β ₄₀ at certain ratios^[207].

Surprisingly, *in vitro* generated mixed fibres of murine and human A β were reported to be more stable than fibres consisting only of human A β ^[208]. This is completely contradictory to *in vivo* results, showing that plaques generated in various transgenic mouse strains (APP/PS1^[113], APP23^[209] or Tg2576^[205, 210]) are generally by far more soluble than those of AD patients. The additional overexpression of murine APP in transgenic APP/PS1 mice accordingly further increased the solubility of generated deposits, but neither accelerated nor increased deposition of human A β ^[113]. Despite its presence in the generated deposits and thus contribution to plaque load, a promoting role of murine A β is therefore unlikely. The present study showed that mean size and growth of individual plaques hardly depend on murine APP expression (section 4.1.1). Hence, murine A β did not critically influence aggregation speed at the level of a single plaque. But as the lack of endogenous murine APP led to the generation of vastly more plaques, the initiation of aggregation may be a depositional bottleneck in transgenic animals where murine A β interferes. This conclusion is in line with previous results, showing that a conformational change during the intermediate aggregation phase of A β renders the process relatively independent of the initial concentration^[29]. It is conceivable that murine A β interferes at this point, as primary and secondary structure is of crucial importance for the conformational change and the subsequent oligomerisation^[29].

However, additional processes related to production, degradation and removal might also contribute to the increased A β deposition to a certain extent. Firstly, an enhanced transgene expression would be possible, though unlikely explanation, because no APP-dependent regulation is known for the utilised Thy1.2-promoter^[211, 212] and Thy1-immunoreactivity even decreases in AD^[213]. The generation of A β is controlled by different proteases, but western blot analysis showed that the expression of the most important proteases is unchanged. Furthermore, utilised mice principally overexpress mutated human presenilin 1, which already expedites the generation of A β . Although APP gene dosis

is generally of crucial importance^[214], the missing competition of murine and human A β for cleavage enzymes most likely facilitates A β deposition to a certain extent^[215, 216].

Immunoassays confirmed the significant influence of endogenous APP expression on the amount of total and deposited (guanidine soluble) cortical A β . Interestingly the levels of soluble A β_{42} (buffer-soluble) initially rose slightly stronger in mAPP^{0/0} mice, indicating an altered A β metabolism (production/elimination). After reaching a peak at 100 to 125 d of age, levels of soluble A β_{42} decreased again and were finally even lower in mAPP^{0/0} mice, underlining the overall enhanced solubility of A β . When comparing plaque load (immunohistochemically determined; section 4.1.1) and amyloid load (biochemically determined; section 4.1.2), it is striking that the difference between mAPP^{0/0} and mAPP^{+/+} mice is more pronounced for plaque than for amyloid load (66% increase in plaque load vs. 27% in amyloid load at 200 d of age, Table 7-3, Table 7-11). The smaller difference in amyloid load can be at least partially explained by the utilised antibodies. While the anti-A β clone 6F3D used for immunohistochemical stains is human-specific, the clone 4G8 from the immunoassays recognises both, human and murine A β . On the contrary, murine A β contributes little to deposits in transgenic animals^[171, 205]. Nevertheless, murine APP-deficiency increased levels of insoluble and decreased levels of soluble A β_{42} in old mice (e.g. +40% soluble and -45% insoluble A β_{42} at 200 d, Table 7-11). These observations plead for the hypothesis of a generally enhanced solubility of A β by simultaneous expression of murine APP in transgenic mice.

Similar observations were made for other proteins that accumulate and aggregate in neurodegenerative diseases. Although endogenous murine tau only sparsely contributes to aggregates in tau transgenic mice^[217], wild-type human tau accumulates solely in the absence of murine tau (in 8c^[163] genetic background)^[162, 166]. Despite the high expression of human tau in 8c mice, no pathological signs were apparent in the presence of murine tau^[162, 163]. Accordingly, the knockout of murine tau facilitated aggregation of mutated human tau and accelerated mortality^[217] in Tg30^[218] mice. The aggregation of α -synuclein, which is implicated in Parkinson's disease^[219] and dementia with Lewy bodies^[220], is inhibited by highly similar β -synuclein^[221]. Another example is the single amino acid substitution in the prion protein found in Fore from Papua New Guinea, which makes them resistant to kuru and classical Creutzfeldt–Jakob disease^[222].

5.1.2 Increased amyloid solubility exacerbates cortical amyloid angiopathy

The expression of murine APP in APP/PS1 transgenic mice expedited the deposition of A β in the walls of leptomeningeal blood vessels (section 4.1.2). Despite the lower amount of A β , young mAPP^{0/0} mice showed a faster developing cerebral amyloid angiopathy, which is thereby opposed to cortical deposition of amyloid. As A β solubility is increased by murine APP expression^[113], generated A β is increasingly subjected to clearance and degradation, including active transport across the blood-

brain barrier. The aggravated CAA might therefore be a result of an overcharged vascular clearance of A β . A similar exacerbation of CAA appeared, when activity or expression of A β transporting proteins like LRP1^[223] or ABCC1^[88] was diminished. Although the used mouse model generally displays only moderate cerebral amyloid angiopathy^[173], the effect of murine APP expression on CAA was clearly evident. The conclusion of an increased solubility as cause of the aggravated CAA is also supported by previous results. In APP/PS1 transgenic mice, the additional overexpression of murine APP further increased A β solubility and enhanced its deposition in vessel walls^[113].

5.1.3 Impact of cellular amyloid clearance

In AD, amyloid plaques are surrounded by astrocytes and microglial cells^[20]. Although this has been long perceived, their role was long debated due to their complex actions. Microglia are nowadays thought to play a changing role during disease progression. They participate in amyloid clearance and eliminate soluble^[54] and fibrillary^[55] forms of A β . However, microglial cells also contribute to neuronal death, as their chronic activation in AD leads to the release of reactive oxygen species^[56], tumor necrosis factor- α ^[224] and nitric oxide^[57].

The pool of cortical microglial cells seemed unchanged upon knockout of murine APP as the total cortical area covered by microglia was similar in mAPP^{0/0} and mAPP^{+/+} mice. With beginning aggregation of A β , plaques became increasingly surrounded by microglial cells. Microglial plaque coverage strongly progressed with age in young animals. But after reaching a peak at 150 d of age, the relative coverage decreased. This general course of microglial plaque coverage has been previously described for the utilised model^[225] and might be the results of an exhausted microglial capacity, while amyloid deposition continues unabatedly. Furthermore, total microglial area typically decreases age-dependently, a process which is dramatically accelerated in AD-models^[226]. Methodically, the results of double-stained slides strongly depend on the intensity ratio of individual stains and fluctuations would heavily affect the results. Although sections were collectively stained fully automated in large batches and the general course of microglial plaque coverage is similar in both groups, a certain influence of staining intensity cannot completely be excluded.

The lack of murine APP expression consistently decreased the microglial coverage of plaques at all ages. The cause for this reduction can only be speculated, because different explanations are reasonable and various factors likely interact. Firstly, the higher number of plaques contributes at least to a certain extent to the lower coverage, since the limited number of microglia distributes to an increased number of plaques in mAPP^{0/0} mice. But despite the similar size of the microglial populations, the proportion of plaque-associated microglial cells is lower in mAPP^{0/0} mice at all ages. The elevated number of plaques is therefore unlikely the only reason for the decreased coverage.

As microglia are able to clear A β , a reduced number or an impaired activation could directly diminish clearance and cause the enhanced deposition. However, the actual extent of microglial contribution in AD pathogenesis is constantly debated. A beneficial role in AD is exemplified by progranulin (PGRN), as reduced expression lowered phagocytic activity and increased amyloid burden in AD mouse models^[60]. Although knockout of microglial fractalkine receptor (CX3CR1) likewise exacerbated AD-related deficits, plaque load was unchanged^[227]. The chronic inflammatory response that accompanies the persistent microglial activation is, on the other hand, primarily considered aggravating and even affects amyloid levels. The interruption of the interleukin-12/interleukin-23 pathway, which is activated in microglia in response to A β , decreased the amyloid burden in transgenic AD mice^[228]. The immunosuppressant rapamycin reduced microglial activation but simultaneously enhanced autophagy and degradation of A β and thus reduced amyloid burden and prevented memory decline^[229]. Epidemiologic studies also supported negative effects of inflammation, as the use of nonsteroidal anti-inflammatory drugs (NSAIDs) decreases the incidence of AD^[230]. The near-complete ablation of microglia in transgenic APP/PS1 mice stressed their janus-faced character in AD, as their absence generally affected neither plaque deposition nor neuritic dystrophy^[231]. Overall, beneficial and deteriorating effects of microglia seem therefore balanced. Although the consequences of the altered microglial reaction can be hardly estimated in the utilised model, they are unlikely the main cause of enhanced A β deposition, especially with regard to decreased CAA.

Finally, microglia and astrocytes are shown to interact and influence each other^[232]. The release of ApoE by astrocytes^[233], for instance, is crucial for microglial clearance of fibrillar A β ^[234]. In APP/PS1 mice, activated astrocytes were shown to suppress the recruitment and activation of microglia^[64]. Thus, attenuation of reactive gliosis increased the abundance of microglial cells in the vicinity plaques and elevated cortical expression of microglial markers CD11b and IBA1^[64]. The knockout of APP has been repeatedly described to induced reactive gliosis in mice^[188, 196, 200]. Despite the expression of human APP, the mAPP^{0/0} mice displayed a significant age-related gliosis (section 4.1.6). Diminished recruitment and decreased elimination of A β by microglia would therefore be a conceivable result. The correlations of the results (section 4.1.9) underpinned the dysregulation of astrocytes in mAPP^{0/0} mice. Cortical astrocyte coverage correlated positively with microglial plaque coverage in mAPP^{+/+} mice, indicating a mutual inflammatory recruitment. Whereas the negative correlation in mAPP^{0/0} mice demonstrated, that the pronounced astroglia was accompanied by a diminished microglial plaque coverage.

A reactive gliosis is also a frequent histopathological feature in AD^[61]. Analogous to microglia, astrocytes thereby not only surround amyloid plaques but ApoE dependently^[235] bind and degrade A β ^[63]. Attenuated reactive gliosis by knockout of GFAP and vimentin (Vim) thus increased plaque

load in APP/PS1 mice^[64]. As GFAP^{0/0}/Vim^{0/0} astrocytes were barely found near plaques, the direct interaction of astrocytes and plaques was hypothesised of fundamental importance for astrocyte dependent amyloid clearance^[64]. Activation of astrocytes by overexpression of murine interleukin-6^[65] or interferon- γ ^[66] in APP transgenic mice induced a pronounced gliosis, promoted microglial phagocytosis and thus decreased plaque load. The distinct gliosis in murine APP-deficient mice might therefore not necessarily promote the deposition of A β .

As previously described, A β is actively cleared from the brain at the BBB^[88] and astrocytes substantially contribute to induction and maintenance of basal BBB properties (reviewed in^[236]). Astrocytes cover capillaries with their endfeet^[237] and induce expression of tight junctions^[238] and ABC-transporters^[239]. Astrocyte-dependent disturbances at the BBB might therefore also contribute to the increased plaque load in murine APP-deficient mice. In summary, due to their various functions and high abundancy^[240, 241] even slight dysregulation or subtle changes in astrocytes could strongly influence A β accumulation.

5.1.4 Neuronal density and apoptosis

The amyloid precursor protein has important developmental and maintenance functions in the brain, e.g. promoting proliferation^[70], differentiation^[77] and migration^[79]. The APP/PS1 transgenic mice lacking murine APP may suffer from the dual effect of missing beneficial APP functions in neuronal development, complemented by negative effects of the age-dependent A β aggregation.

However, the density of cortical neurons was not significantly altered in APP-deficient mice. Additionally, the expression of caspase-3 and -9 was neither genotype- nor age-dependently changed, emphasising the absence of enhanced apoptosis in mAPP^{0/0} mice at the analysed ages. This is in accordance with the previous results, showing that neuronal loss is not evident until eight months of age in the utilised mouse model^[173].

5.1.5 Perspective and implications for research

For the treatment of Alzheimer's disease five symptomatic^[242] medications have been so far approved by the FDA^[243]. These are acetylcholinesterase inhibitors (donepezil, rivastigmine and galantamine), a NMDA receptor antagonist (memantine) and, since recently, a combination of both (donepezil and memantine)^[243]. Causal therapeutics are still in development and have not been approved so far^[242]. Most of the causal therapeutic strategies are directed against amyloid and can be divided by three general mechanisms of action: (i) inhibition of production, (ii) prevention of aggregation and (iii) promotion of clearance^[244]. The latter two thereby exceptionally depend on the exact reproduction of the aggregation process in the utilised models. A decreased aggregation propensity not only restricts amyloid accumulation, but makes A β more available for degradation^[207]

and therefore promotes elimination. The extent of aggregation interference^[245, 246], peripheral^[247] and central^[248] degradation or efflux by LRP1^[86] and different ABC-transporters^[87, 88] might therefore been estimated inaccurately. Because murine APP and its products could interference with A β deposition and decisively influence the obtained results, the co-expression of endogenous APP impedes transferability between species and spreads uncertainty.

The logical alternative would be the use of A β -humanised mice as background for transgenic models. Although the mutagenesis of murine APP has already been reported a long time ago^[206, 249], it attracted only little interest so far. The humanisation of APP at the three sites differing between murine and human A β (positions 5, 10 and 13) increased the production A β to the level of the human sequence^[206]. In the TgAPP^{Swe-KI}^[249] model, humanisation of the three amino acids is complemented by the Swedish *APP* mutation [KM670/671NL]. That's why these mice express normal levels of human APP in absence of murine and already produce increased amounts of A β ₄₀ and A β ₄₂ without deposition^[250]. However, already the additional mutagenesis of murine PS1 [P264L] induced plaque formation by further elevating A β level and A β ₄₂/A β ₄₀ ratio and without any overexpression^[250-252]. This approach has the major advantage, that by keeping *APP* in its chromosomal position with the natural promoter, the developmental, cell- and tissue-specific expression pattern is preserved^[249].

5.2 Octodon degus

The degu (*Octodon degus*) is a small, diurnal, herbivorous rodent from central Chile^[253]. The high average lifespan (up to ten years) in captivity and the particular similarity to human A β (97.5% identical)^[182] made degus an interesting model for age-related diseases. Degus were subjected to AD research in recent years, whereby prominent intra- and extracellular A β deposits were described in cortices and hippocampi of wild type animals^[182, 254] upon two years of age^[254]. Thus, degus were the first rodents described depositing A β without any genetic modification. However, the knowledge on neurodegeneration in degus is so far sparse and the recent results are conflicting. To further elucidate the processes during natural aging in degus, this study histologically analysed degus with defined age, namely young (1-year-old) and aged (5-year-old) animals.

5.2.1 Natural aging without development of marked neurodegeneration

Basic histological H&E stains of degus revealed no obvious age-related changes, specific lesions or degeneration in any of the analysed brain regions. Such conflicting results have been previously described. Groen et al. reported the absence of specific neuronal differences between 3- and 6-year-old degus in Nissl-stained sections and a stable density of blood vessels^[255].

Silver impregnations and thioflavin T stains were performed in this study to reveal neuronal destruction and potential amyloidosis. But extended degeneration and extracellular aggregates were neither apparent in any of the analysed degus. More sensitive immunohistochemically stained sections of young and aged animals showed similarly sparse intracellular but no extracellular reactivity. Groen and colleagues likewise found no evidence for neuronal degeneration or significant age-dependent differences in degus^[255]. However, these results are completely contradictory to the initial description by Inestrosa et al., which found aggregates ubiquitously in all cortical layers and large thioflavin S positive plaques in frontal, parietal and entorhinal cortex and hippocampus upon three years of age^[182]. A most recent publication of Inestrosa's group reported a similar manifestation of ThS positive plaques even upon 24 months^[254], unfortunately, using the identical images initially published as 'over 3-year-old' degus^[182]. Finally, plaque deposition was proclaimed to start even earlier, as already twelve months old animals presented with several ThS positive plaques^[183]. Altogether, the generation of plaques in degus during normal aging is still questionable, as actually only one group was able to detect the deposits. To cap it all, aged degus were shown to generate large amounts of the heavily doubted^[256] dodecameric A β *56^[183].

Although degus have a higher degree of homology to humans in terms of A β than mice or rats, the distinct physiological aggregation previously described is surprising and contradicts a large body of conclusive data. The histidine at position 13 (His¹³), which is changed to arginine in degus^[182], is thought to be of crucial importance for aggregation and toxicity^[257, 258]. In human A β , His¹³ is involved

in early N-terminal β -sheet formation^[259] and thus its substitution by arginine [H13R] diminishes aggregation propensity and cytotoxicity^[260]. The [H13G] substitution further significantly lowered neuronal binding and related toxicity^[261].

The role of histidine 13 is well established regarding general^[29, 257] but also pH-^[262] and metal ion-^[263] dependent aggregation of A β . Coordination of metal ions such as nickel^[264], copper^[265], and zinc^[264] by β -amyloid requires His¹³. Interestingly, regions with zinc-enriched neurons are the primary sites for amyloid deposition^[266]. Accordingly, zinc was found to trigger aggregation of A β ^[267] and become enriched in plaques^[268]. In many rodents, A β has a significantly lower affinity for zinc and thus a lower aggregation propensity^[264], which is merely reproduced by the H13R substitution^[264, 265, 269]. The significance of zinc-induced aggregation is further highlighted by zinc transporter 3 (ZnT3), which loads Zn²⁺ to synaptic vesicles^[270]. The knockout of ZnT3 resulted in reduced A β deposition in cortices of Tg2576 mice^[271]. Copper is likewise enriched in plaques^[268] and promotes A β aggregation^[267, 272] by formation of high-affinity complexes^[273]. As His¹³ is crucial for Cu²⁺-binding^[265], H13R substitution^[274] or methylation of imidazole side chains^[258, 275] alter A β 's affinity for copper and thereby reduce its toxicity. The H13R substitution in degus thereby substantially reduces A β 's aggregation propensity compared to human A β .

The histidine-residues further regulate the redox activity^[276], as A β functionally binds metal ions at a superoxide dismutase-like binding site^[277] and subsequently generates toxic H₂O₂ by reduction of Cu²⁺^[277-279] or Fe³⁺^[279]. The generation of H₂O₂ and accompanied cytotoxicity of A β was prevented by either Cu²⁺ chelators^[277] or platinum complexes, which coordinate A β 's histidine residues^[280].

Because of its crucial importance for aggregation, His¹³ is a constant target for treatment strategies. A range of platinum^[280-282] iridium^[282, 283] and ruthenium^[282, 284, 285] based complexes have been developed, which interact with His¹³ and thus inhibit aggregation. The Zn²⁺/Cu²⁺-chelator clioquinol, which halved A β deposition in Tg2576 mice^[286], even reached phase IIb trial in 2004^[287, 288]. Clioquinol was afterwards abandoned due to the emergence of toxic by-products during synthesis. It was 'replaced' by second generation hydroxyquinoline, which entered phase IIa trials in 2006 for Alzheimer's disease^[289, 290] and in 2012 for Huntington's disease^[291].

These results further detail the crucial importance of histidine at position 13 of human A β . The substitution of histidine by arginine, which appears in most rodents, thereby interferes with various mechanisms of aggregation and cytotoxicity involved in AD pathogenesis.

It is therefore not surprising that the naked mole rat (*Heterocephalus glaber*), which has the same A β sequence as degus, does not develop plaques^[292]. Although, young naked mole rats naturally exhibit pronounced oxidative stress^[293] and high levels of A β , similar to those of 3xTg-AD mice^[292, 293]. However, the H13R substitution in their A β protects naked mole rats, because it significantly lowers the aggregation propensity of A β ^[292]. Even guinea pigs (*Cavia porcellus*), which have long been used

as research models^[294], have human identic A β ^[295] and a very similar APP processing^[296], do not develop dense amyloid deposits^[297]. In that light, plaque deposition in degus appears highly questionable.

5.2.2 Phosphorylation of cytoskeletal tau

The intracellular formation of neurofibrillary tangles, a hallmark of AD, was already part of the initial report on AD-like pathology in degus^[182]. At first glance, tangle formation in degus seems not unreasonable, because the tau-sequence is similar to the human variant. Degus further exhibit the 'VQIVYK' motif (Table 7-1), which is necessary for tau aggregation^[298] and only 2 deviations in the assembly domain of tau, compared to the human sequence ([A239T], [K257R], Table 7-1).

To unveil intracellular accumulation of hyperphosphorylated tau, sections were immunostained for phosphorylation of different tau epitopes. Beside a high background staining, intracellular reactivity was apparent in most cortical and hippocampal neurons of young and aged degus. But the labelled phospho-tau did neither morphologically resembled neurofibrillary tangles nor increased or intensified age-dependently. While tangles primarily affect entorhinal cortex or hippocampal CA1-region in AD^[19], degus showed strongest reactivity against phospho-tau in hippocampal CA3-region and mossy fibres. Furthermore, reactivity appeared consistently throughout the brain including in cerebral cortex, hippocampus, thalamus, hypothalamus, brainstem and cerebellum. A previous study by Groen et al. found only punctual tau accumulation in hippocampal axons of old (six years) animals, but likewise no tangles^[255]. By contrast, degus were initially described with intracellular aggregates of tau and ubiquitin in cortical and hippocampal areas upon three years of age^[182, 183].

However, it is important to note that tau phosphorylation in general is not specific for AD, but occurs also physiologically^[299] with important implications for development^[300] and plasticity^[301]. In naked mole rats which are closely related to degus, large amounts of phosphorylated tau are present without accumulation or generation of tangles^[302]. The high intracellular levels of phosphorylated tau therefore not necessarily constitute tangles or lead to their generation. Just like reported in this study for degus, the highest levels of phosphorylated tau in naked mole rats were located in hippocampal CA3-region (mossy fibres) and not in CA1-region or cortex^[302]. The particular phosphorylation of tau in CA3-region is contradictorily discussed^[303], as it rarely appears in animal disease models^[153].

5.2.3 Cellular clearance, molecular markers and cognitive defects

In AD, microglia and astrocytes gather in the vicinity of amyloid deposits. This clustering of activated cells is an early but unspecific sign of pathology. While a recent paper questioned the emergence of a cortical gliosis in degus^[304], they were originally described with an age-related increase of abundance and activation of hippocampal microglia^[255, 304] and an extended cortical and hippocampal astrogliosis^[182, 255]. Although astro- and microgliosis are unspecific signs for neurodegeneration that also appear in lesions of different genesis, they principally accompany the deposition of amyloid.

In the current study, microglial marker IBA1 revealed homologous populations of resting microglia in young and aged degus without any clustering. Astrocytes (GFAP⁺) were mainly located in cortical layer I and the vicinity of blood vessels. Age-dependent alterations in phenotype, density or spatial distribution, pinpointing to an inflammatory process, could not be detected for microglia or astrocytes. The lack of an age-dependent astro- or microgliosis in the analysed animals is thereby in line with the absence of other signs for related neuropathological changes.

5.2.4 Degus as model for natural aging

A further series of age-dependent and AD-linked changes has been reported for degus. Nucleoporin 62, a marker for AD, was reported to increase by more than 60% in old degus (> 4 year)^[304]. However, levels of nucleoporin 62 actually decrease in AD^[305] and elevated levels are considered protective^[306]. Furthermore, markers for reactive oxygen (4-Hydroxynonenal^[307]) and nitrogen species (nitrotyrosine^[308]) were increased in aged degus^[304]. Hippocampal levels of caspase-3 increased age-dependently in degus and indicated enhanced apoptosis^[304]. Long-term potentiation (LTP) and long-term depression (LTD) were also impaired in hippocampal neurons (CA1 - CA3-region) in 3 to 5 year old degus. Behavioural tests (T-maze and novel object recognition task) finally illustrated the age-dependent decline in memory performance^[183].

While this sounds plausible in connection with amyloid and tau pathology, it is of paramount importance to consider the specificity of the previously described changes of AD-linked markers in the particular experimental context. Although these characteristics occur in AD, they not only overlap with other neurodegenerative diseases, but also physiologically emerge in normal aging. Because young degus served as 'healthy' control for the aged animals with 'AD-like' symptoms, characteristics of normal aging should not be misinterpreted to model AD. Well established and frequently used behavioural tests (Morris water maze^[309-312], Barnes maze^[313] and Novel object recognition task^[310, 314]) revealed significant, age-dependent impairments in learning and cognition of aged, wild-type mice. Old mice further present with decreased performance in hippocampal LTP (CA1-region)^[309, 310, 313], increased frequency of apoptosis and higher levels of caspase-3^[309, 315]. The aforementioned markers for reactive oxygen and nitrogen species Hydroxynonenal^[316] and nitrotyrosine^[317] likewise

increase age-dependently. Interestingly, even levels of APP and sAPP β and the A β_{42} /A β_{40} ratio elevate with normal aging in wild-type mice^[315]. The described examples clearly show that these frequently applied tests and markers are only reasonable and significant if used in combination with appropriate controls. The previous approaches of using young animals as ‘healthy’ controls are problematic and questionable, as by definition, physiological aging is neglected and all alterations are regarded as disease symptoms.

5.2.5 Conclusion

The present study contributes basic knowledge and new insights on animal disease models with pathological aggregation of proteins. In mice, as the most important model species, the remaining expression of murine APP significantly changed the aggregation of transgenic human A β . The knockout of endogenous APP markedly increased the number of plaques, whereas vascular deposition of amyloid was simultaneously delayed. The levels of cortical A β_{42} were also generally higher in mAPP^{0/0} animals, but the difference was less pronounced. At the cellular level, murine APP-deficient animals presented with a notable, age-dependent gliosis and diminished microglial coverage of plaques. However, apoptosis markers and neuronal density were not significantly changed. Overall, the co-expression of endogenous APP in transgenic models was shown to decisively influence disease characteristics and therefore impedes the transferability of results to the human system. This study thereby not only demonstrated the necessity of re-evaluating and refining currently used models, but already presents a starting point for improvements.

The second part of the study focused on the small rodent *Octodon degus*, which was made a promising model as it was presumed to ‘naturally’ resemble the full pathological spectrum of Alzheimer’s disease. In this study, comprehensive histological analyses revealed no signs for extracellular aggregation of amyloid, the histopathological hallmark of the disease. Unspecific signs like astrogliosis, clustering of activated microglia or increased neuronal death were likewise non-existent. In sum, the present results indicate rather physiological aging than distinct neurodegeneration and therefore preclude the utilisation of degus as model of Alzheimer’s disease under the described conditions.

6 References

1. Przedborski, S., Vila, M., and Jackson-Lewis, V., *Neurodegeneration: what is it and where are we?* J Clin Invest, 2003. **111**(1): p. 3-10.
2. Jellinger, K. A., *Basic mechanisms of neurodegeneration: a critical update.* J Cell Mol Med, 2010. **14**(3): p. 457-87.
3. Jellinger, K. A., *Recent advances in our understanding of neurodegeneration.* J Neural Transm, 2009. **116**(9): p. 1111-62.
4. Amor, S., Peferoen, L. A., Vogel, D. Y., Breur, M., van der Valk, P., Baker, D., and van Noort, J. M., *Inflammation in neurodegenerative diseases--an update.* Immunology, 2014. **142**(2): p. 151-66.
5. Swart, C., Haylett, W., Kinnear, C., Johnson, G., Bardien, S., and Loos, B., *Neurodegenerative disorders: dysregulation of a carefully maintained balance? Exp Gerontol, 2014. 58: p. 279-91.*
6. Herczenik, E. and Gebbink, M. F., *Molecular and cellular aspects of protein misfolding and disease.* FASEB J, 2008. **22**(7): p. 2115-33.
7. Johri, A. and Beal, M. F., *Mitochondrial dysfunction in neurodegenerative diseases.* J Pharmacol Exp Ther, 2012. **342**(3): p. 619-30.
8. Invernizzi, G., Papaleo, E., Sabate, R., and Ventura, S., *Protein aggregation: mechanisms and functional consequences.* Int J Biochem Cell Biol, 2012. **44**(9): p. 1541-54.
9. Spillantini, M. G. and Goedert, M., *Tau pathology and neurodegeneration.* Lancet Neurol, 2013. **12**(6): p. 609-22.
10. Bennett, M. C., *The role of alpha-synuclein in neurodegenerative diseases.* Pharmacol Ther, 2005. **105**(3): p. 311-31.
11. Brettschneider, J., Del Tredici, K., Lee, V. M., and Trojanowski, J. Q., *Spreading of pathology in neurodegenerative diseases: a focus on human studies.* Nat Rev Neurosci, 2015. **16**(2): p. 109-20.
12. Alzheimer, A., *Über eine eigenartige Erkrankung der Hirnrinde.* Allgemeine Zeitschrift für Psychiatrie und Psychiatrisch-gerichtliche Medizin, 1907. **Jan**(64): p. 146-8.
13. Alzheimer's Association, *Basics of Alzheimer's Disease*, 2015, Alzheimer's Association.
14. Quiroz, Y. T., Schultz, A. P., Chen, K., Protas, H. D., Brickhouse, M., Fleisher, A. S., Langbaum, J. B., Thiyyagura, P., Fagan, A. M., Shah, A. R., Muniz, M., Arboleda-Velasquez, J. F., Munoz, C., Garcia, G., Acosta-Baena, N., Giraldo, M., Tirado, V., Ramirez, D. L., Tariot, P. N., Dickerson, B. C., Sperling, R. A., Lopera, F., and Reiman, E. M., *Brain Imaging and Blood Biomarker Abnormalities in Children With Autosomal Dominant Alzheimer Disease: A Cross-Sectional Study.* JAMA Neurol, 2015.
15. Brunnstrom, H. R. and Englund, E. M., *Cause of death in patients with dementia disorders.* Eur J Neurol, 2009. **16**(4): p. 488-92.
16. Ferri, C. P., Prince, M., Brayne, C., Brodaty, H., Fratiglioni, L., Ganguli, M., Hall, K., Hasegawa, K., Hendrie, H., Huang, Y., Jorm, A., Mathers, C., Menezes, P. R., Rimmer, E., Sczufca, M., and Alzheimer's Disease, I., *Global prevalence of dementia: a Delphi consensus study.* Lancet, 2005. **366**(9503): p. 2112-7.
17. Reitz, C., Brayne, C., and Mayeux, R., *Epidemiology of Alzheimer disease.* Nat Rev Neurol, 2011. **7**(3): p. 137-52.
18. Qiu, C., Kivipelto, M., and von Strauss, E., *Epidemiology of Alzheimer's disease: occurrence, determinants, and strategies toward intervention.* Dialogues Clin Neurosci, 2009. **11**(2): p. 111-28.
19. Serrano-Pozo, A., Frosch, M. P., Masliah, E., and Hyman, B. T., *Neuropathological alterations in Alzheimer disease.* Cold Spring Harb Perspect Med, 2011. **1**(1): p. a006189.
20. Suh, Y. H. and Checler, F., *Amyloid precursor protein, presenilins, and alpha-synuclein: molecular pathogenesis and pharmacological applications in Alzheimer's disease.* Pharmacol Rev, 2002. **54**(3): p. 469-525.
21. Coburger, I., Dahms, S. O., Roeser, D., Guhrs, K. H., Hortschansky, P., and Than, M. E., *Analysis of the overall structure of the multi-domain amyloid precursor protein (APP).* PLoS One, 2013. **8**(12): p. e81926.
22. Nicolas, M. and Hassan, B. A., *Amyloid precursor protein and neural development.* Development, 2014. **141**(13): p. 2543-8.
23. Zhang, Y. W., Thompson, R., Zhang, H., and Xu, H., *APP processing in Alzheimer's disease.* Mol Brain, 2011. **4**: p. 3.
24. Zhang, X., Li, Y., Xu, H., and Zhang, Y. W., *The gamma-secretase complex: from structure to function.* Front Cell Neurosci, 2014. **8**: p. 427.
25. Kummer, M. P. and Heneka, M. T., *Truncated and modified amyloid-beta species.* Alzheimers Res Ther, 2014. **6**(3): p. 28.
26. Thinakaran, G. and Koo, E. H., *Amyloid precursor protein trafficking, processing, and function.* J Biol Chem, 2008. **283**(44): p. 29615-9.
27. Haass, C. and Selkoe, D. J., *Soluble protein oligomers in neurodegeneration: lessons from the Alzheimer's amyloid beta-peptide.* Nat Rev Mol Cell Biol, 2007. **8**(2): p. 101-12.
28. Bitan, G., Kirkitadze, M. D., Lomakin, A., Vollers, S. S., Benedek, G. B., and Teplow, D. B., *Amyloid beta -protein (Abeta) assembly: Abeta 40 and Abeta 42 oligomerize through distinct pathways.* Proc Natl Acad Sci U S A, 2003. **100**(1): p. 330-5.
29. Garai, K. and Frieden, C., *Quantitative analysis of the time course of Abeta oligomerization and subsequent growth steps using tetramethylrhodamine-labeled Abeta.* Proc Natl Acad Sci U S A, 2013. **110**(9): p. 3321-6.
30. Berriman, J., Serpell, L. C., Oberg, K. A., Fink, A. L., Goedert, M., and Crowther, R. A., *Tau filaments from human brain and from in vitro assembly of recombinant protein show cross-beta structure.* Proc Natl Acad Sci U S A, 2003. **100**(15): p. 9034-8.

31. Bancher, C., Brunner, C., Lassmann, H., Budka, H., Jellinger, K., Wiche, G., Seitelberger, F., Grundke-Iqbal, I., Iqbal, K., and Wisniewski, H. M., *Accumulation of abnormally phosphorylated tau precedes the formation of neurofibrillary tangles in Alzheimer's disease*. *Brain Res*, 1989. **477**(1-2): p. 90-9.
32. Bramblett, G. T., Goedert, M., Jakes, R., Merrick, S. E., Trojanowski, J. Q., and Lee, V. M., *Abnormal tau phosphorylation at Ser396 in Alzheimer's disease recapitulates development and contributes to reduced microtubule binding*. *Neuron*, 1993. **10**(6): p. 1089-99.
33. Ksiazek-Reding, H., Liu, W. K., and Yen, S. H., *Phosphate analysis and dephosphorylation of modified tau associated with paired helical filaments*. *Brain Res*, 1992. **597**(2): p. 209-19.
34. Ittner, L. M. and Gotz, J., *Amyloid-beta and tau--a toxic pas de deux in Alzheimer's disease*. *Nat Rev Neurosci*, 2011. **12**(2): p. 65-72.
35. Lloret, A., Fuchsberger, T., Giraldo, E., and Vina, J., *Molecular mechanisms linking amyloid beta toxicity and Tau hyperphosphorylation in Alzheimers disease*. *Free Radic Biol Med*, 2015. **83**: p. 186-91.
36. van Swieten, J. and Spillantini, M. G., *Hereditary frontotemporal dementia caused by Tau gene mutations*. *Brain Pathol*, 2007. **17**(1): p. 63-73.
37. Cruts, M., Theuns, J., and Van Broeckhoven, C., *Locus-specific mutation databases for neurodegenerative brain diseases*. *Hum Mutat*, 2012. **33**(9): p. 1340-4.
38. Jin, M., Shepardson, N., Yang, T., Chen, G., Walsh, D., and Selkoe, D. J., *Soluble amyloid beta-protein dimers isolated from Alzheimer cortex directly induce Tau hyperphosphorylation and neuritic degeneration*. *Proc Natl Acad Sci U S A*, 2011. **108**(14): p. 5819-24.
39. Gotz, J., Chen, F., van Dorpe, J., and Nitsch, R. M., *Formation of neurofibrillary tangles in P301L tau transgenic mice induced by Abeta 42 fibrils*. *Science*, 2001. **293**(5534): p. 1491-5.
40. Lewis, J., Dickson, D. W., Lin, W. L., Chisholm, L., Corral, A., Jones, G., Yen, S. H., Sahara, N., Skipper, L., Yager, D., Eckman, C., Hardy, J., Hutton, M., and McGowan, E., *Enhanced neurofibrillary degeneration in transgenic mice expressing mutant tau and APP*. *Science*, 2001. **293**(5534): p. 1487-91.
41. Bolmont, T., Clavaguera, F., Meyer-Luehmann, M., Herzog, M. C., Radde, R., Staufenbiel, M., Lewis, J., Hutton, M., Tolnay, M., and Jucker, M., *Induction of tau pathology by intracerebral infusion of amyloid-beta -containing brain extract and by amyloid-beta deposition in APP x Tau transgenic mice*. *Am J Pathol*, 2007. **171**(6): p. 2012-20.
42. Zhang, X. and Song, W., *The role of APP and BACE1 trafficking in APP processing and amyloid-beta generation*. *Alzheimers Res Ther*, 2013. **5**(5): p. 46.
43. BiotechSpain. *Human Alzheimer Amyloid Precursor Protein (APP)*. 2013 Retrieved 27.12.2014, from https://biotechspain.com/en/moleculare.cfm?iid=human_alzheimer_amyloid_precursor_protein_moleculare.
44. Sabuncu, M. R., Desikan, R. S., Sepulcre, J., Yeo, B. T., Liu, H., Schmansky, N. J., Reuter, M., Weiner, M. W., Buckner, R. L., Sperling, R. A., Fischl, B., and Alzheimer's Disease Neuroimaging, I., *The dynamics of cortical and hippocampal atrophy in Alzheimer disease*. *Arch Neurol*, 2011. **68**(8): p. 1040-8.
45. Scahill, R. I., Schott, J. M., Stevens, J. M., Rossor, M. N., and Fox, N. C., *Mapping the evolution of regional atrophy in Alzheimer's disease: unbiased analysis of fluid-registered serial MRI*. *Proc Natl Acad Sci U S A*, 2002. **99**(7): p. 4703-7.
46. Franko, E., Joly, O., and Alzheimer's Disease Neuroimaging, I., *Evaluating Alzheimer's disease progression using rate of regional hippocampal atrophy*. *PLoS One*, 2013. **8**(8): p. e71354.
47. Schonheit, B., Zarski, R., and Ohm, T. G., *Spatial and temporal relationships between plaques and tangles in Alzheimer-pathology*. *Neurobiol Aging*, 2004. **25**(6): p. 697-711.
48. Braak, H. and Braak, E., *Neuropathological staging of Alzheimer-related changes*. *Acta Neuropathol*, 1991. **82**(4): p. 239-59.
49. Cupino, T. L. and Zabel, M. K., *Alzheimer's silent partner: cerebral amyloid angiopathy*. *Transl Stroke Res*, 2014. **5**(3): p. 330-7.
50. Pahnke, J., Frohlich, C., Paarmann, K., Krohn, M., Bogdanovic, N., Arslan, D., and Winblad, B., *Cerebral ABC transporter-common mechanisms may modulate neurodegenerative diseases and depression in elderly subjects*. *Arch Med Res*, 2014. **45**(8): p. 738-43.
51. Heneka, M. T., Carson, M. J., El Khoury, J., Landreth, G. E., Brosseron, F., Feinstein, D. L., Jacobs, A. H., Wyss-Coray, T., Vitorica, J., Ransohoff, R. M., Herrup, K., Frautschy, S. A., Finsen, B., Brown, G. C., Verkhratsky, A., Yamanaka, K., Koistinaho, J., Latz, E., Halle, A., Petzold, G. C., Town, T., Morgan, D., Shinohara, M. L., Perry, V. H., Holmes, C., Bazan, N. G., Brooks, D. J., Hunot, S., Joseph, B., Deigendesch, N., Garaschuk, O., Boddeke, E., Dinarello, C. A., Breitner, J. C., Cole, G. M., Golenbock, D. T., and Kummer, M. P., *Neuroinflammation in Alzheimer's disease*. *Lancet Neurol*, 2015. **14**(4): p. 388-405.
52. Hickman, S. E., Allison, E. K., and El Khoury, J., *Microglial dysfunction and defective beta-amyloid clearance pathways in aging Alzheimer's disease mice*. *J Neurosci*, 2008. **28**(33): p. 8354-60.
53. Lee, C. Y. and Landreth, G. E., *The role of microglia in amyloid clearance from the AD brain*. *J Neural Transm*, 2010. **117**(8): p. 949-60.
54. Mandrekar, S., Jiang, Q., Lee, C. Y., Koenigsnecht-Talboo, J., Holtzman, D. M., and Landreth, G. E., *Microglia mediate the clearance of soluble Abeta through fluid phase macropinocytosis*. *J Neurosci*, 2009. **29**(13): p. 4252-62.
55. Koenigsnecht, J. and Landreth, G., *Microglial phagocytosis of fibrillar beta-amyloid through a beta1 integrin-dependent mechanism*. *J Neurosci*, 2004. **24**(44): p. 9838-46.
56. Colton, C. A. and Gilbert, D. L., *Production of superoxide anions by a CNS macrophage, the microglia*. *FEBS Lett*, 1987. **223**(2): p. 284-8.
57. Boje, K. M. and Arora, P. K., *Microglial-produced nitric oxide and reactive nitrogen oxides mediate neuronal cell death*. *Brain Res*, 1992. **587**(2): p. 250-6.

58. Bhaskar, K., Maphis, N., Xu, G., Varvel, N. H., Kokiko-Cochran, O. N., Weick, J. P., Staugaitis, S. M., Cardona, A., Ransohoff, R. M., Herrup, K., and Lamb, B. T., *Microglial derived tumor necrosis factor-alpha drives Alzheimer's disease-related neuronal cell cycle events*. *Neurobiol Dis*, 2014. **62**: p. 273-85.
59. Ma, J., Jiang, T., Tan, L., and Yu, J. T., *TYROBP in Alzheimer's disease*. *Mol Neurobiol*, 2015. **51**(2): p. 820-6.
60. Minami, S. S., Min, S. W., Krabbe, G., Wang, C., Zhou, Y., Asgarov, R., Li, Y., Martens, L. H., Elia, L. P., Ward, M. E., Mucke, L., Farese, R. V., Jr., and Gan, L., *Progranulin protects against amyloid beta deposition and toxicity in Alzheimer's disease mouse models*. *Nat Med*, 2014. **20**(10): p. 1157-64.
61. Canning, D. R., McKeon, R. J., DeWitt, D. A., Perry, G., Wujek, J. R., Frederickson, R. C., and Silver, J., *beta-Amyloid of Alzheimer's disease induces reactive gliosis that inhibits axonal outgrowth*. *Exp Neurol*, 1993. **124**(2): p. 289-98.
62. Furman, J. L., Sama, D. M., Gant, J. C., Beckett, T. L., Murphy, M. P., Bachstetter, A. D., Van Eldik, L. J., and Norris, C. M., *Targeting astrocytes ameliorates neurologic changes in a mouse model of Alzheimer's disease*. *J Neurosci*, 2012. **32**(46): p. 16129-40.
63. Wyss-Coray, T., Loike, J. D., Brionne, T. C., Lu, E., Anankov, R., Yan, F., Silverstein, S. C., and Husemann, J., *Adult mouse astrocytes degrade amyloid-beta in vitro and in situ*. *Nat Med*, 2003. **9**(4): p. 453-7.
64. Kraft, A. W., Hu, X., Yoon, H., Yan, P., Xiao, Q., Wang, Y., Gil, S. C., Brown, J., Wilhelmsson, U., Restivo, J. L., Cirrito, J. R., Holtzman, D. M., Kim, J., Pekny, M., and Lee, J. M., *Attenuating astrocyte activation accelerates plaque pathogenesis in APP/PS1 mice*. *FASEB J*, 2013. **27**(1): p. 187-98.
65. Chakrabarty, P., Jansen-West, K., Beccard, A., Ceballos-Diaz, C., Levites, Y., Verbeeck, C., Zubair, A. C., Dickson, D., Golde, T. E., and Das, P., *Massive gliosis induced by interleukin-6 suppresses Abeta deposition in vivo: evidence against inflammation as a driving force for amyloid deposition*. *FASEB J*, 2010. **24**(2): p. 548-59.
66. Chakrabarty, P., Ceballos-Diaz, C., Beccard, A., Janus, C., Dickson, D., Golde, T. E., and Das, P., *IFN-gamma promotes complement expression and attenuates amyloid plaque deposition in amyloid beta precursor protein transgenic mice*. *J Immunol*, 2010. **184**(9): p. 5333-43.
67. Kang, J., Lemaire, H. G., Unterbeck, A., Salbaum, J. M., Masters, C. L., Grzeschik, K. H., Multhaup, G., Beyreuther, K., and Muller-Hill, B., *The precursor of Alzheimer's disease amyloid A4 protein resembles a cell-surface receptor*. *Nature*, 1987. **325**(6106): p. 733-6.
68. Goldgaber, D., Lerman, M. I., McBride, O. W., Saffiotti, U., and Gajdusek, D. C., *Characterization and chromosomal localization of a cDNA encoding brain amyloid of Alzheimer's disease*. *Science*, 1987. **235**(4791): p. 877-80.
69. Mucke, L., Masliah, E., Johnson, W. B., Ruppe, M. D., Alford, M., Rockenstein, E. M., Forss-Petter, S., Pietropaolo, M., Mallory, M., and Abraham, C. R., *Synaptotrophic effects of human amyloid beta protein precursors in the cortex of transgenic mice*. *Brain Res*, 1994. **666**(2): p. 151-67.
70. Hayashi, Y., Kashiwagi, K., Ohta, J., Nakajima, M., Kawashima, T., and Yoshikawa, K., *Alzheimer amyloid protein precursor enhances proliferation of neural stem cells from fetal rat brain*. *Biochem Biophys Res Commun*, 1994. **205**(1): p. 936-43.
71. Pruitt, K. D., Brown, G. R., Hiatt, S. M., Thibaud-Nissen, F., Astashyn, A., Ermolaeva, O., Farrell, C. M., Hart, J., Landrum, M. J., McGarvey, K. M., Murphy, M. R., O'Leary, N. A., Pujar, S., Rajput, B., Rangwala, S. H., Riddick, L. D., Shkeda, A., Sun, H., Tamez, P., Tully, R. E., Wallin, C., Webb, D., Weber, J., Wu, W., DiCuccio, M., Kitts, P., Maglott, D. R., Murphy, T. D., and Ostell, J. M., *RefSeq: an update on mammalian reference sequences*. *Nucleic Acids Res*, 2014. **42**(Database issue): p. D756-63.
72. Maglott, D., Ostell, J., Pruitt, K. D., and Tatusova, T., *Entrez Gene: gene-centered information at NCBI*. *Nucleic Acids Res*, 2007. **35**(Database issue): p. D26-31.
73. Cunningham, F., Amode, M. R., Barrell, D., Beal, K., Billis, K., Brent, S., Carvalho-Silva, D., Clapham, P., Coates, G., Fitzgerald, S., Gil, L., Giron, C. G., Gordon, L., Hourlier, T., Hunt, S. E., Janacek, S. H., Johnson, N., Juettemann, T., Kahari, A. K., Keenan, S., Martin, F. J., Maurel, T., McLaren, W., Murphy, D. N., Nag, R., Overduin, B., Parker, A., Patricio, M., Perry, E., Pignatelli, M., Riat, H. S., Sheppard, D., Taylor, K., Thormann, A., Vullo, A., Wilder, S. P., Zadissa, A., Aken, B. L., Birney, E., Harrow, J., et al., *Ensembl 2015*. *Nucleic Acids Res*, 2015. **43**(Database issue): p. D662-9.
74. Nalivaeva, N. N. and Turner, A. J., *The amyloid precursor protein: a biochemical enigma in brain development, function and disease*. *FEBS Lett*, 2013. **587**(13): p. 2046-54.
75. Aydin, D., Weyer, S. W., and Muller, U. C., *Functions of the APP gene family in the nervous system: insights from mouse models*. *Exp Brain Res*, 2012. **217**(3-4): p. 423-34.
76. Shariati, S. A. and De Strooper, B., *Redundancy and divergence in the amyloid precursor protein family*. *FEBS Lett*, 2013. **587**(13): p. 2036-45.
77. Freude, K. K., Penjwini, M., Davis, J. L., LaFerla, F. M., and Blurton-Jones, M., *Soluble amyloid precursor protein induces rapid neural differentiation of human embryonic stem cells*. *J Biol Chem*, 2011. **286**(27): p. 24264-74.
78. van der Kant, R. and Goldstein, L. S., *Cellular functions of the amyloid precursor protein from development to dementia*. *Dev Cell*, 2015. **32**(4): p. 502-15.
79. Rice, H. C., Townsend, M., Bai, J., Suth, S., Cavanaugh, W., Selkoe, D. J., and Young-Pearse, T. L., *Pancortins interact with amyloid precursor protein and modulate cortical cell migration*. *Development*, 2012. **139**(21): p. 3986-96.
80. Wang, P., Yang, G., Mosier, D. R., Chang, P., Zaidi, T., Gong, Y. D., Zhao, N. M., Dominguez, B., Lee, K. F., Gan, W. B., and Zheng, H., *Defective neuromuscular synapses in mice lacking amyloid precursor protein (APP) and APP-Like protein 2*. *J Neurosci*, 2005. **25**(5): p. 1219-25.
81. Wang, Z., Wang, B., Yang, L., Guo, Q., Aithmitti, N., Songyang, Z., and Zheng, H., *Presynaptic and postsynaptic interaction of the amyloid precursor protein promotes peripheral and central synaptogenesis*. *J Neurosci*, 2009. **29**(35): p. 10788-801.

82. Lee, K. J., Moussa, C. E., Lee, Y., Sung, Y., Howell, B. W., Turner, R. S., Pak, D. T., and Hoe, H. S., *Beta amyloid-independent role of amyloid precursor protein in generation and maintenance of dendritic spines*. Neuroscience, 2010. **169**(1): p. 344-56.
83. Hardy, J. and Selkoe, D. J., *The amyloid hypothesis of Alzheimer's disease: progress and problems on the road to therapeutics*. Science, 2002. **297**(5580): p. 353-6.
84. Mawuenyega, K. G., Sigurdson, W., Ovod, V., Munsell, L., Kasten, T., Morris, J. C., Yarasheski, K. E., and Bateman, R. J., *Decreased clearance of CNS beta-amyloid in Alzheimer's disease*. Science, 2010. **330**(6012): p. 1774.
85. Saido, T. and Leissring, M. A., *Proteolytic degradation of amyloid beta-protein*. Cold Spring Harb Perspect Med, 2012. **2**(6): p. a006379.
86. Shibata, M., Yamada, S., Kumar, S. R., Calero, M., Bading, J., Frangione, B., Holtzman, D. M., Miller, C. A., Strickland, D. K., Ghiso, J., and Zlokovic, B. V., *Clearance of Alzheimer's amyloid-ss(1-40) peptide from brain by LDL receptor-related protein-1 at the blood-brain barrier*. J Clin Invest, 2000. **106**(12): p. 1489-99.
87. Lam, F. C., Liu, R., Lu, P., Shapiro, A. B., Renoir, J. M., Sharom, F. J., and Reiner, P. B., *beta-Amyloid efflux mediated by p-glycoprotein*. J Neurochem, 2001. **76**(4): p. 1121-8.
88. Krohn, M., Lange, C., Hofrichter, J., Scheffler, K., Stenzel, J., Steffen, J., Schumacher, T., Bruning, T., Plath, A. S., Alfen, F., Schmidt, A., Winter, F., Rateitschak, K., Wree, A., Gsponer, J., Walker, L. C., and Pahnke, J., *Cerebral amyloid-beta proteostasis is regulated by the membrane transport protein ABCC1 in mice*. J Clin Invest, 2011. **121**(10): p. 3924-31.
89. Abuznait, A. H. and Kaddoumi, A., *Role of ABC transporters in the pathogenesis of Alzheimer's disease*. ACS Chem Neurosci, 2012. **3**(11): p. 820-31.
90. Qosa, H., Abuznait, A. H., Hill, R. A., and Kaddoumi, A., *Enhanced brain amyloid-beta clearance by rifampicin and caffeine as a possible protective mechanism against Alzheimer's disease*. J Alzheimers Dis, 2012. **31**(1): p. 151-65.
91. Abuznait, A. H., Cain, C., Ingram, D., Burk, D., and Kaddoumi, A., *Up-regulation of P-glycoprotein reduces intracellular accumulation of beta amyloid: investigation of P-glycoprotein as a novel therapeutic target for Alzheimer's disease*. J Pharm Pharmacol, 2011. **63**(8): p. 1111-8.
92. Hofrichter, J., Krohn, M., Schumacher, T., Lange, C., Feistel, B., Walbroel, B., Heinze, H. J., Crockett, S., Sharbel, T. F., and Pahnke, J., *Reduced Alzheimer's disease pathology by St. John's Wort treatment is independent of hyperforin and facilitated by ABCC1 and microglia activation in mice*. Curr Alzheimer Res, 2013. **10**(10): p. 1057-69.
93. Schellenberg, G. D. and Montine, T. J., *The genetics and neuropathology of Alzheimer's disease*. Acta Neuropathol, 2012. **124**(3): p. 305-23.
94. Bekris, L. M., Yu, C. E., Bird, T. D., and Tsuang, D. W., *Genetics of Alzheimer disease*. J Geriatr Psychiatry Neurol, 2010. **23**(4): p. 213-27.
95. Haass, C., Lemere, C. A., Capell, A., Citron, M., Seubert, P., Schenk, D., Lannfelt, L., and Selkoe, D. J., *The Swedish mutation causes early-onset Alzheimer's disease by beta-secretase cleavage within the secretory pathway*. Nat Med, 1995. **1**(12): p. 1291-6.
96. Citron, M., Oltersdorf, T., Haass, C., McConlogue, L., Hung, A. Y., Seubert, P., Vigo-Pelfrey, C., Lieberburg, I., and Selkoe, D. J., *Mutation of the beta-amyloid precursor protein in familial Alzheimer's disease increases beta-protein production*. Nature, 1992. **360**(6405): p. 672-4.
97. Scheuner, D., Eckman, C., Jensen, M., Song, X., Citron, M., Suzuki, N., Bird, T. D., Hardy, J., Hutton, M., Kukull, W., Larson, E., Levy-Lahad, E., Viitanen, M., Peskind, E., Poorkaj, P., Schellenberg, G., Tanzi, R., Wasco, W., Lannfelt, L., Selkoe, D., and Younkin, S., *Secreted amyloid beta-protein similar to that in the senile plaques of Alzheimer's disease is increased in vivo by the presenilin 1 and 2 and APP mutations linked to familial Alzheimer's disease*. Nat Med, 1996. **2**(8): p. 864-70.
98. Rovelet-Lecrux, A., Hannequin, D., Raux, G., Le Meur, N., Laquerriere, A., Vital, A., Dumanchin, C., Feuillet, S., Brice, A., Vercelletto, M., Dubas, F., Frebourg, T., and Campion, D., *APP locus duplication causes autosomal dominant early-onset Alzheimer disease with cerebral amyloid angiopathy*. Nat Genet, 2006. **38**(1): p. 24-6.
99. Sleegers, K., Brouwers, N., Gijssels, I., Theuns, J., Goossens, D., Wauters, J., Del-Favero, J., Cruts, M., van Duijn, C. M., and Van Broeckhoven, C., *APP duplication is sufficient to cause early onset Alzheimer's dementia with cerebral amyloid angiopathy*. Brain, 2006. **129**(Pt 11): p. 2977-83.
100. Head, E., Powell, D., Gold, B. T., and Schmitt, F. A., *Alzheimer's Disease in Down Syndrome*. Eur J Neurodegener Dis, 2012. **1**(3): p. 353-364.
101. Nilsberth, C., Westlind-Danielsson, A., Eckman, C. B., Condron, M. M., Axelman, K., Forsell, C., Sten, C., Luthman, J., Teplow, D. B., Younkin, S. G., Naslund, J., and Lannfelt, L., *The 'Arctic' APP mutation (E693G) causes Alzheimer's disease by enhanced Abeta protofibril formation*. Nat Neurosci, 2001. **4**(9): p. 887-93.
102. Ono, K., Condron, M. M., and Teplow, D. B., *Effects of the English (H6R) and Tottori (D7N) familial Alzheimer disease mutations on amyloid beta-protein assembly and toxicity*. J Biol Chem, 2010. **285**(30): p. 23186-97.
103. Hori, Y., Hashimoto, T., Wakutani, Y., Urakami, K., Nakashima, K., Condron, M. M., Tsubuki, S., Saido, T. C., Teplow, D. B., and Iwatsubo, T., *The Tottori (D7N) and English (H6R) familial Alzheimer disease mutations accelerate Abeta fibril formation without increasing protofibril formation*. J Biol Chem, 2007. **282**(7): p. 4916-23.
104. Lan, M. Y., Liu, J. S., Wu, Y. S., Peng, C. H., and Chang, Y. Y., *A novel APP mutation (D678H) in a Taiwanese patient exhibiting dementia and cerebral microvasculopathy*. J Clin Neurosci, 2014. **21**(3): p. 513-5.
105. Pawar, A. P., Dubay, K. F., Zurdo, J., Chiti, F., Vendruscolo, M., and Dobson, C. M., *Prediction of "aggregation-prone" and "aggregation-susceptible" regions in proteins associated with neurodegenerative diseases*. J Mol Biol, 2005. **350**(2): p. 379-92.

106. Van Nostrand, W. E., Melchor, J. P., Romanov, G., Zeigler, K., and Davis, J., *Pathogenic effects of cerebral amyloid angiopathy mutations in the amyloid beta-protein precursor*. *Ann N Y Acad Sci*, 2002. **977**: p. 258-65.
107. Tomiyama, T., Nagata, T., Shimada, H., Teraoka, R., Fukushima, A., Kanemitsu, H., Takuma, H., Kuwano, R., Imagawa, M., Ataka, S., Wada, Y., Yoshioka, E., Nishizaki, T., Watanabe, Y., and Mori, H., *A new amyloid beta variant favoring oligomerization in Alzheimer's-type dementia*. *Ann Neurol*, 2008. **63**(3): p. 377-87.
108. Di Fede, G., Catania, M., Morbin, M., Rossi, G., Suardi, S., Mazzoleni, G., Merlin, M., Giovagnoli, A. R., Prioni, S., Erbetta, A., Falcone, C., Gobbi, M., Colombo, L., Bastone, A., Beeg, M., Manzoni, C., Francescucci, B., Spagnoli, A., Cantu, L., Del Favero, E., Levy, E., Salmona, M., and Tagliavini, F., *A recessive mutation in the APP gene with dominant-negative effect on amyloidogenesis*. *Science*, 2009. **323**(5920): p. 1473-7.
109. Jonsson, T., Atwal, J. K., Steinberg, S., Snaedal, J., Jonsson, P. V., Bjornsson, S., Stefansson, H., Sulem, P., Gudbjartsson, D., Maloney, J., Hoyte, K., Gustafson, A., Liu, Y., Lu, Y., Bhangale, T., Graham, R. R., Huttenlocher, J., Bjornsdottir, G., Andreassen, O. A., Jonsson, E. G., Palotie, A., Behrens, T. W., Magnusson, O. T., Kong, A., Thorsteinsdottir, U., Watts, R. J., and Stefansson, K., *A mutation in APP protects against Alzheimer's disease and age-related cognitive decline*. *Nature*, 2012. **488**(7409): p. 96-9.
110. Maloney, J. A., Bainbridge, T., Gustafson, A., Zhang, S., Kyauk, R., Steiner, P., van der Brug, M., Liu, Y., Ernst, J. A., Watts, R. J., and Atwal, J. K., *Molecular mechanisms of Alzheimer disease protection by the A673T allele of amyloid precursor protein*. *J Biol Chem*, 2014. **289**(45): p. 30990-1000.
111. Puzzo, D., Gulisano, W., Palmeri, A., and Arancio, O., *Rodent models for Alzheimer's disease drug discovery*. *Expert Opin Drug Discov*, 2015. **10**(7): p. 703-11.
112. Bundesministerium für Ernährung und Landwirtschaft. *Versuchstierzahlen 2013*. 2014 Retrieved 26.06.2015, from <http://www.bmel.de/SharedDocs/Downloads/Tier/Tierschutz/2013-TierversuchszahlenGesamt.pdf>.
113. Jankowsky, J. L., Younkin, L. H., Gonzales, V., Fadale, D. J., Slunt, H. H., Lester, H. A., Younkin, S. G., and Borchelt, D. R., *Rodent A beta modulates the solubility and distribution of amyloid deposits in transgenic mice*. *J Biol Chem*, 2007. **282**(31): p. 22707-20.
114. Quon, D., Wang, Y., Catalano, R., Scardina, J. M., Murakami, K., and Cordell, B., *Formation of beta-amyloid protein deposits in brains of transgenic mice*. *Nature*, 1991. **352**(6332): p. 239-41.
115. Wirak, D. O., Bayney, R., Ramabhadran, T. V., Fracasso, R. P., Hart, J. T., Hauer, P. E., Hsiao, P., Pekar, S. K., Scangos, G. A., Trapp, B. D., and et al., *Deposits of amyloid beta protein in the central nervous system of transgenic mice*. *Science*, 1991. **253**(5017): p. 323-5.
116. Sandhu, F. A., Salim, M., and Zain, S. B., *Expression of the human beta-amyloid protein of Alzheimer's disease specifically in the brains of transgenic mice*. *J Biol Chem*, 1991. **266**(32): p. 21331-4.
117. Yamaguchi, F., Richards, S. J., Beyreuther, K., Salbaum, M., Carlson, G. A., and Dunnett, S. B., *Transgenic mice for the amyloid precursor protein 695 isoform have impaired spatial memory*. *Neuroreport*, 1991. **2**(12): p. 781-4.
118. Neve, R. L., Finch, E. A., and Dawes, L. R., *Expression of the Alzheimer amyloid precursor gene transcripts in the human brain*. *Neuron*, 1988. **1**(8): p. 669-77.
119. Johnson, S. A., Pasinetti, G. M., May, P. C., Ponte, P. A., Cordell, B., and Finch, C. E., *Selective reduction of mRNA for the beta-amyloid precursor protein that lacks a Kunitz-type protease inhibitor motif in cortex from Alzheimer brains*. *Exp Neurol*, 1988. **102**(2): p. 264-8.
120. Tanaka, S., Nakamura, S., Ueda, K., Kameyama, M., Shiojiri, S., Takahashi, Y., Kitaguchi, N., and Ito, H., *Three types of amyloid protein precursor mRNA in human brain: their differential expression in Alzheimer's disease*. *Biochem Biophys Res Commun*, 1988. **157**(2): p. 472-9.
121. Higgins, L. S., Holtzman, D. M., Rabin, J., Mobley, W. C., and Cordell, B., *Transgenic mouse brain histopathology resembles early Alzheimer's disease*. *Ann Neurol*, 1994. **35**(5): p. 598-607.
122. Jucker, M., Walker, L. C., Martin, L. J., Kitt, C. A., Kleinman, H. K., Ingram, D. K., and Price, D. L., *Age-associated inclusions in normal and transgenic mouse brain*. *Science*, 1992. **255**(5050): p. 1443-5.
123. Koistinaho, M., Kettunen, M. I., Goldsteins, G., Keinanen, R., Salminen, A., Ort, M., Bures, J., Liu, D., Kauppinen, R. A., Higgins, L. S., and Koistinaho, J., *Beta-amyloid precursor protein transgenic mice that harbor diffuse A beta deposits but do not form plaques show increased ischemic vulnerability: role of inflammation*. *Proc Natl Acad Sci U S A*, 2002. **99**(3): p. 1610-5.
124. Higgins, L. S., Rodems, J. M., Catalano, R., Quon, D., and Cordell, B., *Early Alzheimer disease-like histopathology increases in frequency with age in mice transgenic for beta-APP751*. *Proc Natl Acad Sci U S A*, 1995. **92**(10): p. 4402-6.
125. Dyrks, T., Weidemann, A., Multhaup, G., Salbaum, J. M., Lemaire, H. G., Kang, J., Muller-Hill, B., Masters, C. L., and Beyreuther, K., *Identification, transmembrane orientation and biogenesis of the amyloid A4 precursor of Alzheimer's disease*. *EMBO J*, 1988. **7**(4): p. 949-57.
126. Kammesheidt, A., Boyce, F. M., Spanoyannis, A. F., Cummings, B. J., Ortegon, M., Cotman, C., Vaught, J. L., and Neve, R. L., *Deposition of beta/A4 immunoreactivity and neuronal pathology in transgenic mice expressing the carboxyl-terminal fragment of the Alzheimer amyloid precursor in the brain*. *Proc Natl Acad Sci U S A*, 1992. **89**(22): p. 10857-61.
127. Lamb, B. T., Sisodia, S. S., Lawler, A. M., Slunt, H. H., Kitt, C. A., Kearns, W. G., Pearson, P. L., Price, D. L., and Gearhart, J. D., *Introduction and expression of the 400 kilobase amyloid precursor protein gene in transgenic mice [corrected]*. *Nat Genet*, 1993. **5**(1): p. 22-30.
128. Dodart, J. C., Mathis, C., Bales, K. R., and Paul, S. M., *Does my mouse have Alzheimer's disease?* *Genes Brain Behav*, 2002. **1**(3): p. 142-55.

129. Kawabata, S., Higgins, G. A., and Gordon, J. W., *Amyloid plaques, neurofibrillary tangles and neuronal loss in brains of transgenic mice overexpressing a C-terminal fragment of human amyloid precursor protein*. *Nature*, 1991. **354**(6353): p. 476-8.
130. Kawabata, S., Higgins, G. A., and Gordon, J. W., *Amyloid plaques, neurofibrillary tangles and neuronal loss in brains of transgenic mice overexpressing a C-terminal fragment of human amyloid precursor protein*. *Nature*, 1992. **356**(6366): p. 265.
131. Kawabata, S., Higgins, G. A., and Gordon, J. W., *Alzheimer's retraction*. *Nature*, 1992. **356**(6364): p. 23.
132. Pearson, B. E. and Choi, T. K., *Expression of the human beta-amyloid precursor protein gene from a yeast artificial chromosome in transgenic mice*. *Proc Natl Acad Sci U S A*, 1993. **90**(22): p. 10578-82.
133. Buxbaum, J. D., Christensen, J. L., Ruefli, A. A., Greengard, P., and Loring, J. F., *Expression of APP in brains of transgenic mice containing the entire human APP gene*. *Biochem Biophys Res Commun*, 1993. **197**(2): p. 639-45.
134. Games, D., Adams, D., Alessandrini, R., Barbour, R., Berthelette, P., Blackwell, C., Carr, T., Clemens, J., Donaldson, T., Gillespie, F., and et al., *Alzheimer-type neuropathology in transgenic mice overexpressing V717F beta-amyloid precursor protein*. *Nature*, 1995. **373**(6514): p. 523-7.
135. Clark, R. F. and Goate, A. M., *Molecular genetics of Alzheimer's disease*. *Arch Neurol*, 1993. **50**(11): p. 1164-72.
136. Goate, A., Chartier-Harlin, M. C., Mullan, M., Brown, J., Crawford, F., Fidani, L., Giuffra, L., Haynes, A., Irving, N., James, L., and et al., *Segregation of a missense mutation in the amyloid precursor protein gene with familial Alzheimer's disease*. *Nature*, 1991. **349**(6311): p. 704-6.
137. Naruse, S., Igarashi, S., Kobayashi, H., Aoki, K., Inuzuka, T., Kaneko, K., Shimizu, T., Iihara, K., Kojima, T., Miyatake, T., and et al., *Mis-sense mutation Val----Ile in exon 17 of amyloid precursor protein gene in Japanese familial Alzheimer's disease*. *Lancet*, 1991. **337**(8747): p. 978-9.
138. Murrell, J., Farlow, M., Ghetti, B., and Benson, M. D., *A mutation in the amyloid precursor protein associated with hereditary Alzheimer's disease*. *Science*, 1991. **254**(5028): p. 97-9.
139. Chen, G., Chen, K. S., Knox, J., Inglis, J., Bernard, A., Martin, S. J., Justice, A., McConlogue, L., Games, D., Freedman, S. B., and Morris, R. G., *A learning deficit related to age and beta-amyloid plaques in a mouse model of Alzheimer's disease*. *Nature*, 2000. **408**(6815): p. 975-9.
140. Dodart, J. C., Meziane, H., Mathis, C., Bales, K. R., Paul, S. M., and Ungerer, A., *Behavioral disturbances in transgenic mice overexpressing the V717F beta-amyloid precursor protein*. *Behav Neurosci*, 1999. **113**(5): p. 982-90.
141. Hsiao, K., Chapman, P., Nilsen, S., Eckman, C., Harigaya, Y., Younkin, S., Yang, F., and Cole, G., *Correlative memory deficits, Abeta elevation, and amyloid plaques in transgenic mice*. *Science*, 1996. **274**(5284): p. 99-102.
142. Mullan, M., Crawford, F., Axelman, K., Houlden, H., Lilius, L., Winblad, B., and Lannfelt, L., *A pathogenic mutation for probable Alzheimer's disease in the APP gene at the N-terminus of beta-amyloid*. *Nat Genet*, 1992. **1**(5): p. 345-7.
143. Jacobsen, J. S., Wu, C. C., Redwine, J. M., Comery, T. A., Arias, R., Bowlby, M., Martone, R., Morrison, J. H., Pangalos, M. N., Reinhart, P. H., and Bloom, F. E., *Early-onset behavioral and synaptic deficits in a mouse model of Alzheimer's disease*. *Proc Natl Acad Sci U S A*, 2006. **103**(13): p. 5161-6.
144. King, D. L. and Arendash, G. W., *Behavioral characterization of the Tg2576 transgenic model of Alzheimer's disease through 19 months*. *Physiol Behav*, 2002. **75**(5): p. 627-42.
145. Tagliabattola, G., Hogan, D., Zhang, W. R., and Dineley, K. T., *Intermediate- and long-term recognition memory deficits in Tg2576 mice are reversed with acute calcineurin inhibition*. *Behav Brain Res*, 2009. **200**(1): p. 95-9.
146. Westerman, M. A., Cooper-Blacketer, D., Mariash, A., Kotilinek, L., Kawarabayashi, T., Younkin, L. H., Carlson, G. A., Younkin, S. G., and Ashe, K. H., *The relationship between Abeta and memory in the Tg2576 mouse model of Alzheimer's disease*. *J Neurosci*, 2002. **22**(5): p. 1858-67.
147. Holcomb, L., Gordon, M. N., McGowan, E., Yu, X., Benkovic, S., Jantzen, P., Wright, K., Saad, I., Mueller, R., Morgan, D., Sanders, S., Zehr, C., O'Campo, K., Hardy, J., Prada, C. M., Eckman, C., Younkin, S., Hsiao, K., and Duff, K., *Accelerated Alzheimer-type phenotype in transgenic mice carrying both mutant amyloid precursor protein and presenilin 1 transgenes*. *Nat Med*, 1998. **4**(1): p. 97-100.
148. Duff, K., Eckman, C., Zehr, C., Yu, X., Prada, C. M., Perez-tur, J., Hutton, M., Buee, L., Harigaya, Y., Yager, D., Morgan, D., Gordon, M. N., Holcomb, L., Refolo, L., Zenk, B., Hardy, J., and Younkin, S., *Increased amyloid-beta42(43) in brains of mice expressing mutant presenilin 1*. *Nature*, 1996. **383**(6602): p. 710-3.
149. Elder, G. A., Gama Sosa, M. A., De Gasperi, R., Dickstein, D. L., and Hof, P. R., *Presenilin transgenic mice as models of Alzheimer's disease*. *Brain Struct Funct*, 2010. **214**(2-3): p. 127-43.
150. Lewis, J., McGowan, E., Rockwood, J., Melrose, H., Nacharaju, P., Van Slegtenhorst, M., Gwinn-Hardy, K., Paul Murphy, M., Baker, M., Yu, X., Duff, K., Hardy, J., Corral, A., Lin, W. L., Yen, S. H., Dickson, D. W., Davies, P., and Hutton, M., *Neurofibrillary tangles, amyotrophy and progressive motor disturbance in mice expressing mutant (P301L) tau protein*. *Nat Genet*, 2000. **25**(4): p. 402-5.
151. Gotz, J., Chen, F., Barmettler, R., and Nitsch, R. M., *Tau filament formation in transgenic mice expressing P301L tau*. *J Biol Chem*, 2001. **276**(1): p. 529-34.
152. Higuchi, M., Ishihara, T., Zhang, B., Hong, M., Andreadis, A., Trojanowski, J., and Lee, V. M., *Transgenic mouse model of tauopathies with glial pathology and nervous system degeneration*. *Neuron*, 2002. **35**(3): p. 433-46.
153. Oddo, S., Caccamo, A., Shepherd, J. D., Murphy, M. P., Golde, T. E., Kaye, R., Metherate, R., Mattson, M. P., Akbari, Y., and LaFerla, F. M., *Triple-transgenic model of Alzheimer's disease with plaques and tangles: intracellular Abeta and synaptic dysfunction*. *Neuron*, 2003. **39**(3): p. 409-21.
154. Guo, Q., Fu, W., Sopher, B. L., Miller, M. W., Ware, C. B., Martin, G. M., and Mattson, M. P., *Increased vulnerability of hippocampal neurons to excitotoxic necrosis in presenilin-1 mutant knock-in mice*. *Nat Med*, 1999. **5**(1): p. 101-6.

155. Billings, L. M., Oddo, S., Green, K. N., McGaugh, J. L., and LaFerla, F. M., *Intraneuronal Abeta causes the onset of early Alzheimer's disease-related cognitive deficits in transgenic mice*. *Neuron*, 2005. **45**(5): p. 675-88.
156. Stover, K. R., Campbell, M. A., Van Winssen, C. M., and Brown, R. E., *Early detection of cognitive deficits in the 3xTg-AD mouse model of Alzheimer's disease*. *Behav Brain Res*, 2015. **289**: p. 29-38.
157. Stevens, L. M. and Brown, R. E., *Reference and working memory deficits in the 3xTg-AD mouse between 2 and 15-months of age: a cross-sectional study*. *Behav Brain Res*, 2015. **278**: p. 496-505.
158. Winton, M. J., Lee, E. B., Sun, E., Wong, M. M., Leight, S., Zhang, B., Trojanowski, J. Q., and Lee, V. M., *Intraneuronal APP, not free Abeta peptides in 3xTg-AD mice: implications for tau versus Abeta-mediated Alzheimer neurodegeneration*. *J Neurosci*, 2011. **31**(21): p. 7691-9.
159. *Retraction. Winton et al., Intraneuronal APP, not free Abeta peptides in 3xTg-AD mice: implications for Tau versus Abeta-mediated Alzheimer neurodegeneration*. *J Neurosci*, 2015. **35**(8): p. 3724.
160. The Jackson Laboratory. *B6;129-Psen1tm1Mpm Tg(APP^{Swe},tauP301L)1Lfa/Mmjax*. JAX® Mice database 2014 Retrieved 05.04.2015, from <http://jaxmice.jax.org/strain/004807.html>.
161. Hall, A. M. and Roberson, E. D., *Mouse models of Alzheimer's disease*. *Brain Res Bull*, 2012. **88**(1): p. 3-12.
162. Andorfer, C., Kress, Y., Espinoza, M., de Silva, R., Tucker, K. L., Barde, Y. A., Duff, K., and Davies, P., *Hyperphosphorylation and aggregation of tau in mice expressing normal human tau isoforms*. *J Neurochem*, 2003. **86**(3): p. 582-90.
163. Duff, K., Knight, H., Refolo, L. M., Sanders, S., Yu, X., Picciano, M., Malester, B., Hutton, M., Adamson, J., Goedert, M., Burki, K., and Davies, P., *Characterization of pathology in transgenic mice over-expressing human genomic and cDNA tau transgenes*. *Neurobiol Dis*, 2000. **7**(2): p. 87-98.
164. Tucker, K. L., Meyer, M., and Barde, Y. A., *Neurotrophins are required for nerve growth during development*. *Nat Neurosci*, 2001. **4**(1): p. 29-37.
165. Polydoro, M., Acker, C. M., Duff, K., Castillo, P. E., and Davies, P., *Age-dependent impairment of cognitive and synaptic function in the htau mouse model of tau pathology*. *J Neurosci*, 2009. **29**(34): p. 10741-9.
166. Castillo-Carranza, D. L., Gerson, J. E., Sengupta, U., Guerrero-Munoz, M. J., Lasagna-Reeves, C. A., and Kaye, R., *Specific targeting of tau oligomers in Htau mice prevents cognitive impairment and tau toxicity following injection with brain-derived tau oligomeric seeds*. *J Alzheimers Dis*, 2014. **40 Suppl 1**: p. S97-S111.
167. Ma, Q. L., Zuo, X., Yang, F., Ubeda, O. J., Gant, D. J., Alaverdyan, M., Teng, E., Hu, S., Chen, P. P., Maiti, P., Teter, B., Cole, G. M., and Frautschy, S. A., *Curcumin suppresses soluble tau dimers and corrects molecular chaperone, synaptic, and behavioral deficits in aged human tau transgenic mice*. *J Biol Chem*, 2013. **288**(6): p. 4056-65.
168. Reyes, J. F., Rey, N. L., and Angot, E., *Transmission of tau pathology induced by synthetic preformed tau filaments*. *J Neurosci*, 2013. **33**(16): p. 6707-8.
169. de Calignon, A., Polydoro, M., Suarez-Calvet, M., William, C., Adamowicz, D. H., Kopeikina, K. J., Pitstick, R., Sahara, N., Ashe, K. H., Carlson, G. A., Spires-Jones, T. L., and Hyman, B. T., *Propagation of tau pathology in a model of early Alzheimer's disease*. *Neuron*, 2012. **73**(4): p. 685-97.
170. Calhoun, M. E., Burgermeister, P., Phinney, A. L., Stalder, M., Tolnay, M., Wiederhold, K. H., Abramowski, D., Sturchler-Pierrat, C., Sommer, B., Staufienbiel, M., and Jucker, M., *Neuronal overexpression of mutant amyloid precursor protein results in prominent deposition of cerebrovascular amyloid*. *Proc Natl Acad Sci U S A*, 1999. **96**(24): p. 14088-93.
171. Mahler, J., Morales-Corraliza, J., Stolz, J., Skodras, A., Radde, R., Duma, C. C., Eisele, Y. S., Mazzella, M. J., Wong, H., Klunk, W. E., Nilsson, K. P., Staufienbiel, M., Mathews, P. M., Jucker, M., and Weggen-Braun, B. M., *Endogenous murine Abeta increases amyloid deposition in APP23 but not in APPPS1 transgenic mice*. *Neurobiol Aging*, 2015. **36**(7): p. 2241-7.
172. Sturchler-Pierrat, C., Abramowski, D., Duke, M., Wiederhold, K. H., Mistl, C., Rothacher, S., Ledermann, B., Burki, K., Frey, P., Paganetti, P. A., Waridel, C., Calhoun, M. E., Jucker, M., Probst, A., Staufienbiel, M., and Sommer, B., *Two amyloid precursor protein transgenic mouse models with Alzheimer disease-like pathology*. *Proc Natl Acad Sci U S A*, 1997. **94**(24): p. 13287-92.
173. Radde, R., Bolmont, T., Kaeser, S. A., Coomaraswamy, J., Lindau, D., Stoltze, L., Calhoun, M. E., Jaggi, F., Wolburg, H., Gengler, S., Haass, C., Ghetti, B., Czech, C., Holscher, C., Mathews, P. M., and Jucker, M., *Abeta42-driven cerebral amyloidosis in transgenic mice reveals early and robust pathology*. *EMBO Rep*, 2006. **7**(9): p. 940-6.
174. Giannakopoulos, P., Silhol, S., Jallageas, V., Mallet, J., Bons, N., Bouras, C., and Delaere, P., *Quantitative analysis of tau protein-immunoreactive accumulations and beta amyloid protein deposits in the cerebral cortex of the mouse lemur, Microcebus murinus*. *Acta Neuropathol*, 1997. **94**(2): p. 131-9.
175. Hartig, W., Goldhammer, S., Bauer, U., Wegner, F., Wirths, O., Bayer, T. A., and Grosche, J., *Concomitant detection of beta-amyloid peptides with N-terminal truncation and different C-terminal endings in cortical plaques from cases with Alzheimer's disease, senile monkeys and triple transgenic mice*. *J Chem Neuroanat*, 2010. **40**(1): p. 82-92.
176. Takahashi, E., Kuribayashi, H., Chambers, J. K., Imamura, E., and Une, Y., *Senile plaques and cerebral amyloid angiopathy in an aged California sea lion (Zalophus californianus)*. *Amyloid*, 2014. **21**(3): p. 211-5.
177. Tekirian, T. L., Cole, G. M., Russell, M. J., Yang, F., Wekstein, D. R., Patel, E., Snowdon, D. A., Markesbery, W. R., and Geddes, J. W., *Carboxy terminal of beta-amyloid deposits in aged human, canine, and polar bear brains*. *Neurobiol Aging*, 1996. **17**(2): p. 249-57.
178. Nelson, P. T., Greenberg, S. G., and Saper, C. B., *Neurofibrillary tangles in the cerebral cortex of sheep*. *Neurosci Lett*, 1994. **170**(1): p. 187-90.
179. Nakamura, S., Nakayama, H., Uetsuka, K., Sasaki, N., Uchida, K., and Goto, N., *Senile plaques in an aged two-humped (Bactrian) camel (Camelus bactrianus)*. *Acta Neuropathol*, 1995. **90**(4): p. 415-8.

180. Johnstone, E. M., Chaney, M. O., Norris, F. H., Pascual, R., and Little, S. P., *Conservation of the sequence of the Alzheimer's disease amyloid peptide in dog, polar bear and five other mammals by cross-species polymerase chain reaction analysis*. Brain Res Mol Brain Res, 1991. **10**(4): p. 299-305.
181. Braidy, N., Munoz, P., Palacios, A. G., Castellano-Gonzalez, G., Inestrosa, N. C., Chung, R. S., Sachdev, P., and Guillemin, G. J., *Recent rodent models for Alzheimer's disease: clinical implications and basic research*. J Neural Transm, 2012. **119**(2): p. 173-95.
182. Inestrosa, N. C., Reyes, A. E., Chacon, M. A., Cerpa, W., Villalon, A., Montiel, J., Merabachvili, G., Aldunate, R., Bozinovic, F., and Aboitiz, F., *Human-like rodent amyloid-beta-peptide determines Alzheimer pathology in aged wild-type Octodon degu*. Neurobiol Aging, 2005. **26**(7): p. 1023-8.
183. Ardiles, A. O., Tapia-Rojas, C. C., Mandal, M., Alexandre, F., Kirkwood, A., Inestrosa, N. C., and Palacios, A. G., *Postsynaptic dysfunction is associated with spatial and object recognition memory loss in a natural model of Alzheimer's disease*. Proc Natl Acad Sci U S A, 2012. **109**(34): p. 13835-40.
184. Fagan, T. *Degu Debut—The New Face of Sporadic Alzheimer's Research?* 2012 Retrieved 02.08.2015, from <http://www.alzforum.org/news/research-news/degu-debut-new-face-sporadic-alzheimers-research>.
185. Kamba, T., Higashi, S., Kamoto, T., Shisa, H., Yamada, Y., Ogawa, O., and Hiai, H., *Failure of ureteric bud invasion: a new model of renal agenesis in mice*. Am J Pathol, 2001. **159**(6): p. 2347-53.
186. Xu, F., Previti, M. L., Nieman, M. T., Davis, J., Schmaier, A. H., and Van Nostrand, W. E., *AbetaPP/APLP2 family of Funtz serine proteinase inhibitors regulate cerebral thrombosis*. J Neurosci, 2009. **29**(17): p. 5666-70.
187. Hefetz-Sela, S., Stein, I., Klieger, Y., Porat, R., Sade-Feldman, M., Zreik, F., Nagler, A., Pappo, O., Quagliata, L., Dazert, E., Eferl, R., Terracciano, L., Wagner, E. F., Ben-Neriah, Y., Baniyash, M., and Pikarsky, E., *Acquisition of an immunosuppressive protumorigenic macrophage phenotype depending on c-Jun phosphorylation*. Proc Natl Acad Sci U S A, 2014. **111**(49): p. 17582-7.
188. Zheng, H., Jiang, M., Trumbauer, M. E., Sirinathsinghji, D. J., Hopkins, R., Smith, D. W., Heavens, R. P., Dawson, G. R., Boyce, S., Conner, M. W., Stevens, K. A., Slunt, H. H., Sisoda, S. S., Chen, H. Y., and Van der Ploeg, L. H., *beta-Amyloid precursor protein-deficient mice show reactive gliosis and decreased locomotor activity*. Cell, 1995. **81**(4): p. 525-31.
189. Hirrlinger, P. G., Scheller, A., Braun, C., Quintela-Schneider, M., Fuss, B., Hirrlinger, J., and Kirchhoff, F., *Expression of reef coral fluorescent proteins in the central nervous system of transgenic mice*. Mol Cell Neurosci, 2005. **30**(3): p. 291-303.
190. Feng, G., Mellor, R. H., Bernstein, M., Keller-Peck, C., Nguyen, Q. T., Wallace, M., Nerbonne, J. M., Lichtman, J. W., and Sanes, J. R., *Imaging neuronal subsets in transgenic mice expressing multiple spectral variants of GFP*. Neuron, 2000. **28**(1): p. 41-51.
191. Chen, Q., Cichon, J., Wang, W., Qiu, L., Lee, S. J., Campbell, N. R., Destefino, N., Goard, M. J., Fu, Z., Yasuda, R., Looger, L. L., Arenkiel, B. R., Gan, W. B., and Feng, G., *Imaging neural activity using Thy1-GCaMP transgenic mice*. Neuron, 2012. **76**(2): p. 297-308.
192. Byun, J., Verardo, M. R., Sumengen, B., Lewis, G. P., Manjunath, B. S., and Fisher, S. K., *Automated tool for the detection of cell nuclei in digital microscopic images: application to retinal images*. Mol Vis, 2006. **12**: p. 949-60.
193. Gottschalk, P. G. and Dunn, J. R., *The five-parameter logistic: a characterization and comparison with the four-parameter logistic*. Anal Biochem, 2005. **343**(1): p. 54-65.
194. Bielschowsky, M., *Zur Kenntnis der Alzheimer'schen Krankheit (präsenilen Demenz mit Herdsymptomen)*. J Psychol Neurol, 1911. **18**: p. 273-292.
195. McLean, C. A., Cherny, R. A., Fraser, F. W., Fuller, S. J., Smith, M. J., Beyreuther, K., Bush, A. I., and Masters, C. L., *Soluble pool of Abeta amyloid as a determinant of severity of neurodegeneration in Alzheimer's disease*. Ann Neurol, 1999. **46**(6): p. 860-6.
196. Dawson, G. R., Seabrook, G. R., Zheng, H., Smith, D. W., Graham, S., O'Dowd, G., Bowery, B. J., Boyce, S., Trumbauer, M. E., Chen, H. Y., Van der Ploeg, L. H., and Sirinathsinghji, D. J., *Age-related cognitive deficits, impaired long-term potentiation and reduction in synaptic marker density in mice lacking the beta-amyloid precursor protein*. Neuroscience, 1999. **90**(1): p. 1-13.
197. Phinney, A. L., Calhoun, M. E., Wolfer, D. P., Lipp, H. P., Zheng, H., and Jucker, M., *No hippocampal neuron or synaptic bouton loss in learning-impaired aged beta-amyloid precursor protein-null mice*. Neuroscience, 1999. **90**(4): p. 1207-16.
198. Senechal, Y., Kelly, P. H., and Dev, K. K., *Amyloid precursor protein knockout mice show age-dependent deficits in passive avoidance learning*. Behav Brain Res, 2008. **186**(1): p. 126-32.
199. Magara, F., Muller, U., Li, Z. W., Lipp, H. P., Weissmann, C., Stagljar, M., and Wolfer, D. P., *Genetic background changes the pattern of forebrain commissure defects in transgenic mice underexpressing the beta-amyloid-precursor protein*. Proc Natl Acad Sci U S A, 1999. **96**(8): p. 4656-61.
200. Seabrook, G. R., Smith, D. W., Bowery, B. J., Easter, A., Reynolds, T., Fitzjohn, S. M., Morton, R. A., Zheng, H., Dawson, G. R., Sirinathsinghji, D. J., Davies, C. H., Collingridge, G. L., and Hill, R. G., *Mechanisms contributing to the deficits in hippocampal synaptic plasticity in mice lacking amyloid precursor protein*. Neuropharmacology, 1999. **38**(3): p. 349-59.
201. Tyan, S. H., Shih, A. Y., Walsh, J. J., Maruyama, H., Sarsoza, F., Ku, L., Eggert, S., Hof, P. R., Koo, E. H., and Dickstein, D. L., *Amyloid precursor protein (APP) regulates synaptic structure and function*. Mol Cell Neurosci, 2012. **51**(1-2): p. 43-52.
202. Yang, L., Wang, Z., Wang, B., Justice, N. J., and Zheng, H., *Amyloid precursor protein regulates Cav1.2 L-type calcium channel levels and function to influence GABAergic short-term plasticity*. J Neurosci, 2009. **29**(50): p. 15660-8.

203. Yang, L., Wang, B., Long, C., Wu, G., and Zheng, H., *Increased asynchronous release and aberrant calcium channel activation in amyloid precursor protein deficient neuromuscular synapses*. *Neuroscience*, 2007. **149**(4): p. 768-78.
204. Puig, K. L. and Combs, C. K., *Expression and function of APP and its metabolites outside the central nervous system*. *Exp Gerontol*, 2013. **48**(7): p. 608-11.
205. Morales-Corraliza, J., Schmidt, S. D., Mazzella, M. J., Berger, J. D., Wilson, D. A., Wesson, D. W., Jucker, M., Levy, E., Nixon, R. A., and Mathews, P. M., *Immunization targeting a minor plaque constituent clears beta-amyloid and rescues behavioral deficits in an Alzheimer's disease mouse model*. *Neurobiol Aging*, 2013. **34**(1): p. 137-45.
206. De Strooper, B., Simons, M., Multhaup, G., Van Leuven, F., Beyreuther, K., and Dotti, C. G., *Production of intracellular amyloid-containing fragments in hippocampal neurons expressing human amyloid precursor protein and protection against amyloidogenesis by subtle amino acid substitutions in the rodent sequence*. *EMBO J*, 1995. **14**(20): p. 4932-8.
207. Benilova, I., Gallardo, R., Ungureanu, A. A., Castillo Cano, V., Snellinx, A., Ramakers, M., Bartic, C., Rousseau, F., Schymkowitz, J., and De Strooper, B., *The Alzheimer disease protective mutation A2T modulates kinetic and thermodynamic properties of amyloid-beta (Abeta) aggregation*. *J Biol Chem*, 2014. **289**(45): p. 30977-89.
208. Fung, J., Frost, D., Chakrabartty, A., and McLaurin, J., *Interaction of human and mouse Abeta peptides*. *J Neurochem*, 2004. **91**(6): p. 1398-403.
209. Kuo, Y. M., Kokjohn, T. A., Beach, T. G., Sue, L. I., Brune, D., Lopez, J. C., Kalback, W. M., Abramowski, D., Sturchler-Pierrat, C., Staufienbiel, M., and Roher, A. E., *Comparative analysis of amyloid-beta chemical structure and amyloid plaque morphology of transgenic mouse and Alzheimer's disease brains*. *J Biol Chem*, 2001. **276**(16): p. 12991-8.
210. Kalback, W., Watson, M. D., Kokjohn, T. A., Kuo, Y. M., Weiss, N., Luehrs, D. C., Lopez, J., Brune, D., Sisodia, S. S., Staufienbiel, M., Emmerling, M., and Roher, A. E., *APP transgenic mice Tg2576 accumulate Abeta peptides that are distinct from the chemically modified and insoluble peptides deposited in Alzheimer's disease senile plaques*. *Biochemistry*, 2002. **41**(3): p. 922-8.
211. Robinson, R. A., Cao, Z., and Williams, C., *Oxidative stress in CD90+ T-cells of AbetaPP/PS-1 transgenic mice*. *J Alzheimers Dis*, 2013. **37**(4): p. 661-6.
212. Cao, Z. and Robinson, R. A., *Proteome characterization of splenocytes from an Abetapp/ps-1 Alzheimer's disease model*. *Proteomics*, 2014. **14**(2-3): p. 291-7.
213. Leifer, D. and Kowall, N. W., *Thy-1 in hippocampus: normal anatomy and neuritic growth in Alzheimer's disease*. *J Neuropathol Exp Neurol*, 1992. **51**(2): p. 133-41.
214. Gardiner, K., *Gene-dosage effects in Down syndrome and trisomic mouse models*. *Genome Biol*, 2004. **5**(10): p. 244.
215. Cataldo, A. M., Petanceska, S., Peterhoff, C. M., Terio, N. B., Epstein, C. J., Villar, A., Carlson, E. J., Staufienbiel, M., and Nixon, R. A., *App gene dosage modulates endosomal abnormalities of Alzheimer's disease in a segmental trisomy 16 mouse model of down syndrome*. *J Neurosci*, 2003. **23**(17): p. 6788-92.
216. Christensen, D. Z., Huettenrauch, M., Mitkovski, M., Pradier, L., and Wirths, O., *Axonal degeneration in an Alzheimer mouse model is PS1 gene dose dependent and linked to intraneuronal Abeta accumulation*. *Front Aging Neurosci*, 2014. **6**: p. 139.
217. Ando, K., Leroy, K., Heraud, C., Yilmaz, Z., Authalet, M., Suain, V., De Decker, R., and Brion, J. P., *Accelerated human mutant tau aggregation by knocking out murine tau in a transgenic mouse model*. *Am J Pathol*, 2011. **178**(2): p. 803-16.
218. Schindowski, K., Bretteville, A., Leroy, K., Begard, S., Brion, J. P., Hamdane, M., and Buee, L., *Alzheimer's disease-like tau neuropathology leads to memory deficits and loss of functional synapses in a novel mutated tau transgenic mouse without any motor deficits*. *Am J Pathol*, 2006. **169**(2): p. 599-616.
219. Lin, M. K. and Farrer, M. J., *Genetics and genomics of Parkinson's disease*. *Genome Med*, 2014. **6**(6): p. 48.
220. Mukaetova-Ladinska, E. B. and McKeith, I. G., *Pathophysiology of synuclein aggregation in Lewy body disease*. *Mech Ageing Dev*, 2006. **127**(2): p. 188-202.
221. Hashimoto, M., Rockenstein, E., Mante, M., Mallory, M., and Masliah, E., *beta-Synuclein inhibits alpha-synuclein aggregation: a possible role as an anti-parkinsonian factor*. *Neuron*, 2001. **32**(2): p. 213-23.
222. Asante, E. A., Smidak, M., Grimshaw, A., Houghton, R., Tomlinson, A., Jeelani, A., Jakubcova, T., Hamdan, S., Richard-Londt, A., Linehan, J. M., Brandner, S., Alpers, M., Whitfield, J., Mead, S., Wadsworth, J. D., and Collinge, J., *A naturally occurring variant of the human prion protein completely prevents prion disease*. *Nature*, 2015. **522**(7557): p. 478-81.
223. Kanekiyo, T., Liu, C. C., Shinohara, M., Li, J., and Bu, G., *LRP1 in brain vascular smooth muscle cells mediates local clearance of Alzheimer's amyloid-beta*. *J Neurosci*, 2012. **32**(46): p. 16458-65.
224. Sawada, M., Kondo, N., Suzumura, A., and Marunouchi, T., *Production of tumor necrosis factor-alpha by microglia and astrocytes in culture*. *Brain Res*, 1989. **491**(2): p. 394-7.
225. Scheffler, K., Stenzel, J., Krohn, M., Lange, C., Hofrichter, J., Schumacher, T., Bruning, T., Plath, A. S., Walker, L., and Pahnke, J., *Determination of spatial and temporal distribution of microglia by 230nm-high-resolution, high-throughput automated analysis reveals different amyloid plaque populations in an APP/PS1 mouse model of Alzheimer's disease*. *Curr Alzheimer Res*, 2011. **8**(7): p. 781-8.
226. Baron, R., Babcock, A. A., Nemirovsky, A., Finsen, B., and Monsonego, A., *Accelerated microglial pathology is associated with Abeta plaques in mouse models of Alzheimer's disease*. *Aging Cell*, 2014. **13**(4): p. 584-95.
227. Cho, S. H., Sun, B., Zhou, Y., Kauppinen, T. M., Halabisky, B., Wes, P., Ransohoff, R. M., and Gan, L., *CX3CR1 protein signaling modulates microglial activation and protects against plaque-independent cognitive deficits in a mouse model of Alzheimer disease*. *J Biol Chem*, 2011. **286**(37): p. 32713-22.

228. Vom Berg, J., Prokop, S., Miller, K. R., Obst, J., Kalin, R. E., Lopategui-Cabezas, I., Wegner, A., Mair, F., Schipke, C. G., Peters, O., Winter, Y., Becher, B., and Heppner, F. L., *Inhibition of IL-12/IL-23 signaling reduces Alzheimer's disease-like pathology and cognitive decline*. Nat Med, 2012. **18**(12): p. 1812-9.
229. Richardson, A., Galvan, V., Lin, A. L., and Oddo, S., *How longevity research can lead to therapies for Alzheimer's disease: The rapamycin story*. Exp Gerontol, 2015. **68**: p. 51-8.
230. McGeer, P. L., Schulzer, M., and McGeer, E. G., *Arthritis and anti-inflammatory agents as possible protective factors for Alzheimer's disease: a review of 17 epidemiologic studies*. Neurology, 1996. **47**(2): p. 425-32.
231. Grathwohl, S. A., Kalin, R. E., Bolmont, T., Prokop, S., Winkelmann, G., Kaeser, S. A., Odenthal, J., Radde, R., Eldh, T., Gandy, S., Aguzzi, A., Staufenbiel, M., Mathews, P. M., Wollburg, H., Heppner, F. L., and Jucker, M., *Formation and maintenance of Alzheimer's disease beta-amyloid plaques in the absence of microglia*. Nat Neurosci, 2009. **12**(11): p. 1361-3.
232. DeWitt, D. A., Perry, G., Cohen, M., Doller, C., and Silver, J., *Astrocytes regulate microglial phagocytosis of senile plaque cores of Alzheimer's disease*. Exp Neurol, 1998. **149**(2): p. 329-40.
233. Terwel, D., Steffensen, K. R., Verghese, P. B., Kummer, M. P., Gustafsson, J. A., Holtzman, D. M., and Heneka, M. T., *Critical role of astroglial apolipoprotein E and liver X receptor-alpha expression for microglial Abeta phagocytosis*. J Neurosci, 2011. **31**(19): p. 7049-59.
234. Bolmont, T., Haiss, F., Eicke, D., Radde, R., Mathis, C. A., Klunk, W. E., Kohsaka, S., Jucker, M., and Calhoun, M. E., *Dynamics of the microglial/amyloid interaction indicate a role in plaque maintenance*. J Neurosci, 2008. **28**(16): p. 4283-92.
235. Koistinaho, M., Lin, S., Wu, X., Esterman, M., Koger, D., Hanson, J., Higgs, R., Liu, F., Malkani, S., Bales, K. R., and Paul, S. M., *Apolipoprotein E promotes astrocyte colocalization and degradation of deposited amyloid-beta peptides*. Nat Med, 2004. **10**(7): p. 719-26.
236. Abbott, N. J., Ronnback, L., and Hansson, E., *Astrocyte-endothelial interactions at the blood-brain barrier*. Nat Rev Neurosci, 2006. **7**(1): p. 41-53.
237. Marques, F., Sousa, J. C., Sousa, N., and Palha, J. A., *Blood-brain-barriers in aging and in Alzheimer's disease*. Mol Neurodegener, 2013. **8**: p. 38.
238. Arthur, F. E., Shivers, R. R., and Bowman, P. D., *Astrocyte-mediated induction of tight junctions in brain capillary endothelium: an efficient in vitro model*. Brain Res, 1987. **433**(1): p. 155-9.
239. Schinkel, A. H., *P-Glycoprotein, a gatekeeper in the blood-brain barrier*. Adv Drug Deliv Rev, 1999. **36**(2-3): p. 179-194.
240. Wang, D. D. and Bordey, A., *The astrocyte odyssey*. Prog Neurobiol, 2008. **86**(4): p. 342-67.
241. Savchenko, V. L., McKanna, J. A., Nikonenko, I. R., and Skibo, G. G., *Microglia and astrocytes in the adult rat brain: comparative immunocytochemical analysis demonstrates the efficacy of lipocortin 1 immunoreactivity*. Neuroscience, 2000. **96**(1): p. 195-203.
242. Oboudiyat, C., Glazer, H., Seifan, A., Greer, C., and Isaacson, R. S., *Alzheimer's disease*. Semin Neurol, 2013. **33**(4): p. 313-29.
243. Cherian, J. and Gohil, K., *Cautious optimism for growth in Alzheimer's disease treatments*. P T, 2015. **40**(4): p. 288-9.
244. Aprahamian, I., Stella, F., and Forlenza, O. V., *New treatment strategies for Alzheimer's disease: is there a hope?* Indian J Med Res, 2013. **138**(4): p. 449-60.
245. Brondino, N., Re, S., Boldrini, A., Cuccomarino, A., Lanati, N., Barale, F., and Politi, P., *Curcumin as a therapeutic agent in dementia: a mini systematic review of human studies*. ScientificWorldJournal, 2014. **2014**: p. 174282.
246. Matharu, B., El-Agnaf, O., Razvi, A., and Austen, B. M., *Development of retro-inverso peptides as anti-aggregation drugs for beta-amyloid in Alzheimer's disease*. Peptides, 2010. **31**(10): p. 1866-72.
247. Walker, J. R., Pacoma, R., Watson, J., Ou, W., Alves, J., Mason, D. E., Peters, E. C., Urbina, H. D., Welzel, G., Althage, A., Liu, B., Tuntland, T., Jacobson, L. H., Harris, J. L., and Schumacher, A. M., *Enhanced proteolytic clearance of plasma Abeta by peripherally administered neprilysin does not result in reduced levels of brain Abeta in mice*. J Neurosci, 2013. **33**(6): p. 2457-64.
248. Iwata, N., Tsubuki, S., Takaki, Y., Watanabe, K., Sekiguchi, M., Hosoki, E., Kawashima-Morishima, M., Lee, H. J., Hama, E., Sekine-Aizawa, Y., and Saido, T. C., *Identification of the major Abeta1-42-degrading catabolic pathway in brain parenchyma: suppression leads to biochemical and pathological deposition*. Nat Med, 2000. **6**(2): p. 143-50.
249. Reaume, A. G., Howland, D. S., Trusko, S. P., Savage, M. J., Lang, D. M., Greenberg, B. D., Siman, R., and Scott, R. W., *Enhanced amyloidogenic processing of the beta-amyloid precursor protein in gene-targeted mice bearing the Swedish familial Alzheimer's disease mutations and a "humanized" Abeta sequence*. J Biol Chem, 1996. **271**(38): p. 23380-8.
250. Flood, D. G., Reaume, A. G., Dorfman, K. S., Lin, Y. G., Lang, D. M., Trusko, S. P., Savage, M. J., Annaert, W. G., De Strooper, B., Siman, R., and Scott, R. W., *FAD mutant PS-1 gene-targeted mice: increased A beta 42 and A beta deposition without APP overproduction*. Neurobiol Aging, 2002. **23**(3): p. 335-48.
251. Chang, E. H., Savage, M. J., Flood, D. G., Thomas, J. M., Levy, R. B., Mahadomrongkul, V., Shirao, T., Aoki, C., and Huerta, P. T., *AMPA receptor downscaling at the onset of Alzheimer's disease pathology in double knockin mice*. Proc Natl Acad Sci U S A, 2006. **103**(9): p. 3410-5.
252. Bachstetter, A. D., Norris, C. M., Sompol, P., Wilcock, D. M., Goulding, D., Neltner, J. H., St Clair, D., Watterson, D. M., and Van Eldik, L. J., *Early stage drug treatment that normalizes proinflammatory cytokine production attenuates synaptic dysfunction in a mouse model that exhibits age-dependent progression of Alzheimer's disease-related pathology*. J Neurosci, 2012. **32**(30): p. 10201-10.

253. Ardiles, A. O., Ewer, J., Acosta, M. L., Kirkwood, A., Martinez, A. D., Ebensperger, L. A., Bozinovic, F., Lee, T. M., and Palacios, A. G., *Octodon degus (Molina 1782): a model in comparative biology and biomedicine*. Cold Spring Harb Protoc, 2013. **2013**(4): p. 312-8.
254. Rios, J. A., Cisternas, P., Arrese, M., Barja, S., and Inestrosa, N. C., *Is Alzheimer's disease related to metabolic syndrome? A Wnt signaling conundrum*. Prog Neurobiol, 2014. **121**: p. 125-46.
255. van Groen, T., Kadish, I., Popovic, N., Popovic, M., Caballero-Bleda, M., Bano-Otalora, B., Vivanco, P., Rol, M. A., and Madrid, J. A., *Age-related brain pathology in Octodon degu: blood vessel, white matter and Alzheimer-like pathology*. Neurobiol Aging, 2011. **32**(9): p. 1651-61.
256. Benilova, I., Karran, E., and De Strooper, B., *The toxic Abeta oligomer and Alzheimer's disease: an emperor in need of clothes*. Nat Neurosci, 2012. **15**(3): p. 349-57.
257. Nie, Q., Du, X. G., and Geng, M. Y., *Small molecule inhibitors of amyloid beta peptide aggregation as a potential therapeutic strategy for Alzheimer's disease*. Acta Pharmacol Sin, 2011. **32**(5): p. 545-51.
258. Tickler, A. K., Smith, D. G., Ciccotosto, G. D., Tew, D. J., Curtain, C. C., Carrington, D., Masters, C. L., Bush, A. I., Cherny, R. A., Cappai, R., Wade, J. D., and Barnham, K. J., *Methylation of the imidazole side chains of the Alzheimer disease amyloid-beta peptide results in abolition of superoxide dismutase-like structures and inhibition of neurotoxicity*. J Biol Chem, 2005. **280**(14): p. 13355-63.
259. Dong, X., Chen, W., Mousseau, N., and Derreumaux, P., *Energy landscapes of the monomer and dimer of the Alzheimer's peptide Abeta(1-28)*. J Chem Phys, 2008. **128**(12): p. 125108.
260. Dai, X., Sun, Y., Gao, Z., and Jiang, Z., *Copper enhances amyloid-beta peptide neurotoxicity and non beta-aggregation: a series of experiments conducted upon copper-bound and copper-free amyloid-beta peptide*. J Mol Neurosci, 2010. **41**(1): p. 66-73.
261. Poduslo, J. F., Howell, K. G., Olson, N. C., Ramirez-Alvarado, M., and Kandimalla, K. K., *Alzheimer's disease amyloid beta-protein mutations and deletions that define neuronal binding/internalization as early stage nonfibrillar/fibrillar aggregates and late stage fibrils*. Biochemistry, 2012. **51**(19): p. 3993-4003.
262. Bhowmik, D., MacLaughlin, C. M., Chandrakesan, M., Ramesh, P., Venkatramani, R., Walker, G. C., and Maiti, S., *pH changes the aggregation propensity of amyloid-beta without altering the monomer conformation*. Phys Chem Chem Phys, 2014. **16**(3): p. 885-9.
263. Atwood, C. S., Obrenovich, M. E., Liu, T., Chan, H., Perry, G., Smith, M. A., and Martins, R. N., *Amyloid-beta: a chameleon walking in two worlds: a review of the trophic and toxic properties of amyloid-beta*. Brain Res Brain Res Rev, 2003. **43**(1): p. 1-16.
264. Liu, S. T., Howlett, G., and Barrow, C. J., *Histidine-13 is a crucial residue in the zinc ion-induced aggregation of the A beta peptide of Alzheimer's disease*. Biochemistry, 1999. **38**(29): p. 9373-8.
265. Miura, T., Suzuki, K., Kohata, N., and Takeuchi, H., *Metal binding modes of Alzheimer's amyloid beta-peptide in insoluble aggregates and soluble complexes*. Biochemistry, 2000. **39**(23): p. 7024-31.
266. Bush, A. I., *The metallobiology of Alzheimer's disease*. Trends Neurosci, 2003. **26**(4): p. 207-14.
267. Chen, W. T., Liao, Y. H., Yu, H. M., Cheng, I. H., and Chen, Y. R., *Distinct effects of Zn²⁺, Cu²⁺, Fe³⁺, and Al³⁺ on amyloid-beta stability, oligomerization, and aggregation: amyloid-beta destabilization promotes annular protofibril formation*. J Biol Chem, 2011. **286**(11): p. 9646-56.
268. Ayton, S., Lei, P., and Bush, A. I., *Metallostasis in Alzheimer's disease*. Free Radic Biol Med, 2013. **62**: p. 76-89.
269. Huang, J., Yao, Y., Lin, J., Ye, Y. H., Sun, W. Y., and Tang Dagger, W. X., *The solution structure of rat Abeta-(1-28) and its interaction with zinc ion: insights into the scarcity of amyloid deposition in aged rat brain*. J Biol Inorg Chem, 2004. **9**(5): p. 627-35.
270. Palmiter, R. D., Cole, T. B., Quaife, C. J., and Findley, S. D., *ZnT-3, a putative transporter of zinc into synaptic vesicles*. Proc Natl Acad Sci U S A, 1996. **93**(25): p. 14934-9.
271. Lee, J. Y., Cole, T. B., Palmiter, R. D., Suh, S. W., and Koh, J. Y., *Contribution by synaptic zinc to the gender-disparate plaque formation in human Swedish mutant APP transgenic mice*. Proc Natl Acad Sci U S A, 2002. **99**(11): p. 7705-10.
272. Atwood, C. S., Scarpa, R. C., Huang, X., Moir, R. D., Jones, W. D., Fairlie, D. P., Tanzi, R. E., and Bush, A. I., *Characterization of copper interactions with alzheimer amyloid beta peptides: identification of an attomolar-affinity copper binding site on amyloid beta1-42*. J Neurochem, 2000. **75**(3): p. 1219-33.
273. Hane, F., Tran, G., Attwood, S. J., and Leonenko, Z., *Cu(2+) affects amyloid-beta (1-42) aggregation by increasing peptide-peptide binding forces*. PLoS One, 2013. **8**(3): p. e59005.
274. Alies, B., Badei, B., Faller, P., and Hureau, C., *Reevaluation of copper(II) affinity for amyloid-beta peptides by competition with ferrozine--an unusual copper(II) indicator*. Chemistry, 2012. **18**(4): p. 1161-7.
275. Smith, D. P., Smith, D. G., Curtain, C. C., Boas, J. F., Pilbrow, J. R., Ciccotosto, G. D., Lau, T. L., Tew, D. J., Perez, K., Wade, J. D., Bush, A. I., Drew, S. C., Separovic, F., Masters, C. L., Cappai, R., and Barnham, K. J., *Copper-mediated amyloid-beta toxicity is associated with an intermolecular histidine bridge*. J Biol Chem, 2006. **281**(22): p. 15145-54.
276. Nakamura, M., Shishido, N., Nunomura, A., Smith, M. A., Perry, G., Hayashi, Y., Nakayama, K., and Hayashi, T., *Three histidine residues of amyloid-beta peptide control the redox activity of copper and iron*. Biochemistry, 2007. **46**(44): p. 12737-43.
277. Opazo, C., Huang, X., Cherny, R. A., Moir, R. D., Roher, A. E., White, A. R., Cappai, R., Masters, C. L., Tanzi, R. E., Inestrosa, N. C., and Bush, A. I., *Metalloenzyme-like activity of Alzheimer's disease beta-amyloid. Cu-dependent catalytic conversion of dopamine, cholesterol, and biological reducing agents to neurotoxic H(2)O(2)*. J Biol Chem, 2002. **277**(43): p. 40302-8.
278. Opazo, C., Ruiz, F. H., and Inestrosa, N. C., *Amyloid-beta-peptide reduces copper(II) to copper(I) independent of its aggregation state*. Biol Res, 2000. **33**(2): p. 125-31.

279. Huang, X., Atwood, C. S., Hartshorn, M. A., Multhaup, G., Goldstein, L. E., Scarpa, R. C., Cuajungco, M. P., Gray, D. N., Lim, J., Moir, R. D., Tanzi, R. E., and Bush, A. I., *The A beta peptide of Alzheimer's disease directly produces hydrogen peroxide through metal ion reduction*. *Biochemistry*, 1999. **38**(24): p. 7609-16.
280. Barnham, K. J., Kenche, V. B., Ciccotosto, G. D., Smith, D. P., Tew, D. J., Liu, X., Perez, K., Cranston, G. A., Johanssen, T. J., Volitakis, I., Bush, A. I., Masters, C. L., White, A. R., Smith, J. P., Cherny, R. A., and Cappai, R., *Platinum-based inhibitors of amyloid-beta as therapeutic agents for Alzheimer's disease*. *Proc Natl Acad Sci U S A*, 2008. **105**(19): p. 6813-8.
281. Streltsov, V. A., Chandana Epa, V., James, S. A., Churches, Q. I., Caine, J. M., Kenche, V. B., and Barnham, K. J., *Structural insights into the interaction of platinum-based inhibitors with the Alzheimer's disease amyloid-beta peptide*. *Chem Commun (Camb)*, 2013. **49**(97): p. 11364-6.
282. Yellol, G. S., Yellol, J. G., Kenche, V. B., Liu, X. M., Barnham, K. J., Donaire, A., Janiak, C., and Ruiz, J., *Synthesis of 2-pyridyl-benzimidazole iridium(III), ruthenium(II), and platinum(II) complexes. study of the activity as inhibitors of amyloid-beta aggregation and neurotoxicity evaluation*. *Inorg Chem*, 2015. **54**(2): p. 470-5.
283. Wong, C. Y., Chung, L. H., Lu, L., Wang, M., He, B., Liu, L. J., Leung, C. H., and Ma, D. L., *Dual Inhibition and Monitoring of Beta-Amyloid Fibrillation by a Luminescent Iridium(III) Complex*. *Curr Alzheimer Res*, 2015. **12**(5): p. 439-44.
284. Vyas, N. A., Bhat, S. S., Kumbhar, A. S., Sonawane, U. B., Jani, V., Joshi, R. R., Ramteke, S. N., Kulkarni, P. P., and Joshi, B., *Ruthenium(II) polypyridyl complex as inhibitor of acetylcholinesterase and Abeta aggregation*. *Eur J Med Chem*, 2014. **75**: p. 375-81.
285. Chan, S. L., Lu, L., Lam, T. L., Yan, S. C., Leung, C. H., and Ma, D. L., *A Novel Tetradentate Ruthenium(II) Complex Containing Tris(2-pyridylmethyl)amine (tpa) as an Inhibitor of Beta-Amyloid Fibrillation*. *Curr Alzheimer Res*, 2015. **12**(5): p. 434-8.
286. Cherny, R. A., Atwood, C. S., Xilinas, M. E., Gray, D. N., Jones, W. D., McLean, C. A., Barnham, K. J., Volitakis, I., Fraser, F. W., Kim, Y., Huang, X., Goldstein, L. E., Moir, R. D., Lim, J. T., Beyreuther, K., Zheng, H., Tanzi, R. E., Masters, C. L., and Bush, A. I., *Treatment with a copper-zinc chelator markedly and rapidly inhibits beta-amyloid accumulation in Alzheimer's disease transgenic mice*. *Neuron*, 2001. **30**(3): p. 665-76.
287. Huckle, R., *PBT-1 Prana Biotechnology*. *Curr Opin Investig Drugs*, 2005. **6**(1): p. 99-107.
288. Sampson, E. L., Jenagaratnam, L., and McShane, R., *Metal protein attenuating compounds for the treatment of Alzheimer's dementia*. *Cochrane Database Syst Rev*, 2014. **2**: p. CD005380.
289. Lannfelt, L., Blennow, K., Zetterberg, H., Batsman, S., Ames, D., Harrison, J., Masters, C. L., Targum, S., Bush, A. I., Murdoch, R., Wilson, J., Ritchie, C. W., and group, P. E. s., *Safety, efficacy, and biomarker findings of PBT2 in targeting Abeta as a modifying therapy for Alzheimer's disease: a phase IIa, double-blind, randomised, placebo-controlled trial*. *Lancet Neurol*, 2008. **7**(9): p. 779-86.
290. Faux, N. G., Ritchie, C. W., Gunn, A., Rembach, A., Tsatsanis, A., Bedo, J., Harrison, J., Lannfelt, L., Blennow, K., Zetterberg, H., Ingelsson, M., Masters, C. L., Tanzi, R. E., Cummings, J. L., Herd, C. M., and Bush, A. I., *PBT2 rapidly improves cognition in Alzheimer's Disease: additional phase II analyses*. *J Alzheimers Dis*, 2010. **20**(2): p. 509-16.
291. Huntington Study Group Reach, H. D. I., *Safety, tolerability, and efficacy of PBT2 in Huntington's disease: a phase 2, randomised, double-blind, placebo-controlled trial*. *Lancet Neurol*, 2015. **14**(1): p. 39-47.
292. Edrey, Y. H., Medina, D. X., Gaczynska, M., Osmulski, P. A., Oddo, S., Caccamo, A., and Buffenstein, R., *Amyloid beta and the longest-lived rodent: the naked mole-rat as a model for natural protection from Alzheimer's disease*. *Neurobiol Aging*, 2013. **34**(10): p. 2352-60.
293. Edrey, Y. H., Oddo, S., Cornelius, C., Caccamo, A., Calabrese, V., and Buffenstein, R., *Oxidative damage and amyloid-beta metabolism in brain regions of the longest-lived rodents*. *J Neurosci Res*, 2014. **92**(2): p. 195-205.
294. Pisani, S., Poirion, J. M., Poirion, M., Guevara, E., and Scherb, N., *[Experimental production of allergic hereditary disposition in guinea pig; preliminary communication]*. *Sem Med*, 1952. **100**(17): p. 516-8.
295. Beck, M., Muller, D., and Bigl, V., *Amyloid precursor protein in guinea pigs--complete cDNA sequence and alternative splicing*. *Biochim Biophys Acta*, 1997. **1351**(1-2): p. 17-21.
296. Beck, M., Bruckner, M. K., Holzer, M., Kaap, S., Pannicke, T., Arendt, T., and Bigl, V., *Guinea-pig primary cell cultures provide a model to study expression and amyloidogenic processing of endogenous amyloid precursor protein*. *Neuroscience*, 2000. **95**(1): p. 243-54.
297. Bates, K., Vink, R., Martins, R., and Harvey, A., *Aging, cortical injury and Alzheimer's disease-like pathology in the guinea pig brain*. *Neurobiol Aging*, 2014. **35**(6): p. 1345-51.
298. von Bergen, M., Friedhoff, P., Biernat, J., Heberle, J., Mandelkow, E. M., and Mandelkow, E., *Assembly of tau protein into Alzheimer paired helical filaments depends on a local sequence motif ((306)VQIVYK(311)) forming beta structure*. *Proc Natl Acad Sci U S A*, 2000. **97**(10): p. 5129-34.
299. Mondragon-Rodriguez, S., Trillaud-Doppia, E., Dudilot, A., Bourgeois, C., Lauzon, M., Leclerc, N., and Boehm, J., *Interaction of endogenous tau protein with synaptic proteins is regulated by N-methyl-D-aspartate receptor-dependent tau phosphorylation*. *J Biol Chem*, 2012. **287**(38): p. 32040-53.
300. Goedert, M., Jakes, R., Crowther, R. A., Six, J., Lubke, U., Vandermeeren, M., Cras, P., Trojanowski, J. Q., and Lee, V. M., *The abnormal phosphorylation of tau protein at Ser-202 in Alzheimer disease recapitulates phosphorylation during development*. *Proc Natl Acad Sci U S A*, 1993. **90**(11): p. 5066-70.
301. Arendt, T., Stieler, J., Strijkstra, A. M., Hut, R. A., Rudiger, J., Van der Zee, E. A., Harkany, T., Holzer, M., and Hartig, W., *Reversible paired helical filament-like phosphorylation of tau is an adaptive process associated with neuronal plasticity in hibernating animals*. *J Neurosci*, 2003. **23**(18): p. 6972-81.

302. Orr, M. E., Garbarino, V. R., Salinas, A., and Buffenstein, R., *Sustained high levels of neuroprotective, high molecular weight, phosphorylated tau in the longest-lived rodent*. *Neurobiol Aging*, 2015. **36**(3): p. 1496-504.
303. Decker, J. M., Kruger, L., Sydow, A., Zhao, S., Frotscher, M., Mandelkow, E., and Mandelkow, E. M., *Pro-aggregant Tau impairs mossy fiber plasticity due to structural changes and Ca(++) dysregulation*. *Acta Neuropathol Commun*, 2015. **3**: p. 23.
304. Inestrosa, N. C., Rios, J. A., Cisternas, P., Tapia-Rojas, C., Rivera, D. S., Braidly, N., Zolezzi, J. M., Godoy, J. A., Carvajal, F. J., Ardiles, A. O., Bozinovic, F., Palacios, A. G., and Sachdev, P. S., *Age Progression of Neuropathological Markers in the Brain of the Chilean Rodent Octodon degus, a Natural Model of Alzheimer's Disease*. *Brain Pathol*, 2014.
305. Ramesh Babu, J., Lamar Seibenhener, M., Peng, J., Strom, A. L., Kemppainen, R., Cox, N., Zhu, H., Wooten, M. C., Diaz-Meco, M. T., Moscat, J., and Wooten, M. W., *Genetic inactivation of p62 leads to accumulation of hyperphosphorylated tau and neurodegeneration*. *J Neurochem*, 2008. **106**(1): p. 107-20.
306. Du, Y., Wooten, M. C., and Wooten, M. W., *Oxidative damage to the promoter region of SQSTM1/p62 is common to neurodegenerative disease*. *Neurobiol Dis*, 2009. **35**(2): p. 302-10.
307. Zhong, H. and Yin, H., *Role of lipid peroxidation derived 4-hydroxynonenal (4-HNE) in cancer: focusing on mitochondria*. *Redox Biol*, 2015. **4**: p. 193-9.
308. Butterfield, D. A., Reed, T., and Sultana, R., *Roles of 3-nitrotyrosine- and 4-hydroxynonenal-modified brain proteins in the progression and pathogenesis of Alzheimer's disease*. *Free Radic Res*, 2011. **45**(1): p. 59-72.
309. Puzzo, D., Bizzoca, A., Loreto, C., Guida, C. A., Gulisano, W., Frasca, G., Bellomo, M., Castorina, S., Gennarini, G., and Palmeri, A., *Role of F3/contactin expression profile in synaptic plasticity and memory in aged mice*. *Neurobiol Aging*, 2015. **36**(4): p. 1702-15.
310. Palmeri, A., Privitera, L., Giunta, S., Loreto, C., and Puzzo, D., *Inhibition of phosphodiesterase-5 rescues age-related impairment of synaptic plasticity and memory*. *Behav Brain Res*, 2013. **240**: p. 11-20.
311. Li, Q., Zhao, H. F., Zhang, Z. F., Liu, Z. G., Pei, X. R., Wang, J. B., Cai, M. Y., and Li, Y., *Long-term administration of green tea catechins prevents age-related spatial learning and memory decline in C57BL/6 J mice by regulating hippocampal cyclic amp-response element binding protein signaling cascade*. *Neuroscience*, 2009. **159**(4): p. 1208-15.
312. Calhoun, M. E., Kurth, D., Phinney, A. L., Long, J. M., Hengemihle, J., Mouton, P. R., Ingram, D. K., and Jucker, M., *Hippocampal neuron and synaptophysin-positive bouton number in aging C57BL/6 mice*. *Neurobiol Aging*, 1998. **19**(6): p. 599-606.
313. Bach, M. E., Barad, M., Son, H., Zhuo, M., Lu, Y. F., Shih, R., Mansuy, I., Hawkins, R. D., and Kandel, E. R., *Age-related defects in spatial memory are correlated with defects in the late phase of hippocampal long-term potentiation in vitro and are attenuated by drugs that enhance the cAMP signaling pathway*. *Proc Natl Acad Sci U S A*, 1999. **96**(9): p. 5280-5.
314. Soontornniyomkij, V., Risbrough, V. B., Young, J. W., Soontornniyomkij, B., Jeste, D. V., and Achim, C. L., *Hippocampal calbindin-1 immunoreactivity correlate of recognition memory performance in aged mice*. *Neurosci Lett*, 2012. **516**(1): p. 161-5.
315. Puzzo, D., Loreto, C., Giunta, S., Musumeci, G., Frasca, G., Podda, M. V., Arancio, O., and Palmeri, A., *Effect of phosphodiesterase-5 inhibition on apoptosis and beta amyloid load in aged mice*. *Neurobiol Aging*, 2014. **35**(3): p. 520-31.
316. Mattson, M. P., *Roles of the lipid peroxidation product 4-hydroxynonenal in obesity, the metabolic syndrome, and associated vascular and neurodegenerative disorders*. *Exp Gerontol*, 2009. **44**(10): p. 625-33.
317. Shin, C. M., Chung, Y. H., Kim, M. J., Lee, E. Y., Kim, E. G., and Cha, C. I., *Age-related changes in the distribution of nitrotyrosine in the cerebral cortex and hippocampus of rats*. *Brain Res*, 2002. **931**(2): p. 194-9.
318. Altschul, S. F., Madden, T. L., Schaffer, A. A., Zhang, J., Zhang, Z., Miller, W., and Lipman, D. J., *Gapped BLAST and PSI-BLAST: a new generation of protein database search programs*. *Nucleic Acids Res*, 1997. **25**(17): p. 3389-402.
319. Altschul, S. F., Wootton, J. C., Gertz, E. M., Agarwala, R., Morgulis, A., Schaffer, A. A., and Yu, Y. K., *Protein database searches using compositionally adjusted substitution matrices*. *FEBS J*, 2005. **272**(20): p. 5101-9.

7 Supplement

Table 7-1: Accession numbers of compared proteins.

Protein sequences were gathered using NCBI protein database (<http://www.ncbi.nlm.nih.gov/protein>) and protein alignments were performed using BLASTP 2.2.30+^[318, 319].

Protein	Species	Accession number
Amyloid precursor protein	<i>Homo sapiens sapiens</i>	P05067.3
	<i>Microcebus murinus</i>	XP_012619906.1
	<i>Macaca mulatta</i>	AFI33610.1
	<i>Canis lupus familiaris</i>	NP_001006601.2
	<i>Ursus maritimus</i>	XP_008699989.1
	<i>Ovis aries</i>	XP_004002849.1
	<i>Camelus bactrianus</i>	XP_010954929.1
	<i>Octodon degus</i>	EHB11615.1
	<i>Heterocephalus glaber</i>	XP_004898345.1
	<i>Cavia porcellus</i>	XP_003467233.1
Tau	<i>Homo sapiens sapiens</i>	NP_058519.3
	<i>Octodon degus</i>	XP_004630049.1
	<i>Heterocephalus glaber</i>	EHB10652.1

Table 7-2: Linear regression analysis of plaque number.

All values of each time point were used for linear regression analysis (R^2 of mean values is ≥ 0.965).

Age		mAPP ^{0/0}	mAPP ^{+/+}
50 d to 100 d	Slope (95% confidence interval)	5.861 (5.064 to 6.658)	3.462 (2.723 to 4.201)
	Y-intercept (95% confidence interval)	-282.0 (-346.0 to -218.1)	-164.9 (-224.7 to -105.2)
	X-intercept (95% confidence interval)	48.12 (42.60 to 52.53)	47.64 (37.97 to 54.40)
	R^2	0.8609	0.7464
125 d to 200 d	Slope (95% confidence interval)	3.526 (2.783 to 4.270)	2.153 (1.445 to 2.861)
	Y-intercept (95% confidence interval)	-113.8 (-237.4 to 9.737)	-22.04 (-138.9 to 94.81)
	X-intercept (95% confidence interval)	32.28 (-3.486 to 55.82)	10.24 (-65.29 to 48.78)
	R^2	0.6965	0.4793

Table 7-3: Statistical analysis of plaque number, size and cortical coverage.

	Age	mAPP ^{0/0}	mAPP ^{+/+}	P value	Ratio of means
Number of cortical plaques in n/10 mm ² ± SEM	50 d	18.40 ± 2.203 (n=11)	8.406 ± 2.035 (n=10)	0.0035	2.1889
	75 d	144.0 ± 8.565 (n=12)	94.19 ± 8.568 (n= 9)	0.0006	1.5286
	100 d	309.5 ± 18.93 (n=15)	181.4 ± 17.25 (n=14)	< 0.0001	1.7058
	125 d	347.8 ± 15.25 (n=10)	255.1 ± 21.75 (n=10)	0.0030	1.3633
	150 d	392.9 ± 20.71 (n=11)	286.8 ± 8.765 (n=11)	0.0004	1.3700
	175 d	488.0 ± 24.50 (n= 9)	360.6 ± 21.33 (n=12)	0.0011	1.3533
	200 d	605.9 ± 21.07 (n=12)	409.1 ± 22.46 (n=10)	< 0.0001	1.4810
Plaque size in μm ² ± SEM	50 d	247.5 ± 13.50 (n=11)	241.2 ± 25.51 (n=10)	0.8289	1.0264
	75 d	386.9 ± 22.15 (n=12)	404.7 ± 17.92 (n= 9)	0.5395	0.9560
	100 d	650.7 ± 37.06 (n=15)	538.8 ± 33.19 (n=14)	0.0328	1.2078
	125 d	679.5 ± 22.12 (n=10)	651.8 ± 54.57 (n=10)	0.6466	1.0425
	150 d	656.9 ± 30.94 (n=11)	645.9 ± 37.22 (n=11)	0.8236	1.0169
	175 d	709.7 ± 17.86 (n= 9)	698.8 ± 27.51 (n=12)	0.7437	1.0156
	200 d	734.0 ± 25.52 (n=12)	654.6 ± 17.40 (n=10)	0.0189	1.1213
Cortical coverage in % ± SEM	50 d	0.047 ± 0.007 (n=11)	0.020 ± 0.005 (n=10)	0.0053	2.3500
	75 d	0.567 ± 0.056 (n=12)	0.390 ± 0.048 (n= 9)	0.0262	1.4538
	100 d	2.091 ± 0.235 (n=15)	1.024 ± 0.140 (n=14)	0.0007	2.0420
	125 d	2.379 ± 0.159 (n=10)	1.689 ± 0.220 (n=10)	0.0214	1.4085
	150 d	2.621 ± 0.237 (n=11)	1.831 ± 0.081 (n=11)	0.0080	1.4315
	175 d	3.463 ± 0.202 (n= 9)	2.555 ± 0.222 (n=12)	0.0069	1.3554
	200 d	4.476 ± 0.270 (n=12)	2.702 ± 0.214 (n=10)	< 0.0001	1.6566

Table 7-4: Two-way analysis of variance (ANOVA) of the obtained parameters.

Parameter	% of total variation			P value		
	Interaction	Age	Genotype	Interaction	Age	Genotype
Number of cortical plaques	2.456	79.50	8.208	< 0.0001	< 0.0001	< 0.0001
Size of plaques	1.229	72.09	0.729	0.3533	< 0.0001	0.0477
Cortical plaque coverage	3.675	71.22	7.655	0.0001	< 0.0001	< 0.0001
Amount of 'small' plaques (< 400 μm ²)	1.125	67.34	7.544	0.3596	< 0.0001	< 0.0001
Amount of 'medium' plaques (400 – 700 μm ²)	2.715	81.69	7.306	< 0.0001	< 0.0001	< 0.0001
Amount of 'large' Plaques (> 700 μm ²)	3.664	67.74	7.343	0.0008	< 0.0001	< 0.0001
Cerebral amyloid angiopathy (affected vessels)	3.766	49.55	2.002	0.0702	< 0.0001	0.0128
Cerebral amyloid angiopathy (severity)	2.130	43.90	1.376	0.4557	< 0.0001	0.0559
Microglial plaque coverage	3.775	48.32	13.09	0.0688	< 0.0001	< 0.0001
Plaque-associated microglia	0.049	20.78	10.16	0.9817	0.0011	0.0078
Cortical astrogliosis	10.44	8.861	10.59	0.0178	0.0281	0.0170
Guanidine-soluble cerebral Aβ ₄₂ level	1.218	48.96	3.068	0.8364	< 0.0001	0.0096
Buffer-soluble cerebral Aβ ₄₂ level	7.079	38.56	0.033	0.0396	< 0.0001	0.7988
Total cerebral Aβ ₄₂ level	0.478	51.05	2.804	0.9804	< 0.0001	0.0122

Table 7-5: Separate analysis of ‘small’, medium and ‘large’ plaques in mAPP^{0/0} and mAPP^{+/+} mice.

	Age	mAPP ^{0/0}	mAPP ^{+/+}	P value
‘small’ plaques in n/10 mm ² ± SEM	50 d	16.12 ± 1.826 (n=11)	8.006 ± 2.016 (n=10)	0.0078
	75 d	86.99 ± 5.747 (n=12)	53.82 ± 3.985 (n= 9)	0.0002
	100 d	105.8 ± 5.907 (n=15)	74.31 ± 6.403 (n=14)	0.0013
	125 d	103.1 ± 5.651 (n=10)	82.15 ± 10.50 (n=10)	0.1008
	150 d	124.1 ± 7.284 (n=11)	99.23 ± 12.91 (n= 9)	0.1175
	175 d	134.1 ± 11.97 (n= 9)	109.8 ± 9.158 (n=12)	0.1268
	200 d	179.6 ± 9.022 (n=12)	134.3 ± 9.611 (n=10)	0.0027
‘medium’ sized plaques in n/10 mm ² ± SEM	50 d	1.253 ± 0.649 (n=3/11)	0.180 ± 0.180 (n=1/10)	0.1380
	75 d	41.91 ± 4.167 (n=12)	29.90 ± 3.968 (n= 9)	0.0507
	100 d	87.99 ± 2.737 (n=15)	55.34 ± 4.232 (n=14)	< 0.0001
	125 d	102.6 ± 4.550 (n=10)	79.87 ± 6.915 (n=10)	0.0146
	150 d	115.1 ± 5.800 (n=11)	91.32 ± 3.708 (n=11)	0.0030
	175 d	148.7 ± 9.781 (n= 9)	97.52 ± 3.919 (n=12)	0.0006
	200 d	162.5 ± 4.027 (n=12)	116.4 ± 3.403 (n=10)	< 0.0001
‘large’ plaques in n/10 mm ² ± SEM	50 d	(n=0/11)	(n=0/10)	-
	75 d	14.13 ± 3.949 (n=9/11)	6.628 ± 2.640 (n=6/9)	0.1329
	100 d	113.8 ± 15.82 (n=15)	46.32 ± 10.54 (n=12/14)	0.0016
	125 d	140.6 ± 11.82 (n=10)	89.44 ± 15.26 (n=10)	0.0168
	150 d	150.4 ± 18.34 (n=11)	101.6 ± 8.829 (n=11)	0.0306
	175 d	202.9 ± 11.93 (n= 9)	149.7 ± 15.23 (n=12)	0.0127
	200 d	261.1 ± 17.43 (n=12)	153.9 ± 13.59 (n=10)	0.0001

Table 7-6: Comparison of cortical amyloid angiopathy in mAPP^{0/0} and mAPP^{+/+} mice.

	Age	mAPP ^{0/0}	mAPP ^{+/+}	P value
Affected vessels in % ± SEM	50 d	9.059 ± 3.194 (n=11)	10.46 ± 2.445 (n=10)	0.7324
	75 d	29.47 ± 5.812 (n=12)	44.22 ± 5.653 (n= 9)	0.0849
	100 d	35.59 ± 6.415 (n=14)	62.26 ± 8.095 (n=11)	0.0177
	125 d	55.14 ± 6.046 (n=10)	64.22 ± 3.813 (n=11)	0.2227
	150 d	57.95 ± 4.866 (n=11)	61.55 ± 5.683 (n=11)	0.6362
	175 d	61.90 ± 4.157 (n= 9)	62.35 ± 4.172 (n=12)	0.9397
	200 d	63.80 ± 5.265 (n=12)	59.34 ± 5.566 (n= 7)	0.5692
Mean severity score ± SEM	50 d	0.094 ± 0.031 (n=11)	0.1092 ± 0.0237 (n=10)	0.7042
	75 d	0.338 ± 0.085 (n=12)	0.5478 ± 0.1070 (n= 9)	0.1432
	100 d	0.520 ± 0.124 (n=14)	0.9360 ± 0.1686 (n=11)	0.0609
	125 d	0.855 ± 0.137 (n=10)	1.015 ± 0.0946 (n=11)	0.3485
	150 d	0.948 ± 0.115 (n=11)	1.112 ± 0.1526 (n=11)	0.4021
	175 d	1.046 ± 0.090 (n= 9)	1.066 ± 0.0941 (n=12)	0.8823
	200 d	1.106 ± 0.145 (n=12)	1.035 ± 0.1585 (n= 7)	0.7464

Table 7-7: Statistical analysis of microglia response in mAPP^{0/0} and mAPP^{+/+} mice.

	age	mAPP ^{0/0}	mAPP ^{+/+}	P value	
mean cortical coverage in % ± SEM	150 d	13.24 ± 0.790 (n=10)	13.36 ± 0.892 (n=10)	0.9216	
Plaque coverage in % ± SEM	all plaques	100 d	21.06 ± 2.792 (n=10)	34.82 ± 6.412 (n= 9)	0.0317
		150 d	31.15 ± 1.808 (n=11)	55.37 ± 5.481 (n=11)	0.0012
		200 d	6.735 ± 1.260 (n=10)	12.02 ± 2.936 (n= 7)	0.1360
	'small' plaques	100 d	30.98 ± 3.712 (n=10)	53.19 ± 12.84 (n= 9)	0.1297
		150 d	53.76 ± 4.261 (n=11)	91.17 ± 13.32 (n=11)	0.0202
		200 d	14.14 ± 2.407 (n=10)	27.43 ± 7.583 (n= 7)	0.1372
	'medium' plaques	100 d	17.82 ± 2.357 (n=10)	30.63 ± 5.565 (n= 9)	0.0579
		150 d	27.84 ± 1.518 (n=11)	44.16 ± 5.818 (n=11)	0.0196
		200 d	6.543 ± 1.199 (n=10)	13.35 ± 3.364 (n= 7)	0.0952
	'large' plaques	100 d	11.39 ± 1.861 (n=10)	20.41 ± 4.309 (n= 9)	0.0811
		150 d	17.71 ± 1.025 (n=11)	26.75 ± 2.884 (n=11)	0.0116
		200 d	3.266 ± 0.610 (n=10)	6.405 ± 1.525 (n= 7)	0.0927
Plaque-associated microglial area per 10 mm ² in % ± SEM	100 d	0.233 ± 0.029 (n=10)	0.409 ± 0.084 (n= 9)	0.0762	
	150 d	0.478 ± 0.047 (n=11)	0.636 ± 0.117 (n=11)	0.2369	
	200 d	0.181 ± 0.027 (n=10)	0.367 ± 0.105 (n= 7)	0.1299	

Table 7-8: Neuronal density in mAPP^{0/0} and mAPP^{+/+} mice.

	mAPP ^{0/0}	mAPP ^{+/+}	P value
Neuronal density in n/mm ² ± SEM	2016 ± 53.67 (n=10)	2114 ± 61.46 (n=12)	0.2458

Table 7-9: Cortical astrocyte coverage in mAPP^{0/0} and mAPP^{+/+} mice.

	Age	mAPP ^{0/0}	mAPP ^{+/+}	P value
Cortical GFAP ⁺ area in % ± SEM	100 d	8.355 ± 0.748 (n=15)	8.336 ± 1.116 (n=12)	0.9886
	200 d	13.56 ± 0.677 (n=11)	8.123 ± 2.078 (n= 7)	0.0405

Table 7-10: Statistical analysis of age-dependent astrogliosis in mAPP^{0/0} and mAPP^{+/+} mice.

	Strain	P value
100 d vs. 200 d	mAPP ^{0/0}	< 0.0001
	mAPP ^{+/+}	0.9301

Table 7-11: Cortical levels of soluble and insoluble A β ₄₂ in mAPP^{0/0} and mAPP^{+/+} mice.

		mAPP ^{0/0}	mAPP ^{+/+}	P value	Ratio of means
Guanidine-soluble A β ₄₂ in pg/mg protein \pm SEM	50 d	4771 \pm 471.9 (n=10)	3845 \pm 883.3 (n= 8)	0.3750	1.2408
	75 d	7049 \pm 881.9 (n=10)	4657 \pm 569.6 (n=10)	0.0373	1.5136
	100 d	13117 \pm 852.5 (n= 9)	10498 \pm 753.0 (n=10)	0.0347	1.2495
	125 d	15322 \pm 1525 (n= 8)	14085 \pm 1925 (n= 8)	0.6227	1.0878
	150 d	21715 \pm 3596 (n= 9)	17370 \pm 1229 (n= 8)	0.2799	1.2501
	175 d	23128 \pm 4735 (n= 7)	18686 \pm 3607 (n= 9)	0.4700	1.2377
	200 d	26120 \pm 5768 (n= 7)	18618 \pm 1912 (n= 7)	0.2552	1.4029
Buffer-soluble A β ₄₂ in pg/mg protein \pm SEM	50 d	654.5 \pm 93.17 (n=10)	660.1 \pm 160.4 (n= 8)	0.9766	0.9915
	75 d	3052 \pm 347.8 (n=10)	2116 \pm 362.6 (n=10)	0.0792	1.4423
	100 d	5540 \pm 592.3 (n= 9)	5283 \pm 796.1 (n=10)	0.7987	1.0486
	125 d	7865 \pm 1232 (n= 8)	4710 \pm 1616 (n= 8)	0.1444	1.6699
	150 d	3271 \pm 486.3 (n= 9)	3917 \pm 618.5 (n= 8)	0.4253	0.8351
	175 d	2230 \pm 659.1 (n= 7)	3675 \pm 967.3 (n= 9)	0.2384	0.6068
	200 d	1898 \pm 377.2 (n= 7)	3428 \pm 948.4 (n= 7)	0.1729	0.5537
A β ₄₂ in pg/mg protein \pm SEM	50 d	5426 \pm 558.8 (n=10)	4505 \pm 1018 (n= 8)	0.4445	1.2044
	75 d	10101 \pm 975.1 (n=10)	6774 \pm 748.0 (n=10)	0.0150	1.4911
	100 d	18657 \pm 1263 (n= 9)	15781 \pm 1135 (n=10)	0.1090	1.1822
	125 d	23187 \pm 1649 (n= 8)	18795 \pm 2272 (n= 8)	0.1421	1.2337
	150 d	24986 \pm 3815 (n= 9)	21287 \pm 1492 (n= 8)	0.3870	1.1738
	175 d	25358 \pm 4993 (n= 7)	22361 \pm 3837 (n= 9)	0.6427	1.1340
	200 d	28018 \pm 5542 (n= 7)	22046 \pm 2528 (n= 7)	0.3543	1.2709

Table 7-12: Nonparametric Spearman correlation coefficients in mAPP^{0/0} mice.

Correlation coefficients with p > 0.05 were excluded.

	insoluble A β ₄₂	soluble A β ₄₂	Plaque size	Cortical plaque coverage in %	Plaque number / 10 mm ²	Plaques <400 μ m ²	Plaques 400-700 μ m ²	Plaques >700 μ m ²	Astrocyte coverage	Microglial plaque coverage
insoluble A β ₄₂										
soluble A β ₄₂	0.363									
Plaque size	0.723	0.401								
Cortical plaque coverage	0.753	0.319	0.899							
Plaque number /10 mm ²	0.759	0.314	0.835	0.987						
Plaques <400 μ m ²	0.622	0.315	0.546	0.798	0.862					
Plaques 400-700 μ m ²	0.650		0.582	0.867	0.928	0.799				
Plaques >700 μ m ²	0.494		0.869	0.988	0.946	0.585	0.777			
Astrocyte coverage	0.635	-0.541	0.510	0.683	0.651	0.406	0.523	0.702		
Microglial plaque coverage				-0.494	-0.514	-0.488	-0.447	-0.512	-0.777	

Table 7-13: Nonparametric Spearman correlation coefficients in mAPP^{+/+} mice.

 Correlation coefficients with $p > 0.05$ were excluded.

	insoluble A β ₄₂	soluble A β ₄₂	Plaque size	Cortical plaque coverage in %	Plaque number / 10 mm ²	Plaques <400 μ m ²	Plaques 400-700 μ m ²	Plaques >700 μ m ²	Astrocyte coverage	Microglial plaque coverage	Neuronal density
insoluble A β ₄₂											
soluble A β ₄₂	0.440										
Plaque size	0.776										
Cortical plaque coverage	0.798		0.902								
Plaque number /10 mm ²	0.768		0.762	0.951							
Plaques <400 μ m ²			0.409	0.702	0.864						
Plaques 400-700 μ m ²	0.776		0.600	0.843	0.940	0.805					
Plaques >700 μ m ²	0.722		0.893	0.989	0.881	0.515	0.748				
Astrocyte coverage											
Microglial plaque coverage						-0.488			0.600		
Neuronal density						-0.886					

Table 7-14: Semi-automatic evaluation of cortical microglia, astrocytes and neurons in degus.

	Young	Aged	P value
Cortical coverage by GFAP ⁺ cells \pm SEM	5.925 \pm 0.457 (n= 4)	5.385 \pm 0.581 (n= 4)	0.4943
Cortical coverage by IBA1 ⁺ cells \pm SEM	5.194 \pm 0.683 (n= 4)	4.112 \pm 0.172 (n= 4)	0.2120
Neuronal density in n/mm ² \pm SEM	1487 \pm 33.57 (n= 4)	1351 \pm 115.6 (n= 4)	0.3295

8 Appendix

8.1 Declaration / Erklärung

Johannes Steffen
Einsteinstraße 12
39104 Magdeburg

Erklärung

Hiermit erkläre ich, dass ich die von mir eingereichte Dissertation zu dem Thema

Analysis of animal models of neurodegenerative diseases with protein deposits

selbstständig verfasst, nicht schon als Dissertation verwendet habe und die benutzten Hilfsmittel und Quellen vollständig angegeben wurden.

Weiterhin erkläre ich, dass ich weder diese noch eine andere Arbeit zur Erlangung des akademischen Grades doctor rerum naturalium (Dr. rer. nat.) an anderen Einrichtungen eingereicht habe.

Magdeburg, 25.08.2015

8.2 Curriculum vitae

Personal Information

Name: Johannes Steffen
Address: Einsteinstraße 12
39104 Magdeburg
Date of Birth: 01.06.1986
Place of Birth: Wismar, Germany
Nationality: German
Email: Johannes.Steffen@t-online.de

Education

10/2012 – 08/2015 Otto von Guericke-University, Magdeburg
Dissertation

10/2009 – 09/2011 University of Rostock
Studies of medical biotechnology
Degree: Master of Science (M.Sc.)

10/2006 – 09/2009 University of Rostock
Studies of medical biotechnology
Degree: Bachelor of Science (B. Sc.)

08/1997 – 07/2006 Gerhart-Hauptmann-Gymnasium Wismar
Secondary education

Magdeburg, 25.08.2015

8.3 List of publications

1. Frohlich, C.* , K. Paarmann*, **J. Steffen***, J. Stenzel*, M. Krohn, H. J. Heinze and J. Pahnke (2013). "Genomic background-related activation of microglia and reduced beta-amyloidosis in a mouse model of Alzheimer's disease." *Eur J Microbiol Immunol (Bp)* 3(1): 21-27.
2. Schumacher, T., M. Krohn, J. Hofrichter, C. Lange, J. Stenzel, **J. Steffen**, T. Dunkelmann, K. Paarmann, C. Frohlich, A. Uecker, A. S. Plath, A. Sommer, T. Bruning, H. J. Heinze and J. Pahnke (2012). "ABC transporters B1, C1 and G2 differentially regulate neuroregeneration in mice." *PLoS One* 7(4): e35613.
3. Krohn, M., C. Lange, J. Hofrichter, K. Scheffler, J. Stenzel, **J. Steffen**, T. Schumacher, T. Bruning, A. S. Plath, F. Alfen, A. Schmidt, F. Winter, K. Rateitschak, A. Wree, J. Gsponer, L. C. Walker and J. Pahnke (2011). "Cerebral amyloid-beta proteostasis is regulated by the membrane transport protein ABCC1 in mice." *J Clin Invest* 121(10): 3924-3931.

*equal contribution

8.4 Acknowledgements

First, I want to thank my supervisor Prof. Jens Pahnke not only for providing the research project and the necessary resources but also for the scientific inspiration, the continuing support and the worldly wisdom. I would also like to thank all my colleagues from the NRL: PAHJ, KROM, BRUT, TURC, FROC, PAAK, SOMA, SHIP, SEVA and ERST for the good collaboration and the fun we had together. It was a great and exciting time. Additionally, I thank Prof. Pahnke, Toni, Claudia and Christina for their critical comments on the manuscript.

I want to thank Rainer, Gisela, Heinrich, Mrs Walter, Mrs Albrecht, Mr Scheewe, Mr Koppe and Prof. Pahnke for arousing and strengthening my interest in natural sciences and imparting the necessary basic and advanced knowledge.

Finally, I am most grateful for the patience, forbearance, trust and support of Rainer, Gisela, Heinrich and especially Amelie and Anne and I want to thank them with all my heart.